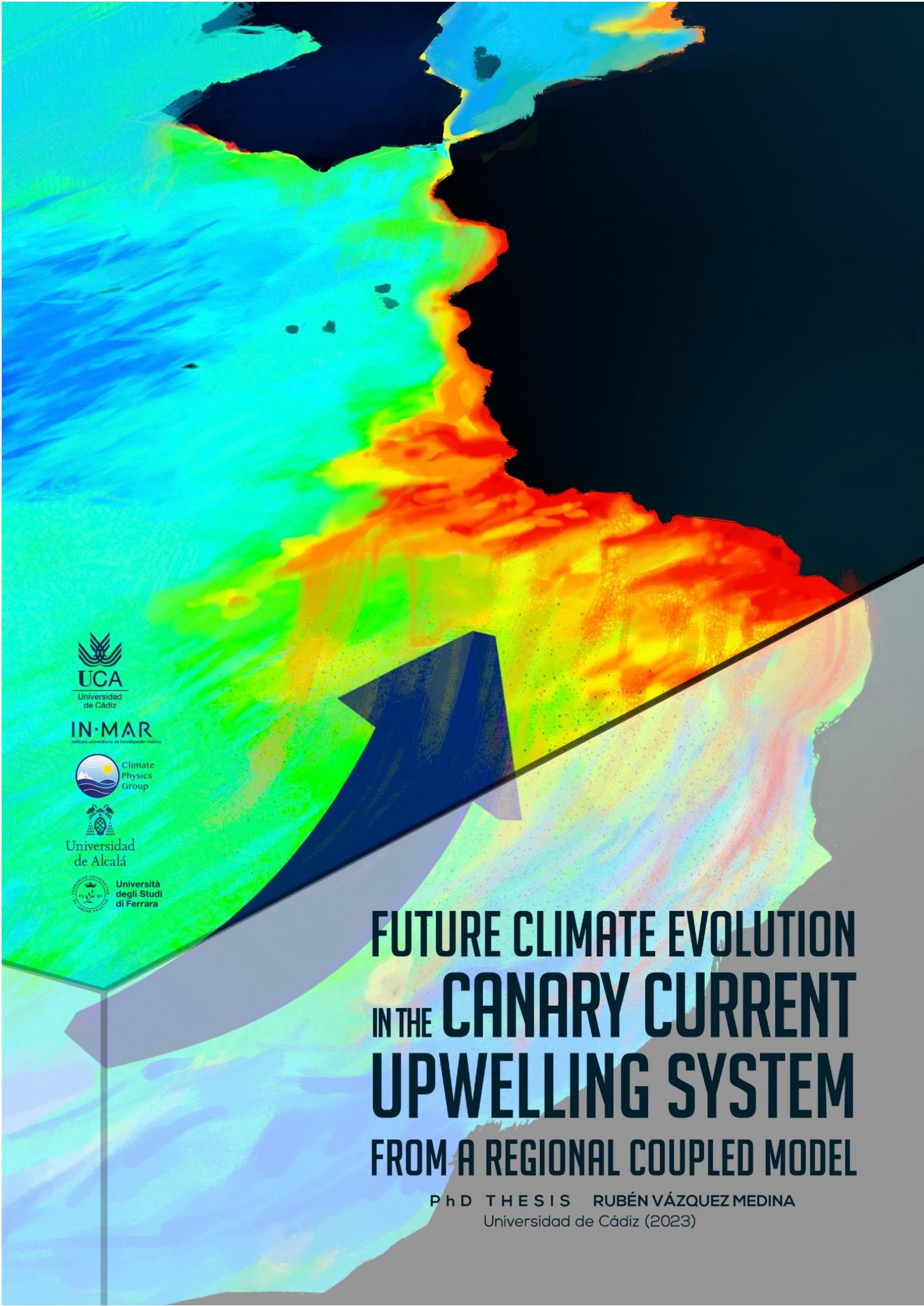

UCA
Universidad de Cádiz

IN·MAR
Instituto universitario de investigación marino

Climate Physics Group

Universidad de Alcalá

Università degli Studi di Ferrara

FUTURE CLIMATE EVOLUTION IN THE CANARY CURRENT UPWELLING SYSTEM FROM A REGIONAL COUPLED MODEL

PhD THESIS RUBÉN VÁZQUEZ MEDINA
Universidad de Cádiz (2023)

Università degli Studi di Ferrara

UCA Universidad de Cádiz

INTERNATIONAL DOCTORAL COURSE IN

"EARTH AND MARINE SCIENCES (EMAS)"

CYCLE 35

COORDINATOR Prof. Paolo Ciavola

FUTURE CLIMATE EVOLUTION IN THE CANARY CURRENT UPWELLING SYSTEM FROM A REGIONAL COUPLED MODEL

Scientific/Disciplinary Sector (SDS) / Physical Oceanography

Firmado por VAZQUEZ MEDINA RUBEN - ***9045** el día 09/05/2023 con un certificado emitido por AC FNMT Usuarios

IZQUIERDO GONZALEZ ALFREDO - 34846311T 2023.05.08 18:44:08 +01'00'

Candidate

Dott. Rubén Vázquez Medina

Supervisor

Prof. Alfredo Izquierdo González

Firmado por CABOS NARVAEZ WILLIAM DAVID - ***3932**

Co-Supervisors

Prof. William David Cabos Narvaez

Years 2019/2023

Università degli Studi di Ferrara

DOTTORATO DI RICERCA IN

"EARTH AND MARINE SCIENCES (EMAS)"

CYCLE 35

COORDINATOR Prof. PAOLO CIAVOLA

FUTURE CLIMATE EVOLUTION IN THE CANARY CURRENT UPWELLING SYSTEM FROM A REGIONAL COUPLED MODEL

Scientific/Disciplinary Sector: Physical Oceanography

Firmado por VAZQUEZ MEDINA RUBEN - ***9045** el día 09/05/2023 con un certificado emitido por AC FNMT Usuarios

IZQUIERDO GONZALEZ ALFREDO - 34846311T

IZQUIERDO GONZALEZ ALFREDO - 34846311T 2023.05.08 18:44:08 +01'00'

Candidate

Rubén Vázquez Medina

Supervisor

Prof. Alfredo Izquierdo González

(University of Cádiz)

Firmado por CABOS NARVAEZ WILLAM DAVID - ***3932**

Co-Supervisor

Prof. William David Cabos Narváez

(University of Alcalá)

UNIVERSIDAD DE CÁDIZ

FACULTAD DE CIENCIAS DEL MAR Y AMBIENTALES

DEPARTAMENTO DE FÍSICA APLICADA

FUTURE CLIMATE EVOLUTION IN THE CANARY CURRENT UPWELLING SYSTEM FROM A REGIONAL COUPLED MODEL

Memoria presentada por Rubén Vázquez Medina para optar al grado de Doctor en Ciencias y Tecnologías Marinas - EMAS

Puerto Real, Marzo 2023

D. ALFREDO IZQUIERDO GONZÁLEZ, Profesor contratado doctor del departamento de Física Aplicada de la Universidad de Cádiz y D. WILLIAM DAVID CABOS NARVÁEZ, Profesor titular del departamento de Física y Matemáticas de la Universidad de Alcalá, como sus directores HACEN CONSTAR:

Que esta memoria titulada "FUTURE CLIMATE EVOLUTION IN THE CANARY CURRENT UPWELLING SYSTEM FROM A REGIONAL COUPLED MODEL" , presentada por Rubén Vázquez Medina, resume su trabajo de Tesis y, considerando que reúne todos los requisitos legales, autorizan su presentación y defensa para optar al grado de Doctor por la Universidad de Cádiz.

Firmado por VAZQUEZ MEDINA RUBEN - ***9045** el día 09/05/2023 con un certificado emitido por AC FNMT Usuarios

IZQUIERDO GONZALEZ ALFREDO - 34846311T

IZQUIERDO GONZALEZ ALFREDO - 34846311T 2023.05.08 18:44:08 +01'00'

Candidato

Rubén Vázquez Medina

Supervisor

Prof. Alfredo Izquierdo González

Firmado por CABOS NARVAEZ WILLIAM DAVID - ***3932**

Co-Supervisor

Prof. William David Cabos Narváez

Pirata de mar y cielo,
si no fui ya, lo seré.

Si no robé la aurora de los mares,
si no la robé,
ya la robaré.

Pirata de cielo y mar,
sobre un cazatorpederos,
con seis fuertes marineros,
alternos de tres en tres.

Si no robé la aurora de los cielos,
si no la robé,
ya la robaré.

Rafel Alberti
Marinero en tierra (1924)

Mira que te diga Abuela, para ti, con todo mi amor.

Agradecimientos

Aunque de manera general nos sentimos agradecidos por multitud de circunstancias, comúnmente los agradecimientos vienen suscritos a una acción concreta. Sin embargo, está demostrado que agradecer impulsa la felicidad y el secreto no es más que serlo siempre sin necesidad de que ocurra algo extraordinario. Aunque la gratitud condicional a menudo puede exaltar el bienestar tanto físico como mental, es poco duradera e irregular. En un periodo como el predoctoral, que sobrepasa todo tipo de barreras temporales y emocionales, se convierte en imprescindible asociar tus emociones a una actitud o un hábito de vida y por ello me gustaría mostrar mi gratitud incondicional a todas esas personas que directa o indirectamente me han ayudado a que a día de hoy pueda estar defendiendo esta tesis doctoral.

Hoy en día no es fácil apostar por la persona y más cuando la excelencia cada vez se asocia más a un expediente. Por ello, en primer lugar me gustaría agradecer a mi director de tesis Alfredo Izquierdo. Alfredo has sido un referente para mí, guiando cada uno de mis pasos durante todo este tiempo. No es fácil comenzar el vuelo solo, cuando has tenido siempre una red de seguridad debajo y de repente, te la quitan. Sin embargo, sí que es sencillo comenzar una nueva ruta con la mochila cargada de aprendizaje y con la confianza de tener un amigo al que preguntar siempre que lo necesite. Me gustaría también agradecer a mi director de tesis William Cabos su confianza y trabajo durante estos casi 4 años. Gracias por trasmitirme tus ganas e ímpetu en avanzar dentro de la ciencia. Además no quería dejar escapar la ocasión sin agradecer tu decisión de apostar por mí en este nuevo proyecto dentro de la Universidad de Alcalá. Quizás al comenzar una nueva aventura los miedos e incertidumbre pueden llegar a inundar mi mente, pero si debo agradecer algo a mis dos directores de tesis, es que siempre han creído en mí, con mis defectos y virtudes y por esto no dejo, no dejaré de agradecerles incondicionalmente su apuesta y ayuda.

Durante más de una década, mi carrera estudiantil-profesional ha estado ligada a una gran persona, Iván. Si caminas solo, irás más rápido, si caminas acompañado, llegarás más lejos, y por ello debo agradecerte que me hayas acompañado durante todos estos años. Juntos hemos crecido de manera exponencial, y lo seguiremos haciendo, ya que aunque parezca un final, es el último paso para un principio y en esto de la ciencia nos queda mucho futuro.

Agradecer a los compañeros del Departamento de Física Aplicada de la Universidad de Cádiz por todo vuestro apoyo durante estos años. En primer lugar, me gustaría recalcar la experiencia que me habéis transmitido los "Seniors" durante estos años, así como vuestra ayuda en todo momento, gracias Rafa, Mike, Óscar y Jesús. Agradecer también aaquellos que aún no eran doctores o acababan de serlos cuando comencé. Gracias Carlitos y Juanxu por acogerme en aquellos comienzos en la "pecera". Dentro de este próspero presente, está una de las personas con mayor progresión en el mundo de la ciencia, Marina. Gracias Marina por ser un ejemplo de lucha, ganas e ímpetu en la ciencia. Estoy seguro de que si hoy en día hay una forma de progresar y avanzar en ciencia es de la manera en que tú lo haces. ¡Gracias por inculcar tu forma de ver la ciencia en los más noveles! Finalmente, agradecer las ganas y la nueva savia de los que estáis inmersos en vuestra tesis, Sara, Carmen, Juanito y Cira. Os agradezco vuestro apoyo en estos últimos coletazos de mi tesis y os animo a que sigáis trabajando y esforzándoos, ya que llegareis muy lejos. También agradecer a uno de los últimos integrantes del grupo Carlos Román, por transmitirme esas ganas de aprender y seguir avanzando en ciencia. Finalmente, me gustaría también agradecer al grupo de clima de la Universidad de Alcalá por haberme acogido como uno más en esta nueva etapa.

La gratitud condicional está ligada a un suceso extraordinario, fuera de lo cotidiano. Sin embargo, en mi vida encuentro un nexo de unión con la gratitud incondicional, mi familia. Tengo la suerte de pertenecer a una familia llena de personas excepcionales, que hacen cada uno de mis días extraordinarios. Gracias a cada uno de los integrantes de mi familia por hacerme partícipe de vuestra vida e influir positivamente en la mía. Gracias Tito Francis y Tita Loli por ser tan increíbles, por acogerme cada fin de semana con una sonrisa, acompañada de una buena tortilla de patatas… esto último imprescindible. Gracias Enrique por alegrarme esos fines de semanas llenos de trabajo, aunque fuera con más trabajo…. Dentro de mi familia más cercana debo añadir a dos personas que desde el primer momento me acogieron en la suya. Gracias Joaquín y Encarni por aportar tanto a mi vida y darme tanto cariño.

El océano Atlántico cobra un papel fundamental en mi vida y no sólo vinculado a este trabajo de tesis. Es el pequeño/gran estrecho que separa/une a parte de las personas más importantes de mi vida. Muchas gracias Rebeca por quererme incondicionalmente, por educarme y enseñarme los valores de la vida durante muchos años. Gracias Jared por cuidar de esta joya tan importante y por supuesto de mis otras dos joyitas, Gabriel y Lucía.

Anexados a mi familia me gustaría agradecer la aportación incondicional de mis amigos. La definición de familia está principalmente asociada a un grupo de personas emparentadas entre sí. Sin embargo, hay parte de tu familia que eliges durante el camino. Ahí, en ese camino me gustaría agradecer a Antonio Pedro que esté en mi vida desde hace ya bastantes años. Gracias por hacerme participe en tu lucha durante todo este tiempo, apostando por las capacidades de las personas, eliminando las etiquetas . Quizás no tenemos la capacidad de cambiar el mundo, pero si nuestro entorno (ANPEHI). Gracias también a mi periodista de confianza, Domi. Aunque probablemente la distancia podría ser un atajo al olvido, nuestra amistad es como nuestra afición, "no cumple años, cumple temporadas". Agradecer también a Luís su forma de ser y de aportar tanto a mi vida. Como no agradecer a mis "Caribues" y en particular a Salva, sin vosotros el comienzo de mis andaduras en Ciencia no hubieran sido igual. También me gustaría agradecer a Ana y Miriam su amistad, ya que muy a mi pesar en primera instancia, habéis conseguido entrar por la puerta grande en mi corazón.

Confianza, sencillez, empatía, generosidad, sinceridad….. amor, virtudes que tiene la persona más especial de mi vida y que me aporta durante en el día a día. Gracias Lorena, por ser parte de mi vida, de mí. Somos el resultado de la suma de todos los pequeños momentos de nuestra vida y tú haces todos ellos inmejorables. Dentro de estos agradecimientos no puedo dejar sin mencionar a mis dos "niñas", Chui y Chica.

Cuesta que fluyan las palabras cuando tienes tanto que agradecer a alguien. Y en este sentido creo que el corazón debe jugar un papel fundamental. Papá y Mamá os debo cada uno de los pilares que sustentan mi vida. Quiero agradeceros que cada uno de los días desde que llegué a este mundo me hayáis querido de manera indefectible. Sois unos padres extraordinarios y eso es un hecho evidente. A día de hoy no estaría en esta tesitura si vosotros no hubierais apostado por mí cada uno de vuestros días y eso os hace los mejores padres del mundo. Podría seguir escribiendo palabras de gratitud y afecto durante días, semanas o meses, pero sé que para vosotros con el simple hecho de existir ya estáis agradecidos de por vida.

Pese a que hace algunos años que te perdimos, mis lágrimas escribiendo este párrafo siguen evidenciando la falta que me haces. Gracias Abuela María por construir una familia sin fronteras, por poner los pilares de nuestro camino y por hacer que el camino que comenzamos hace años como unos niños fueran basados en el afecto, el amor y la familia. Es frecuente en mi vida hacer examen de conciencia e intentar identificar sobre dónde camina mi vida y a menudo me pregunto si en algún tramo me alejo de mi familia o de las personas que

precisamente hacen importantes estos agradecimiento. En este punto siempre apareces tú, tan sencilla y tan increíble. Gracias abuela por guiarme en los momentos difíciles y por hacer que tu inquebrantable ímpetu de amar a tus seres queridos sea la cruz de guía de mi vida.

Acknowledgements

The author would like to thank Dr. Dmitry Sein from Alfred Wegener Institute (AWI) for providing the simulations of the ROM model which have been the focus on the present thesis. The author would like to grate the Climate Dynamics section in the AWI and particularly to Dr. Sergei Danilov for your welcoming and helping during the research stay. Finally, the author would like to thank Dr. Dmitry Sidorenko and Dr. Aldo Drago for being the referees of this thesis.

Moreover, the authors acknowledge the Copernicus marine services (http:// marine. coper nicus. eu), because part of this study has been conducted using CMEMS modeled products (GLORYS12v1) and observational data sources (ESA). The authors also thank the coordinating body of AFRICA-CORDEX (http:// www. csag. uct. ac. za/ cordex- africa) and the responsible panel for CMIP5

This thesis is supported by the PhD program “Earth and Marine Science” of the University of Cádiz (Spain) and the University of Ferrara (Italy).

Table of Contents

List of figures

Wind differences between the last 30 years of ROM_P2 (2070-2099) and ROM_P1 (1976-2005) are represented over the MSLP trends for each period. The black box (b) represents the MSUR (12ºN-19ºN).

Fig. 5.6 Brunt-Väisälä frequency (s^{-1}) averaged from surface to 150 m in the closest grid points to coast for Period 1 (a), Period 2 (b) and Period 3 (c) for ROM_P1 (red shading; Historical) and the differences between ROM_P2 and ROM_P1 (black shading; RCP8.5 - Historical). The mask used is shown in the panel d.

Fig. 5.7 Upwelling source water depth (m) in the closest grid points to coast (Fig. 5.6d) for Period 1 (a), Period 2 (b) and Period 3 (c) both for ROM_P1 (red shading; Historical) and the differences between ROM_P2 and ROM_P1 (black shading; RCP8.5 - Historical). The mask used is shown in Fig. 5.6d.

Fig. 5.8 MSLP trends averaged from 1950 to 2099 for each period. Wind differences between the last 30 years of ROM_P2 (2070-2099) and ROM_P1 (1976-2005) are represented over the MSLP trends for each period. The domain is represented in the Fig. 5.5b with a black box.

Fig. 5.9 Temperature differences between ROM_P2 and ROM_P1 averaged from surface to the maximum depth in the closest grid points to coast (Mask in Fig. 5.6d) for Period 1 (a), Period 2 (b) and Period 3 (c).

Fig. 5.10 Upwelling source water depth differences (m) in the closest grid points to coast (Fig. 5.6d) for Period 1 (a), Period 2 (b) and Period 3 (c) between ROM_P2UI (green shading), ROM_P2N (blue shading), ROM_P2 (dashed line) and ROM_P1. The mask used is shown in Fig. 5.6d. ROM_P2UI is calculated by maintaining the *N* of the historical simulation and the *UI* of the future (ROM_P2UI), and ROM_PN is calculated by maintaining the *UI* of the present and the *N* of the future (ROM_P2N).

Fig. 6.1 Schematic representation of our suggested impact of climate change on coastal upwelling in the CCUS. We show a competitive mechanism as an increase of the upwelling favourable winds along with an enhanced ocean stratification (left) and a complementary mechanism as a decrease of the upwelling favourable winds along with an enhanced ocean stratification (right).

List of tables

Abbreviations

AMOC	Atlantic Meridional Overturning Circulation
ATSR	Along Track Scanning Radiometer
AVHRR	Advanced Very High Resolution Radiometer
CCUS	Canary Current Upwelling System
CMEMS	Copernicus Marine Environment Monitoring Services
CMIP	Coupled Model Intercomparison Project
CORDEX	Coordinated Regional Climate Downscaling Experiment
DJF	December-January-February
EBUSs	Eastern Boundary Upwelling Systems
ECHAM	ECmwf HAMburg
ECMWF	European Centre for Medium-Weather Forecasts
ENSO	El Niño-Southern Oscillation
ESA	European Space Agency
ETOPO	Earth TOPOgraphy
GCMs	Global Climate Models
GLORYS	GLobal Ocean ReanalYsis and Simulation
HAMOCC	Hamburg Model Ocean Carbon Cycle
HD	Hydrological Discharge
ITCZ	Intertropical Convergence Zone
IPCC	Intergovernmental Panel on Climate Change
IUR	Iberian Upwelling Region
JJA	June-July-August
LMEs	Large Marine Ecosystems

LR	Low Resolution
MODIS	Moderate Resolution Imaging Spectroradiometer
MPI-ESM	Max Plank Institute-Earth System Model
MPIOM	Max Plank Institute Ocean Model
MR	Medium Resolution
MSUR	Mauritania-Senegalese Upwelling Region
NW	North Western
OISST	Optimum Interpolation Sea Surface Temperature
PUR	Permanent Upwelling Region
RCMs	Regional Climate Models
RCSMs	Regional Climate System Models
RCP	Representative Concentration Pathways
REMO	Regional Atmosphere Model
ROM	REMO-OASIS-MPIOM
SODA	Simple Ocean Data Assimilation
SST	Sea Surface Temperature
UI	Upwelling Index
WOD	World Ocean Database
WPUR	Weak Permanent Upwelling Region

Summary

The Canary current upwelling system (CCUS) is one of the major eastern boundary coastal upwelling systems in the world, bearing a high productive ecosystem and commercially important fisheries. The CCUS has a large latitudinal extension, and it is divided into upwelling zones with different characteristics. Eddies, filaments and other mesoscale processes characterize upwelling dynamics and are known to have an impact in the upwelling productivity. Thus, for a proper representation of the CCUS, a high horizontal resolution is required. In this study we assess present and future climate of the CCUS using an atmosphere–ocean regionally coupled model. The regional coupled model consists of a global oceanic component with increased horizontal resolution along the northwestern African coast (reaching the 5 km in Cape Ghir) coupled to a high-resolution regional atmosphere (25 km), which extends its domain to the North Atlantic, including the whole CCUS region. We assess the model's present-time performance over the CCUS against relevant reanalysis data sets and compared with an ensemble of global climate models (GCMs) and an ensemble of atmosphere-only regional climate models (RCMs) to evaluate the role of the horizontal resolution. The coupled system reproduces the larger scale pattern of the CCUS and its latitudinal and seasonal variability over the coastal band, improving the GCMs outputs. The model properly reproduces mesoscale structures and is able to simulate the upwelling filaments events off Cape Ghir, which are not well represented in most of GCMs. Our results demonstrate the ability of the regionally coupled model to reproduce both the larger scale and mesoscale processes over the CCUS.

Under RCP8.5 scenario in summer (winter), the upwelling favourable winds increase (decrease) along the Iberian coast and decrease (increase) for the African region. The model simulations suggest that the Azores high is the main driver of these variations in winter, while in summer, the changes are attributed to the intensification of the Iberian thermal low along with an increase in mean sea level pressure over the British islands. This increase may be associated with a weakening of the Atlantic meridional overturning circulation (AMOC). The southernmost region in CCUS, the Mauritania-Senegal upwelling region (MSUR), is expected to experience seasonal changes mainly defined by Cap-Vert (15ºN), where the upwelling favourable winds in the northern subregion will be intensified throughout the year in the future. In the southern MSUR, the upwelling favourable winds are expected to weaken in April-May and strengthen during the winter months. This pattern has been associated with an

intensification of the Azores high in winter and spring. Moreover, our study highlights the importance of the high resolution in reproducing coastal upwelling, as we detected changes in upwelling associated with local increases in air temperature over Sahel. During summer, a drastic thermal rise in the African continent will intensify the Saharan thermal low, increasing the upwelling favourable winds in the northern region of MSUR.

However, the efforts of the scientific community to evaluate the effects of climate change on EBUSs have not only focused on the upwelling favourable winds; changes in ocean stratification may also have a significant impact on these upwelling systems. Although both the wind patterns and ocean stratification responses can provide useful information on the future of these vulnerable ecosystems, obtaining a joint response from both mechanisms is essential. In this context, we obtained a joint response from the upwelling source water depth, which is highly dependent on the latitudinal and seasonal variability of the CCUS. We found that ocean stratification plays a primary role in the two northern regions of the CCUS, while in the PUR and MSUR, it plays a secondary role. Nevertheless, both ocean stratification and wind patterns have a significant impact on the future of the CCUS, and our results reveal the importance of studying both mechanisms seasonally and latitudinally.

Resumen

El sistema de afloramiento canario es uno de los principales sistemas de afloramiento de contorno oriental oceánico en el mundo, los cuales soportan un ecosistema de alta productividad generando regiones muy importantes comercialmente para el sector pesquero. El sistema de afloramiento de la corriente canaria (CCUS) tiene una gran extensión latitudinal, normalmente dividido en subregiones de afloramiento con diferentes características estacionales. Remolinos, filamentos y otros procesos de meso-escala tienen un gran impacto en la productividad del afloramiento, por lo que para una apropiada representación de la CCUS es requerida una alta resolución horizontal. Aquí evaluamos la CCUS en un clima presenta a través de un modelo atmósfera-océano regionalmente acoplado. Este modelo presenta una componente oceánica global con resolución horizontal incrementada a lo largo de la costa noroccidental Africana acoplado a un modelo atmosférico de alta resolución, que extiende su dominio al Atlántico norte, incluyendo toda la CCUS. Su actuación es evaluada a través de relevantes conjuntos de datos de reanálisis y comparado con un ensemble de modelos climáticos globales (GCMs) y un ensemble de modelos regionales atmosféricos (RCMs) con el objetivo de evaluar el rol de la resolución horizontal. El modelo reproduce los patrones de larga escala de la CCUS y su variabilidad latitudinal y estacional sobre la banda costera, mejorando las salidas de los GCMs. El modelo es capaz de reproducir apropiadamente las estructuras meso-escalares, siendo capaz de simular los eventos de filamentos sobre Cabo Ghir, los cuales no son bien representados en la mayoría de los GCMs. Nuestros resultados muestran la habilidad del sistema de modelo regional climático para reproducir la mayor escala así como los procesos locales sobre la CCUS.

Bajo el escenario RCP8.5 en verano (invierno), los vientos favorables de afloramiento incrementan (descienden) sobre el sistema de afloramiento Ibérico y desciende (incrementa) para las regiones Africanas. Las simulaciones del modelo muestran que el alto de las Azores es el principal responsable de esas variaciones en invierno, mientras que en verano los cambios son debidos tanto a la intensificación de la baja térmica Ibérica junto con un incremento en la presión media atmosférica a nivel del mar sobre las islas Británicas, que podría estar asociado con un debilitamiento de la circulación meridional de retorno atlántica (AMOC). La región de afloramiento más al sur de la CCUS, la región Mauritana-Senegalesa (MSUR), presenta cambios estacionales en el futuro definido por Cabo Verde (15ºN), donde los vientos de afloramiento de la subregión norte son intensificados en el futuro y en la subregión sur

debilitados para Abri-Mayo. Este patrón fue asociado con la intensificación de las Azores en invierno y primavera. Además, nosotros identificamos la importancia de la alta resolución para reproducir los afloramientos costeros, ya que detectamos cambios en el afloramiento asociados a incrementos locales de temperatura del aire sobre Sahel. En verano un aumento drástico de la temperatura en el continente Africano intensificará la baja térmica Sahariana, fortaleciendo así los vientos favorables de afloramiento en la región norte del MSUR.

Sin embargo, los esfuerzos de la comunidad científica para evaluar los efectos del cambio climático en los EBUS no solo se han centrado en los vientos favorables de surgencia; los cambios en la estratificación del océano también pueden tener un impacto significativo en estos sistemas de surgencia. Aunque tanto los patrones de viento como las respuestas de estratificación del océano pueden proporcionar información útil sobre el futuro de estos ecosistemas vulnerables, obtener una respuesta conjunta de ambos mecanismos es esencial. En este contexto, obtuvimos una respuesta conjunta de la profundidad del agua de origen de la surgencia, que depende en gran medida de la variabilidad latitudinal y estacional del CCUS. Encontramos que la estratificación del océano desempeña un papel primordial en las dos regiones del norte del CCUS, mientras que en el PUR y MSUR desempeña un papel secundario. Sin embargo, tanto la estratificación del océano como los patrones de viento tienen un impacto significativo en el futuro del CCUS, y nuestros resultados revelan la importancia de estudiar ambos mecanismos de manera estacional y latitudinal.

Riassunto

Il sistema di upwelling associato nelle isole Canarie è uno dei principali sistemi di risalita costiera di acque profonde del confine orientale nel mondo, con un ecosistema altamente produttivo che genera zone importanti dal punto di vista commerciale per il settore peschiero. Il Sistema di Upwelling associato alla Corrente delle Canarie (CCUS) ha una grande estensione latitudinale, normalmente suddivisa in zone di risalita con caratteristiche differenti. Vortici, filamenti, e altri processi di mesoscala hanno un grande impatto sulla produttività nei processi di upwelling, risulta quindi necessaria una elevata risoluzione orizzontale per avere una corretta rappresentazione della CCUS. In questo lavoro si valuta il clima attuale della CCUS mediante un modello regionale accoppiato atmosfera-oceano. Il modello accoppiato regionale presenta una componente oceanica globale con una maggiore risoluzione orizzontale lungo la costa nord-occidentale dell'Africa accoppiato a un modello atmosferico ad alta risoluzione, che estende il suo dominio al Nord Atlantico, includendo l'intero CCUS. Sue prestazioni rispetto alla CCUS vengono valutate mediante un set di dati di rianalisi pertinenti e confrontate con un ensemble di modelli climatici globali (GCMs) e un ensemble di modelli climatici regionali (RCMs) con l'obiettivo di valutare il ruolo della risoluzione orizzontale. Il modello riproduce lo schema, a scala maggiore, della CCUS e la sua variabilità latitudinale e stagionale sulla fascia costiera, migliorando gli output dei GCMs. Il modello è capace di riprodurre correttamente le strutture di mesoscala, essendo capace di simulare gli eventi dei filamenti su Capo Ghir, non ben rappresentati nella maggior parte dei GCMs. Il nostro risultato dimostra l'abilità del sistema accoppiato di modello regionale nel riprodurre processi di larga scala così come processi di mesoscala sulla CCUS.

Nello scenario RCP8.5 in estate (invierno), i venti favorevoli all'upwelling aumentano (diminuiscono) nel sistema di risalita Iberico e diminuiscono (aumentano) per le regioni dell'Africa. Le simulazioni del modello mostrano che l'alta delle Azzorre è la principale responsabile di tali variazioni in inverno, mentre in estate i cambiamenti sono dovuti all'intensificazione della bassa termica iberica insieme accanto ad un aumento della pressione atmosferica media a livello del mare sulle isole britanniche, che potrebbe essere associato ad un indebolimento del capovolgimento meridionale della circolazione atlantica (AMOC). La regione più meridionale del CCUS, regione di upwelling Mauritana-Senegalese (MSUR), regali cambiamenti stagionali in futuro principalmente definito da Capo Verde (15ºN), dove i venti favorevoli di risalita nella subregione settentrionale saranno intensificati per tutto l'anno

in futuro. Nella subregione meridionale i venti favorevoli di risalita sono attenuati in aprile-maggio e rafforzati nei mesi invernali. Questo schema è stato associato all'intensificazione delle Azzorre in inverno e in primavera. Inoltre, abbiamo identificato l'importanza dell'alta risoluzione per riprodurre upwellings costieri, poiché sono stati rilevati cambiamenti di risalita associati agli aumenti locali della temperatura dell'aria sopra il Sahel. In estate, un drastico aumento della temperatura nel continente africano intensificherà la bassa termica sahariana, rafforzando così i venti di risalita favorevoli nella regione settentrionale del MSUR.

Tuttavia, gli sforzi della comunità scientifica per valutare gli effetti del cambiamento climatico sugli EBUS non si sono concentrati solo sui venti favorevoli alla risalita; i cambiamenti nella stratificazione dell'oceano possono avere anche un impatto significativo su questi sistemi di risalita. Anche se sia i modelli di vento che le risposte di stratificazione dell'oceano possono fornire informazioni utili sul futuro di questi ecosistemi vulnerabili, ottenere una risposta congiunta da entrambi i meccanismi è essenziale. In questo contesto, abbiamo ottenuto una risposta congiunta dalla profondità dell'acqua di origine della risalita, che dipende in gran parte dalla variabilità latitudinale e stagionale del CCUS. Abbiamo scoperto che la stratificazione dell'oceano svolge un ruolo primario nelle due regioni settentrionali del CCUS, mentre nel PUR e MSUR svolge un ruolo secondario. Tuttavia, sia la stratificazione dell'oceano che i modelli di vento hanno un impatto significativo sul futuro del CCUS, e i nostri risultati rivelano l'importanza di studiare entrambi i meccanismi in modo stagionale e latitudinale.

CHAPTER 1:

General Introduction

1.1 Introduction

The ocean covers about 71% of Earth's surface, with most of the water masses (approximately the 90%) corresponding to the low-productive open ocean (oligotrophic waters). The remaining constitutes the large marine ecosystems (LMEs; Sherman and Hempel 2008) regions where a 10% of area represents the 80% of the ocean productivity. All LMEs require supply of nutrients to support their productivity. Thus, these ecosystems are strongly controlled by the availability of nutrients (e.g., nitrogen, phosphorus, silica, iron). Depending on the region, this nutrient supply comes from land (large rivers and estuaries), ocean's interior (including seabed), vertical movement of the water column (upwelling) or by the vertical stirring of nutrient-enriched sub-surface water towards the surface (Kampf and Champman 2016).

The upwelling systems are associated to an upward movement of water, which enrich the warmer and usually nutrient-depleted surface waters. The nutrient-rich upwelled water stimulates the growth and reproduction of primary producers such as phytoplankton. The increased availability of nutrients in upwelling regions results in high levels of primary production and increased fishery production. The upward movement can be induced by different mechanisms, but the largest and most persistent upwelling regions are wind-driven. There are three persistent wind-driven upwelling forms: (i) coastal upwelling, (ii) equatorial upwelling and (iii) ice-edge upwelling. Besides these, there are other types of upwelling, related to different mechanisms, described in Kampf and Champman (2016)

- Ekman pumping
- Dynamic uplift
- Tidally-induced upwelling
- Upwelling in the wake of islands
- Topographically caused upwelling
- Transient upwelling caused by the passage of coastally trapped waves

Here we will focus on the wind-driven upwelling.

1.2 Wind-driven Upwelling

The three wind-driven upwelling mechanisms, mentioned in the previous section, are generated by the combined action of wind, Coriolis force, and Ekman transport. When surface water

layers move by the force of the wind, the Coriolis effect moves the surface water at a 45º angle from the wind direction to the right in the Northern Hemisphere and to the left in the Southern Hemisphere. The frictional movement of the topmost layer of water sets in motion the layer directly underneath it, which then sets in motion the next layer under that, and so on as the water gets deeper. Increasing depth in the upper boundary layer, the current speed is reduced, and the direction rotates farther away from the wind direction following a spiral, which usually penetrates to about 100 m deep before the motion ceases. Finally, the resulting net mass transport of the upper 100 m is 90º shifted relative to the original wind direction and is called Ekman transport (Ekman, 1905).

Therefore, near oceanic eastern boundaries, which typically have nominally meridional orientation, equatorward wind stress produces offshore Ekman transport. Since the velocity across the coastal boundary is zero, offshore Ekman transport results in cross-shelf mass flux divergence (coastal divergence) that must be compensated by mass flux convergence in the alongshore or vertical directions (Jacox et al. 2018). Assuming no alongshore variations, water displaced offshore must be compensated from below, and the wind-driven Ekman transport is equal to the vertical transport into the Ekman layer (Halpern, 2002).

In addition to upwelling resulting from coastal divergence, vertical transport can be driven also by Ekman transport divergence associated with spatial variability in wind stress, specifically wind stress curl, where the wind stress curl-driven vertical velocity at the base of the Ekman (Stommel, 1958). While Ekman transport may extend to large scales alongshore (around 100 km), the wind stress curl may enhance upwelling locally on smaller scales (around 10 km; Wang et al. 2011). In the northern hemisphere, positive curl draws water from depth into the Ekman layer (upwelling), a process referred to as Ekman suction, while negative curl (Ekman pumping) pumps near surface water downward into the ocean interior (downwelling). In the southern hemisphere, positive and negative wind stress curl are associated with Ekman pumping and Ekman suction, respectively (Renault, Hall and McWilliams, 2016). To date, some studies have tried to difference upwelling due to coastal divergence from upwelling due to wind stress curl, in terms of both their magnitude and their ecological impacts (Pickett and Paduan, 2003; Rykaczewski and Checkley, 2008). Nevertheless, they are not spatially distinct and upwelling neither can be attributed solely to coastal divergence or wind stress curl (Jacox et al. 2018).

Horizontal surface currents also play a role in the vertical movements of deeper water by contributing to mixing the upper water column. When upwelling occurs horizontal surface currents have to be divergent in order to fulfill mass conservation. There are three types of upwelling mechanisms driven by the winds: Coastal upwelling, Equatorial upwelling and Ice-edge upwelling.

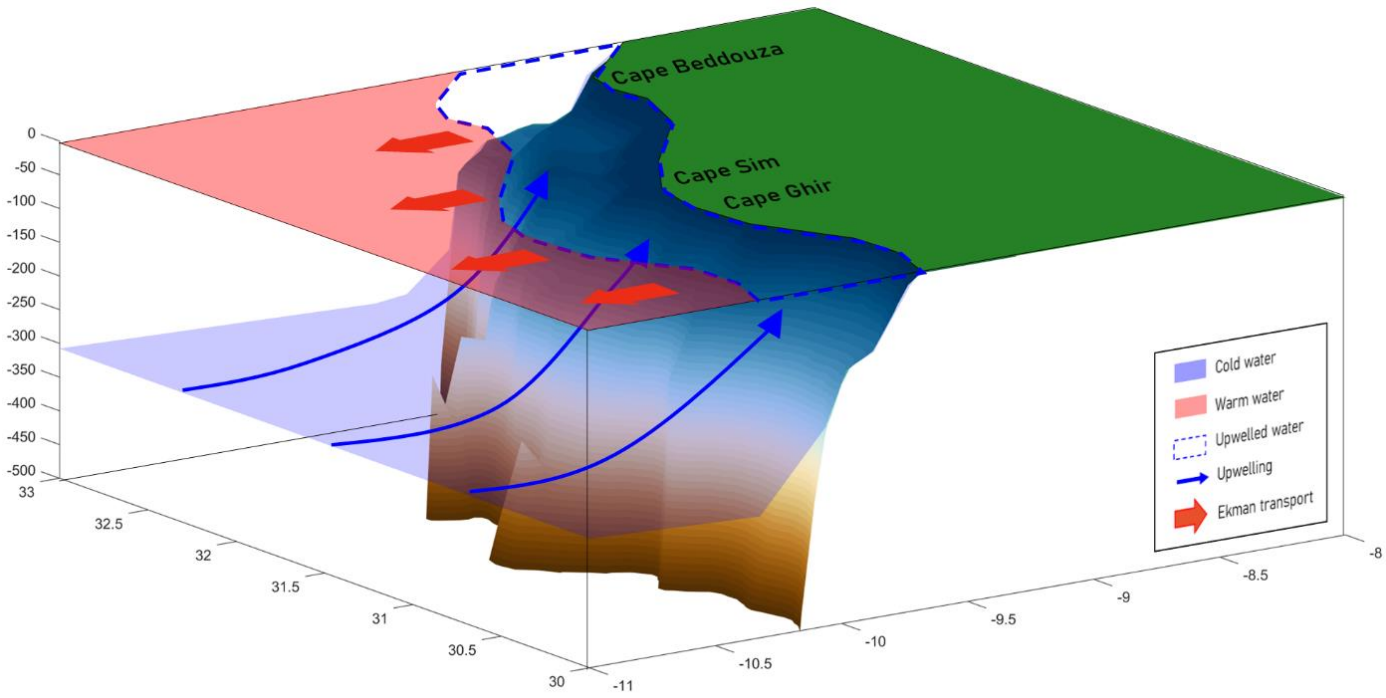

Fig 1.1 Coastal upwelling scheme. This coastal upwelling corresponds to the Canary current upwelling system, from 30ºN to 33ºN (weak permanent upwelling region).

- **Coastal upwelling**: Coastal upwelling (Fig. 1.1) is the process by which stable winds blow along the coasts of continents and, in conjunction with the earth's rotation, cause the surface waters to be pushed offshore. Water from the ocean depths is then upwelled to the surface to take its place.

- **Equatorial upwelling**: In the equatorial, the trade winds blow the North and South Equatorial Currents towards the west, while Ekman transport causes the upper layers to move to the north and south in their respective hemispheres. This creates a divergence zone, and a region of upwelling and high productivity.

- **Ice-edge upwelling**: In the Antarctic, the west wind drift (Antarctic Circumpolar Current) is flowing parallel to, but in the opposite direction of the east wind drift. As both currents flow in the Southern Hemisphere, the Ekman transport will result to the left, creating a divergence zone with high productivity

The opposite process to the upwelling is the downwelling, where Ekman transport moves surface waters toward the coast, the water piles up and sinks. Since surface water is usually low in nutrients, downwelling leads to low productivity zones. An example of a downwelling region is located off the Labrador coast in Canada, where the Gulf Stream, Labrador, and East Greenland Currents converge.

Therefore, coastal upwelling regions are associated with winds that linger during days and weeks. There are four large regions that present these conditions, forming the main LMEs at the world. These regions are called Eastern Boundary Upwelling Systems (EBUSs) and cover only the 2% of the ocean areas while representing the 20% of the fishery catches at the world (Pauly and Christesen, 1995).

1.3 Eastern Boundary Upwelling Systems

EBUSs are productive ocean areas, where cold waters upwell by the action of the alongshore favourable winds. These systems, located in the Pacific (California and Humboldt currents) and Atlantic (Canary and Benguela currents) oceans (Fig. 1.2), provide ecosystem, economic, and recreational services to about 80 million people living along their coasts and in their immediate hinterlands (García-Reyes et al. 2015). The alongshore favourable winds in the EBUSs result from large-scale atmospheric pressure systems that favour equatorward winds, transporting the surface water offshore. In these systems, the upwelled nutrient-rich water typically comes from relatively shallow depths of 100-200 m (Kampf and Chapman 2016). There are four large EBUSs: California current upwelling system, Humboldt current upwelling system, Canary current upwelling system and Benguela current upwelling system.

- **California current upwelling system**: The California upwelling system is found in the eastern limb of the North Pacific gyre along the western coastline of North America and stretches from the US-Canadian (48ºN) border to the tip of the Baja California Peninsula (23ºN; Kampf and Champman, 2016). This system experiences significant

natural variability mainly related to El Niño–Southern Oscillation (ENSO) and the Pacific Decadal Oscillation with important ecosystem consequences (García-Reyes et al. 2015).

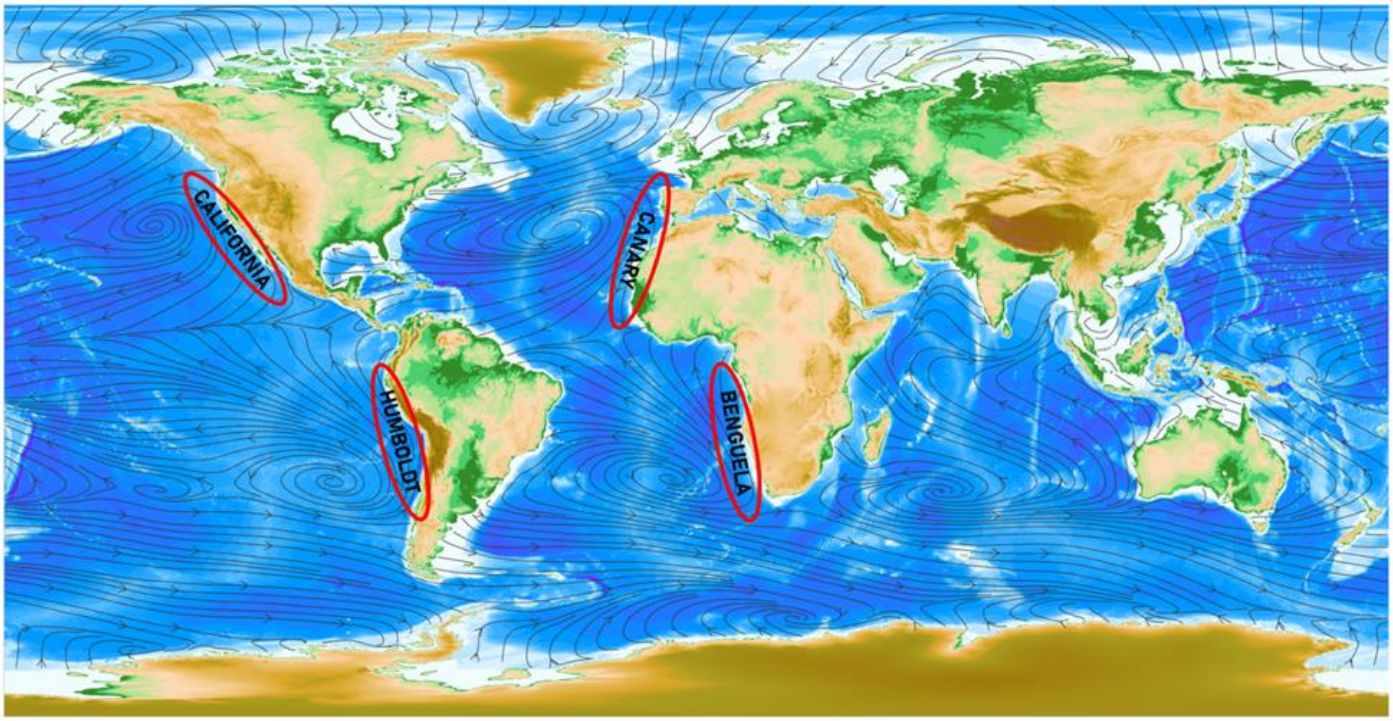

Fig 2.2 Global wind field from ERA5 reanalysis, showing the four large eastern boundary upwelling systems with its high pressure centres. The wind field is overlaying to the topography from ETOPO dataset.

- **Humboldt current upwelling system**: The Humboldt upwelling system is in the eastern South Pacific, extending along the west coast of South America from southern-central Chile up to Ecuador and the Galapagos islands. This system is highly influenced by ENSO and it is classified as a highly productive LME (Garcia-Reyes et al. 2015).

- **Benguela current upwelling system:** The Benguela upwelling system stretches along the southwest coast of Africa, from 15ºS in Angola to Cape Agulhas, the southern tip of the Africa continent close to 35ºS. It is largely influenced by the variability of the Agulhas current (Kampf and Chapman, 2016).

- **Canary current upwelling system:** The Canary Current is an eastern branch of the subtropical gyre in the North Atlantic ocean. This region is highly influenced by the intensity and position of the Azores high (Cropper et al. 2014), which generate different upwelling subregions that shape the Canary Current Upwelling System (CCUS).

This thesis is focused on the CCUS, which is specifically detailed in the next section as our study area.

1.4 Canary Current Upwelling System

The CCUS is one of the most important fishery grounds in the world (Aristegui et al. 2006), being the second most productive ocean region (Carr, 2001). The along-shore favourable winds are the northeasterly alongshore component of the Trade winds, associated with the Azores High pressure system, which shifts north-south between winter and summer (Wooster et al., 1976; Mittelstaedt, 1991; Van Camp et al., 1991; Nykjær and Van Camp, 1994). This fact generates a high latitudinal variability within the own CCUS, as well as a strong geographical diversity (e.g., Nykjær and Van Camp, 1994; Barton et al., 1998; Aristegui et al., 2009).

As a result and like previous studies (Arístegui et al. 2009; Pardo et al. 2011; Crooper et al. 2014), we can distinguish four regions well seasonally differentiated along the CCUS (Fig. 1.3): Iberian upwelling region (IUR), weak permanent upwelling region (WPUR), permanent upwelling region (PUR) and Mauritania-Senegalese upwelling region (MSUR).

The IUR is the northernmost region of the CCUS, from the northern tip of the Iberian Peninsula (43ºN) to the Strait of Gibraltar (33ºN), which is the major interruption in the continuity of the system (Kampf and Chapman, 2016). This sub-region is mainly characterized by downwelling favourable winds in winter and upwelling favourable winds in summer. The differences among seasons are related to the position and intensity of the Azores high (Fig. 1.3), being located close to the Iberian Peninsula in winter, which favours the downwelling processes specially in the northern region. In summer, the western displacement of the Azores high generates the upwelling favourable winds in practically the whole western Iberian coast.

Continuing southward, it is located the WPUR, from the Strait of Gibraltar to Cape Juby (around 26ºN). This sub-region presents year-round upwelling favourable winds, with increased intensity in summer. In this sub-region there are some geographical features, as Cape

Sim, Cape Ghir or Cape Juby, triggering mesoscale processes. The irregular topography of the capes produces substantial variability in the flow of the coastal currents, generating instabilities that give rise to these mesoscale processes (Barton et al., 1998; Capet et al., 2014). In this context, one of the most relevant characteristics of the EBUSs is the capacity to export part of the coastal high production to oligotrophic open areas through filaments and eddies.

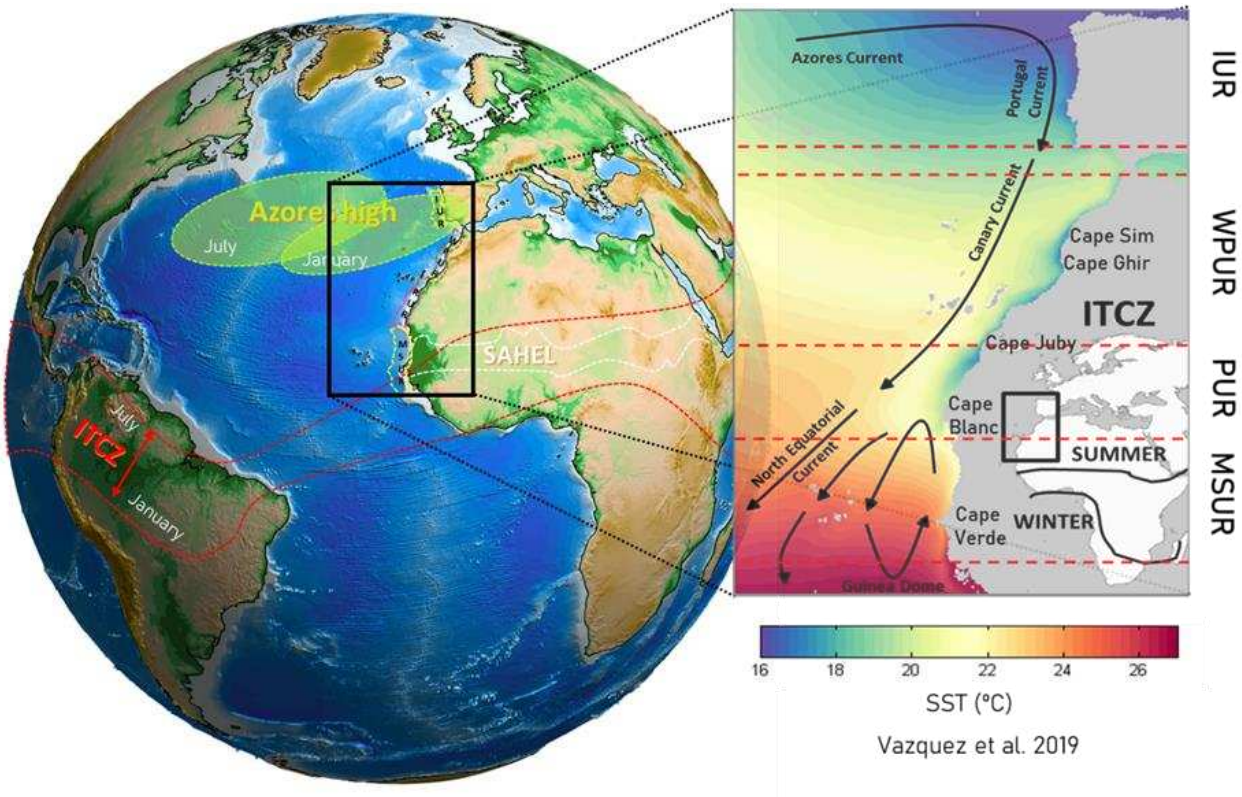

Fig 3.3 Seasonal Azores high and Intertropical convergence zone (ITCZ) behavior. The inset panel shows the sea surface temperature (°C) and a scheme of upper ocean circulation in the Canary current system. This figure has been modified from Vázquez et al. 2019, adding the different regions of the Canary current upwelling system.

as WPUR, PUR presents year-round upwelling favourable winds. However, in this sub-region the magnitude of the upwelling favourable winds is stronger than in the WPUR. Stronger upwelling is present in summer, associated with the trade-wind migration (Crooper et al. 2014). In this sub-region is located the largest filament known as “Giant Cape Blanc filament” (Pelegrí et al. 2005), which is a tongue of cold upwelled waters, spreading several hundreds of kilometers offshore (Gabric et al., 1993; Van Camp et al., 1991).

Finally, the southernmost region, the MSUR is influenced both by the position and intensity of the Azores high and the latitudinal migration of the Intertropical Convergence Zone (ITCZ) (Sylla et al. 2019). During the winter months, the strong northeastern equatorward trade winds cause upwelling in the coast of Guinea, Senegal and Mauritania (12ºN-19ºN), due to the southern position of the ITCZ. Nevertheless, the ITCZ migrates to the north in summer, weakening the winds in the whole region. Consequently, the coastal upwelling is reduced, even reversing to downwelling in the Senegalese region (Cropper et al. 2014), due to the appearance of the onshore monsoonal winds (Gomez-Letona et al 2017). Within MSUR we can identify two sub-regions mainly defined by the migration of the ITCZ (Pardo et al. 2011; Cropper et al. 2014; Benazzouz et al. 2015) and divided by Cap Vert (~15ºN), with year-round upwelling winds in the northern region and downwelling winds during the summer months in the southern region.

Therefore, the CCUS presents a large complexity, due to the high latitudinal and seasonal variability. Thus, it is the great importance to understand the mechanisms that could affect this vulnerable ecosystem under climate change.

1.5 Context and state of knowledge

The EBUSs are vulnerable to the impact of climate change with large regional variation (Blasiak et al. 2017) and sensitive to climate variability (Macias et al. 2012; Garcia-Reyes et al. 2015).

In the last decades many authors have explored the effects of climate change in the EBUSs due to their ecological and large socio-economic importance. In 1990, Bakun proposed that the increase in the ocean-land thermal gradient due to greenhouse warming would result in stronger alongshore winds, increasing the upwelling of the deeper water to the surface. Sydeman et al. (2014), through a meta-analysis of the existing literature on upwelling favourable wind intensification, revealed contradictory results between observational data and model-data reanalysis. Their results showed equivocal wind intensification in the Canary upwelling, in agreement with the analysis of Varela et al. (2015), which also highlighted the importance of a high-resolution wind database to properly resolve conditions at the coastal length-scale in intense and localized upwelling zones. However, significant trends of upwelling intensification are evident at the higher latitude for all EBUSs (Rykaczewski et al. 2015).

In consequence, Rykcazewski et al. (2015) proposed an alternative hypothesis: changes in the magnitude, timing or location of upwelling favourable winds could be associated with poleward migration and intensification of major atmospheric high-pressure cells in response to increased greenhouse gas concentrations. The upwelling systems might be more sensitive to this mechanism than to ocean-land thermal gradient increase as proposed Bakun (Garcia-Reyes et al. 2015).

However, along-shore winds are not the sole driver of climate change in the EBUSs. In the Humboldt current, Oyarzún and Brierley (2019) showed an increase of the ocean stratification as result of global warming, becoming the major mechanism of change in the 21st Century. Therefore, there are contradictory views regarding the future of EBUSs due to the opposite effects of intensifying winds and increasing vertical thermal stratification. Hence, it is needed to consider both mechanisms to project changes in coastal upwelling for the future.

Regarding the CCUS, Wang et al. (2015) found a strong correlation between the land-sea air temperature increase and the upwelling favourable winds in the northern regions of the CCUS, with 22 CMIP5 (Coupled Model Intercomparison Project) Global Climate models (GCMs). However, Rykaczewski et al. (2015) and Sousa et al. (2017) reported changes in the position and intensity of the Azores high, which affected the magnitude and timing of the alongshore favourable winds in the three northern regions of the CCUS. Sylla et al. (2019) with a CMIP5 ensemble model identified a weakening of the upwelling favourable winds in the MSUR, associated with changes both in the Azores high and the Sahara thermal low. However, the thermal vertical structure under climate changes in the CCUS are still uncertain and both stratification and wind changes may be complementary or competitive (Bonino et al. 2019).

The last report of the Intergovernmental Panel on Climate Change (IPCC) in 2019 (Bindoff et al., 2019) concluded that there is low confidence in projections regarding upwelling zones. The low confidence is due to the heterogeneity of the EBUS physical characteristics and the coarse resolution of the global climate models (GCMs) to represent the local processes in the upwelling systems (Garcia-Reyes et al., 2015). Although the models from CMIP6 and High Resolution Model Intercomparsion project (Haarsma et al., 2016) present an opportunity for nearshore analysis (Varela et al. 2022; Sylla et al. 2022), they still have a resolution coarser than 25 km. In fact, recent studies (García-Reyes et al. 2015; Wang et al. 2015; Sein et al. 2017; Gómez-Letona et al. 2017; Bindoff et al. 2019; Vázquez et al. 2022) showed the need for much

higher horizontal resolution for the representation of mesoscale processes in the upwelling systems that are partly masked in the current GCMs.

However, Regional Climate System Models (RCSMs), with higher horizontal resolution, will allow to represent smaller scale processes of the EBUSs that are partly masked in the GCMs (Sein et al. 2017; Xiu et al. 2018; Bindoff et al. 2019; Vázquez et al. 2022). Therefore, downscaling global models to the coastal domain of EBUSs is required to get an adequate representation of upwelling dynamics.

1.6 Hypothesis and Objectives

Our working hypothesis considers that the CCUS will experiment significant changes as consequence of global warming that will be detectable in physical variables, changes in circulation and as well as in the vertical structure of the water column. The use of the RCSMs will allow a substantial progress in the quantification and analysis of these parameters, contributing to improve the estimation of the climate change effects on the present and future climate.

Therefore, the general objective is to assess the changes of the future climate in the CCUS with the high-resolution regionally coupled atmosphere-ocean model ROM (abbreviated as ROM from REMO–OASIS–MPIOM; Sein et al., 2015). To reach the general objective, we propose the next specific objectives, which are organized in three chapters:

Chapter 3: The main goal of this chapter is to evaluate the ROM performance in a present time for the three northern regions of the CCUS, compared to different observational and reanalysis datasets. The subobjectives of this chapter can be summarized as follows:

- First, to validate the representation of the inter-annual variability and the seasonal cycle of the three northern regions of the CCUS with a Regional Climate System Model (RCSM).
- Second, to compare the performance of our regionally coupled model with regional climate models (RCMs) and GCMs to highlight the advantages and disadvantages of the AORCMs in reproducing the CCUS dynamics.

Chapter 4: The main objective of this chapter is to assess the future impact of climate change on the three northern regions of the CCUS with a RCSM. For this, we propose two sub-objectives:

- First, to understand the impact of climate change in the wind field, identifying the main driver of changes in the alongshore winds for the future.
- Second, to assess the impact on the coastal upwelling of the ocean stratification changes due to global warming.

Chapter 5: This chapter aims to analyze the evolution of the Mauritania-Senegalese upwelling region under the RCP8.5 scenario. For this we propose two sub-objectives:

- First, to validate the representation of the main variables in the MSUR.
- Second, to assess the projected climate change signal in the MSUR under the RCP8.5 scenario.

CHAPTER 2:

Methodology

2.1 ROM configuration

In this thesis we will work with the regional climate system model (RCSM) ROM (REMO-OASIS-MPIOM; Sein et al. 2015). ROM (Sein et al., 2015) comprises the regional atmosphere model (REMO; Jacob et al., 2001), the Max Planck Institute Ocean Model (MPIOM; Marsland et al., 2003; Jungclaus et al., 2013), the Hamburg Ocean Carbon Cycle (HAMOCC) model (Maier-Reimer et al., 2005), the hydrological discharge (HD) model (Hagemann and Gates, 1998, 2001), the soil model of REMO (Rechid and Jacob, 2006) and a dynamic thermodynamic sea ice model (Hibler, 1979), which are coupled via the OASIS3 (Valcke, 2013) coupler and abbreviated as ROM from REMO–OASIS–MPIOM.

Atmospheric model (REMO)

The atmospheric component of ROM is the REgional atmosphere MOdel (REMO) (e.g., Jacob, 2001). The dynamical core of the model as well as the discretization in space and time are based on the Europa-Model of the German Weather service (Majewski, 1991). The physical parameterizations are taken from the global climate model ECHAM versions 4 and 5 (Roeckner et al., 1996, 2003). To avoid the largely different extensions of the grid cells close to the poles, REMO uses a rotated grid, with the equator of the rotated system in the middle of the model domain with a constant resolution of 25 km (Sein et al. 2015), extending its domain to the North Atlantic, the eastern tropical Pacific and the Mediterranean Sea regions, including the whole CCUS region (Fig. 3.1b).

Oceanic model (MPIOM)

The oceanic component of ROM is MPIOM, a global oceanic model developed at the Max Planck Institute for Meteorology (Hamburg, Germany). MPIOM is a free surface, primitive equations ocean model, which uses the Boussinesq and incompressibility approximations. MPIOM is formulated on an orthogonal curvilinear Arakawa C-grid (Arakawa and Lamb, 1977) with variable spatial resolution. The MPIOM configuration used for all experiments features the grid poles over North America and Northwestern Africa. The horizontal resolution ranges from 5 km (close to the NW African coast) to 100 km in the southern oceans. This feature allows a local high resolution in the region of interest allowing the study of local-scale processes while maintaining a global domain (e.g. Izquierdo and Mikolajewicz, 2019). The model has 40 vertical levels with increasing level thickness towards the ocean bottom (Sein et al. 2015; Parras-Berrocal et al. 2020).

REMO-OASIS-MPIOM

In the region covered by REMO, the atmosphere and the ocean interact while the rest of the global ocean is driven by energy fluxes, momentum and mass from global atmospheric data used as external

forcing. In the experiments analyzed in this thesis, data from ERA-Interim reanalysis (Dee et al., 2011) and MPI-ESM-LR (low resolution) (Giorgetta et al., 2013) are used to provide lateral boundary conditions to REMO and to force MPIOM outside the coupling region. The spin-up of MPIOM was done according to the procedure described in Sein et al. (2015). MPIOM is started with climatological temperature and salinity data (Levitus et al. 1998). Subsequently, it is integrated six times through the 1958–2002 period forced by ERA-40 and one time by ERA-Interim reanalysis (1979–2012) and with 60 min of the coupling frequency.

Therefore, we use two configurations of ROM to analyze the CCUS: (i) ROM forced by ERA-Interim. (ii) ROM forced by MPI-ESM-LR.

- **ROM forced by ERA-Interim (ROM_P0):** In chapter 3 and chapter 5, we use this configuration to validate the ROM performance to reproduce the present time against different datasets in the CCUS.

- **ROM forced by MPI-ESM-LR:** In the chapter 4 and the second part of the chapter 5, we use this configuration to evaluate the effects of the climate change in the CCUS. In these cases, ROM presents two simulations, first a historical time as control period (1950-2005; ROM_P1) and second from 2006 to 2099 under Representative Concentration Pathway 8.5 (RCP 8.5) CMIP5 scenario (ROM_P2).

The Coupled Model Intercomparison Project Phase 5 (CMIP5) projections have as objective to improve the knowledge about the past, present and future climate change in a multi-model context and for this, it makes use of Representative Concentration Pathways (RCPs), which are designed to provide plausible future scenarios of anthropogenic forcing spanning a range from a low emission scenario characterized by active mitigation (RCP 2.6), through two intermediate scenarios (RCP 4.5 and RCP6.0), to a high emission scenario (RCP 8.5). Each RCP is associated with plausible combinations of projected population growth, economic activity, energy intensity, and socio-economic development. The RCP scenarios were named based on their total radiative forcing by (or post) 2100.

2.2 Datasets: Observational data, reanalysis and climate models

In order to know the behaviour of the climate system, it is necessary to obtain information about it through measurements and observations, remote monitoring systems (satellite or radars), allowing the development of models that are very useful for the study of climate and its evolution. As, for example, reanalysis (regular gridded observational and modelled data)

and modelled data (numerical climate models). In this work we use different datasets, to evaluate, compare and force the ROM model.

Observational data: Observations are key elements to deepen our knowledge of the ocean and the atmosphere, as well as for climate research. They are essential for climate change assessment, the development of policy responses, the development of climate services or testing climate and weather forecasting models. To evaluate the ROM model in the chapter three, we use four observational data: OISST, ESA, WOD18 and Aqua MODIS.

- The daily Optimum Interpolation Sea Surface Temperature (OISST) is a SST dataset that incorporates observations from different platforms (satellites, ships, buoys and Argo floats) into a regular global grid with a horizontal resolution of 0.25º (Reynolds et al. 2007).

- The European Space Agency (ESA) SST dataset provides a globally-complete daily analysis of sea surface temperature (SST) on a 0.05º lon-lat grid. It combines data from both the Advanced Very High Resolution Radiometer (AVHRR) and Along Track Scanning Radiometer (ATSR) Climate Data Records, using a data assimilation method to provide SST where there were no measurements. This dataset is part of the climate change initiative sea surface temperature project (Merchant et al. 2019).

- The World Ocean Database (WOD) is a powerful dataset for oceanographic, climatic, and environmental research, that presents the world's largest collection of uniformly formatted, quality controlled, publicly available ocean profile data (Boyer et al. 2019).

- Aqua MODIS (or Moderate Resolution Imaging Spectroradiometer) is a key instrument a board Aqua satellite. Aqua MODIS views the entire Earth's surface every 2 days, acquiring data in 36 spectral bands. These data improve our understanding of global dynamics and processes occurring in the oceans. MODIS plays a vital role in the development of validated, global, interactive Earth system models able to predict global change accurately enough to assist policy makers in making sound decisions concerning the protection of our environment (Hall and Riggs 2007).

Reanalysis: The retrospective analysis or reanalysis are climate datasets that describe the recent history of the atmosphere, land surface and the oceans. An advantage of reanalysis is that it offers long time series of multiple climate variables in a regular grid. However, limitations arise due to observational constraints that introduce false variability and trends (Geralo et al. 2017), varying depending on the location, time period and variable considered. In the work we have used three reanalyses: ERA5, SODA and GLORYS.

- Within the marine Copernicus services, the European Centre for Medium-Range Weather Forecasts has developed the ERA5 reanalysis, which provides hourly estimates of a large number of atmospheric, land and oceanic climate variables, covering the Earth on a 30 km grid. ERA5 combines vast amounts of historical observations into global estimates using advanced modelling and data assimilation systems and has a temporal cover from 1950 to present (Hersbach et al. 2020).

- Simple Ocean Data Assimilation (SODA) is an ocean reanalysis dataset consisting of gridded variables for the global ocean, as well as several derived fields. SODA used an atmospheric forcing from the NOAA Twentieth Century Reanalysis version 2. The goal is to provide an improved estimate of ocean state from those based solely on observations or numerical simulations. SODA covers from 1980 to the present time (Carton et al. 2018).

- GLORYS (GLobal Ocean ReanalYsis and Simulation) is implemented in the framework of the Copernicus Marine Environment Monitoring Services (CMEMS), that produces and distributes global ocean reanalysis at eddy-permitting (1/4°) resolution that aim to describe the mean and time-varying state of the ocean circulation with a focus on the period from 1993 to present (Drèvillon et al. 2018).

Climate models: Climate models represent the evolution of climatic variables by solving the conservation equations of dynamics and thermodynamics that govern the atmosphere, ocean, and the land surface processes (Flato et al. 2014). There are different types of climate models, depending on the domain covered.

The global climate models (GCMs) are a fundamental tool in the study of climate, being a complex mathematical representation of the major climate system components (atmosphere,

land surface, ocean, and sea ice), and their interactions. These models allow to evaluate the global climate from a general view, but its coarser resolution is not able to resolve some of the processes of smaller scales (e.g. Xiu et al. 2018; Vázquez et al. 2022).

We compare the ROM model outputs with those from an ensemble of four Global Climate Models from the CMIP5 project. Moreover, along with these GCMs, we compared our model with the Max-Plank Institute-Earth System Model (MPI-ESM; Giorgetta et al. 2013). MPI-ESM consists in a global coupled model, with the same ocean component (MPIOM) of ROM. Moreover, MPI-ESM presents the atmosphere model ECHAM6 (Stevens et al., 2013). MPI-ESM has been used in different configurations for Coupled Model Intercomparison Project phase 5 (CMIP5) in a series of climate change experiments. In the thesis we use two MPI-ESM configurations: The low resolution (LR) configuration uses for the ocean a bipolar grid with 1.5° resolution and the medium resolution (MR) decreases the horizontal grid spacing of the ocean to 0.4° with a tripolar grid, two poles localized in Siberia and Canada and a third pole at the South Pole. MPI-ESM-LR was used not only to compare ROM model, but also as external forcing and driver in the historical and RCP8.5 simulations.

Regional Climate Models (RCMs) are numerical climate prediction models that simulate atmospheric and land surface processes, while accounting for high-resolution topographical data, land-sea contrasts, surface characteristics, and other components of the Earth-system within a limited domain with the goal to simulate the climate variability with regional refinements. RCMs need lateral and ocean conditions from a GCMs or reanalysis. RCMs allow a more detailed study and simulation of regional and local conditions (Laprise et al. 2008; Rummukainen, 2010; Giorgi, 2019). In this context born the Coordinated Regional Climate Downscaling Experiment (CORDEX; Giorgi et al. 2009), with the objective to advance and coordinate the science and application of regional climate downscaling through global partnerships. The coordination focuses on different regions worldwide, including Africa in the specific AFRICA-CORDEX part of the project. Two ensemble mean from AFRICA-CORDEX were used for the evaluation of ROM. First, using seven atmosphere models with a horizontal resolution of 0.44º and second three atmosphere models with an increased horizontal resolution (0.22º). These AFRICA-CORDEX models were collected with the external forcing from ERA-Interim.

2.3 GCMs, RCMs and RCSMs

Numerical models are very powerful tools to evaluate the complex mechanisms associated with the climate and environmental sciences. Thus, the development of GCMs include coupled representations of the ocean, atmosphere, land use, vegetation, biogeochemistry, atmospheric chemistry, and the hydrological cycle (Taylor et al. 2012). GCMs can be used to simulate both the longer-term evolution of the Earth's climate on decadal and longer time, as the short and medium-range weather forecasts and seasonal predictions (Sein et al. 2015). However, GCMs are not able to capture some physical phenomena due to a low horizontal resolution, thus hampering the accuracy of climate projections on regional and local scales (Marotzke et al., 2016; Xie et al., 2015), especially in the north Atlantic ocean (Sein et al. 2020).

The regional climate models (RCMs) is a good opportunity to improve the low resolution of current GCMs. RCMs take the initial conditions, lateral conditions, and surface boundary conditions from GCMs and provide dynamically downscaled climate information within the region of interest with a higher resolution than GCMs. Additionally, they allow a better understanding of various aspects of air-sea interaction processes important for the climate. However, in the literature there is various views on the added value of the RCMs to determinate the regional responses to climate change, since often, GCMs reproduce well the larger-scale mechanisms and the spatial extension of these phenomena and patterns is in most cases larger than the domain size of most RCMs (Sein et al. 2015).

To date, most RCMs are composed of only atmospheric component coupled to a land surface scheme and driven over ocean areas by prescribed sea surface temperature (SST) and sea ice cover (Sein et al. 2015). However, there are cases where the RCMs are not sufficient due to the lack of atmosphere-ocean feedbacks, which can substantially influence the spatial and temporal structure of regional climate (Li et al., 2012). Recent studies have shown that Regional Climate System Models (RCSMs) are capable of simulating these features of the climate system (Soares et al. 2019; Parras-Berrocal et al. 2020; de la Vara et al. 2021). Compared to GCMs, RCSMs can achieve much higher resolution and detailed parameterizations, providing a more accurate representation of the relevant small-scale processes (Sein et al. 2020) and compared to RCMs, the interaction between the ocean and atmosphere in RCMSs also give a more realistic representation of the physic mechanisms than in atmosphere and ocean only regional models (Sein et al. 2015). In this thesis, we use the RCSM, ROM, which introduces the novel approach of implementing a global ocean model with high horizontal resolution at regional scales. This

allows us to obtain information of the global ocean maintaining the high spatial resolution in the coupling area.

CHAPTER 3:

Assessment of the Canary Current Upwelling System in a regionally coupled climate model

The contents of this chapter have been published in:

Vázquez, R., Parras-Berrocal, I., Cabos, W., Sein, DV., Mañanes, R. and Izquierdo, A. (2022) Assessment of the Canary current upwelling system in a regionally coupled climate model. Clim Dyn 58, 69–85. https://doi.org/10.1007/s00382-021-05890-x

3.1 Introduction

The Eastern Boundary Upwelling Systems (EBUSs) are among the major fishery grounds in the world, contributing more than 20% to global fish catches, while covering only 2% of the global ocean surface (Pauly and Christesen 1995). Coastal upwelling systems are generated by the action of the equatorward along-shore winds, which transport coastal surface water offshore, causing the upwelling of the cold and nutrient-rich deep waters by Ekman dynamics. These systems have a large ecological and economic importance (Garcia-Reyes et al. 2015; Varela et al. 2015), hence knowing the response of coastal upwelling to changing climate is of uttermost importance. There are four EBUSs: Canary Current Upwelling System (CCUS), Benguela Current Upwelling System, Humboldt Current Upwelling System and California Current Upwelling System.

In the EBUSs, the large-scale pressure gradients between are the main drivers of upwelling favourable winds (Bakun 1990; Garcia-Reyes et al. 2015). Bakun (1990) hypothesized that the strengthening of the ocean-land thermal gradient under the greenhouse warming would result in stronger alongshore winds, increasing the upwelling of the deeper water to the surface during the second half of the 20th Century. This hypothesis was supported by Wang et al. (2015), who found a robust relationship between the increase of the land-sea temperature differences and the upwelling intensity in the 21st Century.

However, Ryckazewski et al. (2015) proposed an alternative hypothesis: changes in the magnitude, timing or location of upwelling winds could be associated with poleward migration and intensification of major atmospheric high-pressure cells in response to increased greenhouse gas concentrations. The upwelling systems may be more sensitive to this mechanism than to the increase of the ocean-land thermal gradient (Garcia-Reyes et al. 2015).

Nevertheless, along-shore winds are not the sole driver of change in the EBUSs. Coastal surface warming may increase the water stratification, reducing the upward nutrient-rich transport to surface (Di Lorenzo et al. 2005; Garcia-Reyes et al. 2015; Brady et al. 2019). For instance, Oyarzún and Brierley (2018) showed that the increase of the ocean stratification, as result of global warming, becomes the major mechanism of change during the 21st Century in the Humboldt Current system. Therefore, the EBUS future behavior is still uncertain and both stratification and wind changes may be complementary or competitive (Bonino et al. 2019).

In this study we focus on the CCUS, which is part of the North Atlantic subtropical gyre, extending from the northern tip of the Iberian Peninsula at 43°N to the south of Senegal at about 10°N (Fig. 3.1a). The coastal upwelling region between Cape Blanc and the Strait of Gibraltar is a year-round phenomenon that becomes stronger to the south of Cape Bojador (Cropper et al. 2014). In the western coast of the Iberian Peninsula (37º-43ºN) there is a marked seasonality with along-shore upwelling favorable winds dominating during spring and summer months (Sousa et al. 2017a, Wooster et al. 1976). The Strait of Gibraltar divides both regions, representing a major discontinuity of the upwelling system due to an abrupt change in the coastline orientation in the Gulf of Cádiz (Kämpf and Chapman 2016).

The resolution of the Global Climate Models (GCMs) is insufficient to reproduce mesoscale features or detailed coastal dynamics (Xiu et al. 2018). In fact, recent studies (Garcia-Reyes et al. 2015; Wang et al. 2015; Sein et al, 2017; Gómez-Letona et al. 2017; Bindoff et al. 2019) stressed the need for much higher horizontal resolution for the explicit representation of mesoscale processes that are important for a correct simulation of the upwelling systems but are partly masked in the current GCMs. Regional climate system models (RCSMs) are able to provide a resolution that allows an explicit representation of these processes and represent a valuable tool for their study.

In this work we use a high-resolution atmosphere-ocean regional coupled model for the study of the CCUS. The main goals of the paper can be summarized as follows:

- First, validating the representation of the inter-annual variability and the seasonal cycle of the CCUS.
- Second, comparing the outputs of regionally coupled model with regional climate models (RCMs) and GCMs to highlight the advantages and disadvantages of the RCSMs in reproducing the CCUS dynamics.

3.2 Data and Methods

ROM (REMO-OASIS-MPIOM; Mikolajewicz et al. 2005; Sein et al. 2015; Sein et al. 2020) is an atmosphere-ocean regional climate model in which the limited area atmospheric model REMO (REgional MOdel; Jacob et al. 2001) is coupled to the global ocean model MPIOM (Max Plank Institute-Ocean Model; Marsland et al. 2003; Jungclaus et al. 2013). These

components are coupled via the OASIS3.0 (Valcke 2013) coupler. ROM also simulates globally the lateral freshwater fluxes at the land surface through the Hydrological Discharge (HD, Hagemann and Gates 1998, 2001) model, which is run as part of REMO. Furthermore, the relevant carbon stocks of the atmosphere, the ocean and the sediments are included through the Hamburg Ocean Carbon Cycle (HAMOCC; Maier-Reimer et al. 2005), which is a MPIOM subsystem (Soares et al. 2018, 2019; Parras-Berrocal et al. 2020).

3.2.1 ROM configuration

The atmospheric component of ROM, REMO, is the only model component that is run in a regional configuration. The REMO domain (Fig. 3.1b) extends to the North Atlantic, the eastern tropical Pacific and the Mediterranean Sea regions, including the whole CCUS region, and has a constant horizontal resolution of 25 km with a rotated grid (Parras-Berrocal et al. 2020).

MPIOM is discretized on a curvilinear grid with variable spatial resolution ranging from 5 km at the West African coast to 100 km in the Southern oceans. In the area of study, the MPIOM resolution is not coarser than 10 km. The MPIOM horizontal resolution in CCUS is sufficiently high to allow for the study of local scale processes in the region while maintaining a global domain with an acceptable computing cost. A similar MPIOM configuration was successfully applied in a process study of the Mediterranean Outflow Waters (Izquierdo and Mikolajewicz, 2019). The model has 40 vertical levels with increasing level thickness towards the ocean bottom (Sein et al. 2015; Parras-Berrocal et al. 2020). The spin-up of MPIOM was done according to the procedure described in Sein et al. (2015). MPIOM is started with climatological temperature and salinity data (Levitus et al. 1998). Subsequently, it is integrated six times through the 1958–2002 period forced by ERA-40 and one time by ERA-Interim reanalysis (1979– 2012) and with 60 min of the coupling frequency.

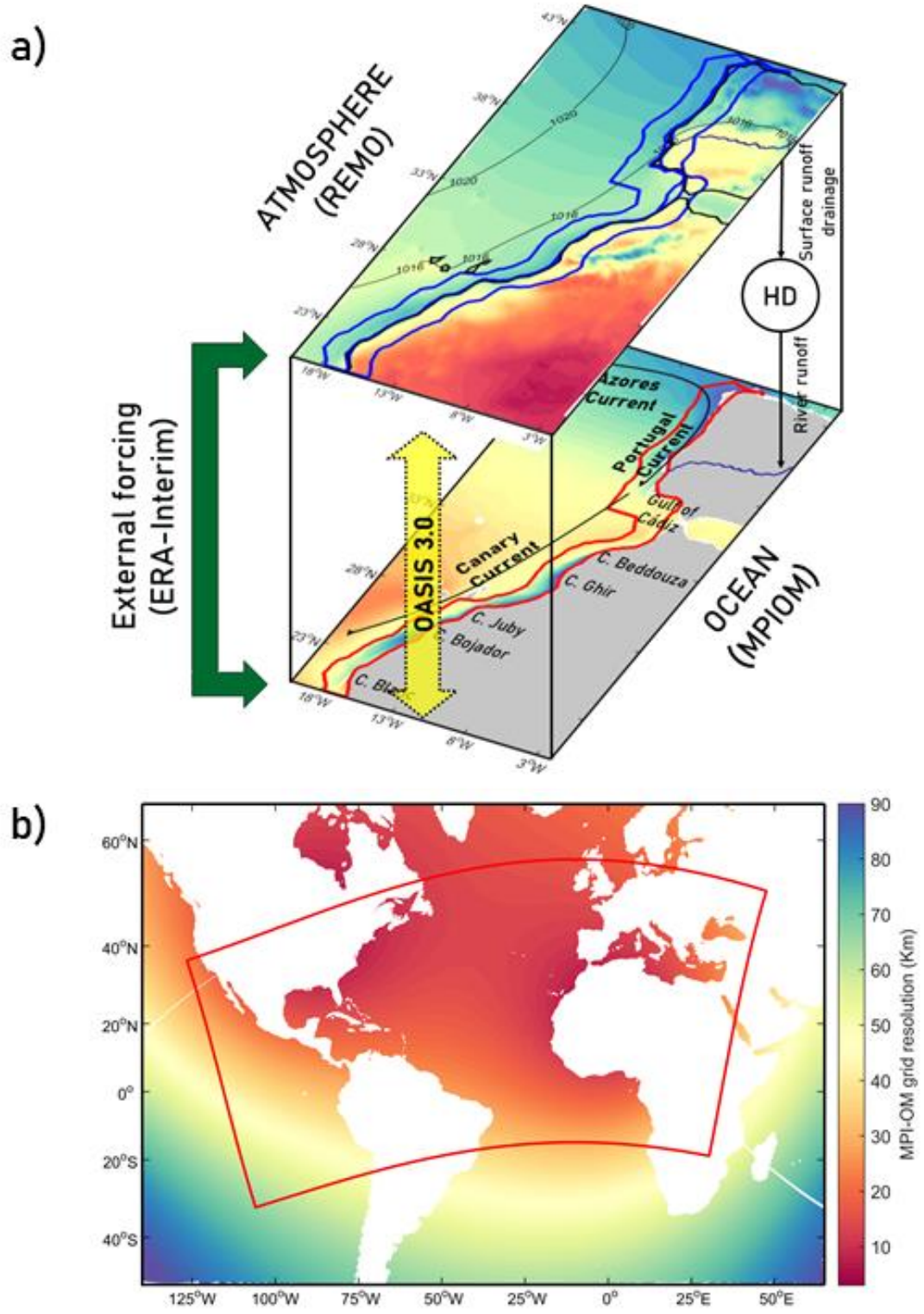

Fig. 3.1 a) ROM coupling scheme, with sea surface temperature (SST) and 2 m air temperature (T2m). The masks used in SST section (red lines) and to calculate the $T2m_{land\text{-}sea}$ differences (blue lines) are overlaid. b) MPIOM grid resolution and REMO domain for ROM (red boundary).

In this work, we assess the ROM performance in the CCUS using a simulation forced by ERA-Interim (ROM_P0; Dee et al. 2011). ERA-Interim provides lateral boundary conditions to REMO and surface forcing to MPIOM outside the coupling region. Both models are hydrostatic and solve the Navier–Stokes equations using the Boussinesq approximation, In this run HAMOCC was disabled.

3.2.2 Assessment strategy and data sets

The model outputs were assessed in terms of seasonal cycle and inter-annual variability, focusing on the larger scale processes, the latitudinal variability and the mesoscale dynamics that characterizes the CCUS. For the validation, we use daily and monthly data of the most representative atmosphere and ocean variables: Near-surface air temperature (T2m), sea surface temperature (SST), wind stress and ocean temperature. This validation is carried out against several observational and reanalysis data sets (Table 1). Additionally, we use the Max Plank Institute - Earth System Model (MPI-ESM), seven RCMs from AFRICA-CORDEX (Table 2) and four GCMs from CMIP5 (Table 3) to assess ROM_P0 performance. The validation strategy addressed:

- **Larger scale:** The CCUS climate at the larger scale was evaluated by means of OISSTv2 (SST) and ERA5 (wind stress) data. The NOAA 1/4° daily OISST (Reynolds et al. 2007) is an analysis constructed by combining observations from different platforms (satellites, ships, buoys, and Argo floats) on a regular global grid. ERA5 (Copernicus Climate Change Services 2017) is a product of the European Centre for Medium Range Weather Forecast (ECMWF) and covers the Earth on a 30 km grid and resolves the atmosphere on 137 levels from the surface up to a height of 80 km. We also used the European Space Agency (ESA) SST Climate Change Initiative (CCI) and C3S global Sea Surface Temperature Reprocessed product (Good et al. 2019), which provides daily averaged SST with a resolution of 5 km (Merchant et al. 2019).

- **Latitudinal variability:** Between the four major EBUSs, the CCUS stands out as the most spatially and seasonally variable one in terms of primary production (Sylla et al. 2019). Based on the seasonality, there are different arguments to divide the CCUS in

sub-regions but without a broad consensus (Aristegui et al. 2009; Pardo et al. 2011; Crooper et al. 2014; Gomez-Letona et al. 2017; Fischer et al. 2019). Here we will focus on the seasonal and latitudinal variability of T2m, wind and SST over the coastal band, allowing an integrated view of the coastal upwelling. The local wind was assessed using an upwelling index (*UI*) based on the offshore wind-driven Ekman transport (*Q*). The UI proposed by Bakun (1973) was calculated following the approach used by Gomez-Gesteira et al. (2006), Crooper et al. (2014) and Sousa et al. (2017a, 2017b):

$$Q_x = \frac{\tau_y}{f\rho_0} \quad \text{Eq. 3.1}$$

$$Q_y = -\frac{\tau_x}{f\rho_0} \quad \text{Eq. 3.2}$$

$$UI = -sin\left(\theta - \frac{\pi}{2}\right) Q_x + cos\left(\theta - \frac{\pi}{2}\right) Q_y \quad \text{Eq. 3.3}$$

where Q_x, Q_y and τ_x, τ_y are the zonal and meridional components of the horizontal Ekman transport and the wind stress vector, respectively; ρ_0 is the reference sea water density (1025 kg m^{-3}); f is the Coriolis parameter and θ is the angle between the coastline and the equator.

- **Thermal vertical structure:** The cross-shelf thermal vertical structure is relevant for the characterization of the coastal upwelling intensity. The vertical structure of the ocean temperature was assessed through SODA (Carton et al. 2018) and GLORYS12V1 (Drèvillon et al. 2018) gridded products and WOD18 (Boyer at al., 2019) in situ data. SODA3.4.1 is the latest version of SODA with 1/4º x 1/4º resolution in 50 vertical levels. The GLORYS12V1 product is the Copernicus Marine Environment Monitoring Service (CMEMS) global ocean eddy-resolving reanalysis with observations assimilated from along track altimeter data, satellite sea surface temperature, sea ice concentration and in situ temperature and salinity vertical profiles. The WOD18 includes in situ measurements of temperature, salinity, dissolved oxygen and nutrients from 1773 to the present. For the evaluation we used a cross-shelf transect along 31ºN (Cape Ghir), a region where the spatial resolution could play a role due to the bathymetry features and coastline.

- **Mesoscale events:** Coastal upwelling filaments are mesoscale structures with a great importance in the transport of organic carbon and nutrient-rich upwelled waters several hundred kilometers offshore and have typical lifetime of a few weeks (Menna et al. 2016), fueling the biological activity of the oligotrophic open waters (Lovecchio et al. 2018). We use two high resolution datasets able to detect the filaments: MODIS Aqua (Hall and Riggs 2007) and GLORYS12V1 (Drèvillon et al. 2018). The Moderate Resolution Imaging Spectroradiometer (MODIS) is a key instrument aboard Aqua satellite, which views the entire Earth's surface every 2 days, acquiring data in 36 spectral bands (Hall and Riggs 2007).

Table 1. Observational and reanalysis data products selected to assess ROM_P0 performance in the CCUS

Dataset	Period	Spatial resolution	Reference
ERA5	1980-2012	31 km	Copernicus Climate Change Services (2017)
OISST	1982-2012	0.25º x 0.25º	Reynolds et al. (2007)
SODA	1980-2012	0.5º x 0.5º	Carton et al. (2018)
WOD18	1980-2012	Not gridded	Boyer et al. (2019)
ESA	1981-2012	5km	Merchant et al. (2019)
MODIS	2002 to present	0.05º x 0.05º	Hall and Riggs (2007)
GLORYS	1993-2012	0.083º x 0.083º	Drèvillon et al. (2018)

3.2.3 Model Intercomparison

We use the Max Plank Institute for Meteorology – Earth System Model (MPI-ESM; Giorgetta et al. 2013) in order to assess the impact of the high resolution of ROM, particularly regarding mesoscale dynamics. MPI-ESM has the same ocean component (MPIOM) than ROM. Here we use the two versions of MPI-ESM contributing to CMIP5. The first, Low Resolution (-LR) uses for the ocean a bipolar grid with 1.5º resolution. The Medium Resolution (-MR) has a tripolar grid with higher ocean horizontal resolution of 0.4º (Giorgetta et al. 2013).

Additionally, we compare ROM output to the ensemble mean of several Regional Climate Models (RCMs) from the AFRICA-CORDEX, with boundary conditions forced by ERA-

Interim. We should note that in AFRICA-CORDEX the available simulations are atmosphere-only and the horizontal resolution available was 0.44º. Following Sousa et al. (2017b), we chose seven RCMs in the study (Table 2).

Table 2. AFRICA-CORDEX simulations used to compare ROM with RCMs

Model	Period	Description
RCA4	1980-2010	Rossby Centre regional atmospheric model (Samuelsson et al. 2015)
RACMO22T	1980-2012	Regional atmospheric Climate model version 2.2 (van Meijgaar et al. 2008)
CRCM5	1980-2012	Canadian Regional Climate Model Fifth generation (Takhsha et al. 2016)
CCLM4-8-17	1989-2008	Climate Limited-Area Modelling Community (Rockel et al. 2008)
REMO2009	1989-2008	Atmospheric Regional Model (Jacob et al. 2001)
HadRM3P	1990-2011	Met Office Hadley Centre Regional climate model version 3 (Jones et al. 2004)
HIRHAM5	1989-2010	High resolution Limited Area Model (HIRLAM) + General circulation models for the atmosphere (ECHAM); (Christensen et al. 2006)

Finally, also following Sousa et al. (2017a), ROM is compared with an ensemble of four Global Climate Models (GCMs) from the CMIP5 project (Table 3).

Table 3. CMIP5 simulations used to compare ROM with GCMs

Model	Spatial resolution	Description
CNRM-CM5	1.4º x 1.4º	Centre National de Recherches Météorologiques Coupled Global Climate Model, version 5 (Voldoire et al. 2013)
EC-EARTH	1.12º x 1.125º	The numerical wather prediction (NWP) system of the European Centre for Medium-Range Weather Forecasts (ECMWF) forms the basis for EC-Earth (Hazeleger et al. 2010)
IPSL-CM5A-MR	1.25º x 2.5º	Institut Pierre Simon Laplace – Climate Modellling Centre Earth System Model version 5 (Dufresne et al. 2013)
HadGEM2-ES	1.25º x 1.875º	Second version of Hadley Centre Global Environmental Model version 2 Earth System configuration (Jones et al. 2011)

3.3 Results

3.3.1 Larger scale

In this section we assess the larger scale climate of the CCUS through the SST, the wind stress and the T2m from the Iberian Peninsula to Cape Blanc. Besides the coastal area, we also analyze an extensive offshore area that contains the CCUS (see the area of study in Fig. 3.2).

The mean SST field in the CCUS for the 1982-2012 period presents a year-round meridional gradient and a colder patch by the NW African and Iberian coasts because of the upwelled waters (Fig. 3.1a). For the evaluation of SST, we compare the output of ROM_P0 with OISST, MPI-ESM-LR, MPI-ESM-MR and CMIP5 for the 1982-2012 period (Fig. 3.2). In DJF, ROM provides a good agreement with OISST, displaying biases smaller than 1.0ºC over most of domain except for the northwest region, where the differences reach 2.5 ºC (Fig. 3.2a). MPI-ESM-LR and MPI-ESM-MR present biases up to 2.0 ºC with larger differences at local regions such as Cape Bojador and Cape Blanc (Figs. 3.2b and 3.2c). CMIP5 ensemble mean shows an overall cold bias with a maximum in the Gulf of Cádiz (Fig. 3.2d).

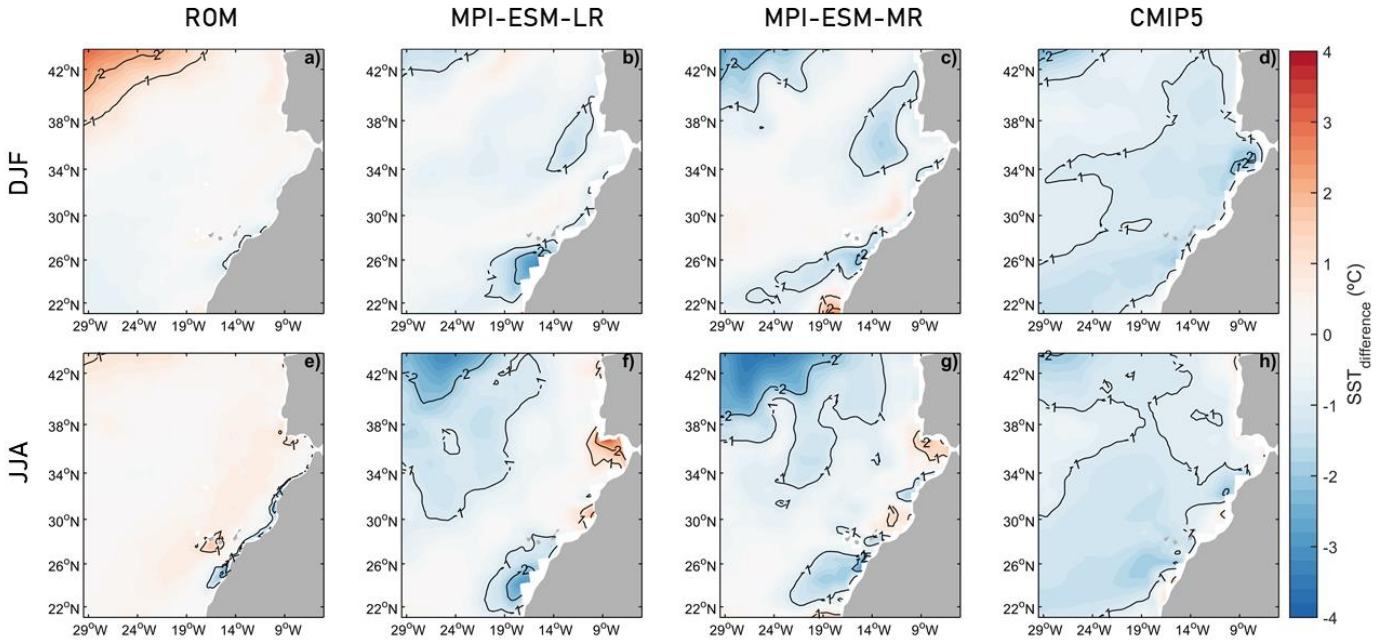

Fig. 3.2. SST biases (ºC) in DJF (upper row) and in JJA (lower row) between ROM (a, e), MPI-ESM-LR (b, f), MPI-ESM-MR (c, g) and CMIP5 (d, h) with OISST.

In JJA, the cooling of coastal surface waters evidences the intensification of the upwelling system. This mechanism seems to be magnified by ROM_P0, which despite of having small differences with OISST throughout the domain presents a cold bias of 2.0 ºC in the coastal strip between 24ºN and 34ºN (Fig. 3.2e), corresponding to the permanent upwelling zone with summer intensification (Arístegui et al. 2009). MPI-ESMs show a patchy bias distribution along the coast (-2.0 to +2.0 ºC) presenting a cold bias (3.0 ºC) in the northwest corner of the domain (Fig. 3.2f and 3.2g). CMIP5 biases present a similar patchy pattern but with lower values along the NW African coast (Fig. 3.2h), where the horizontal resolution seems to play an important role.

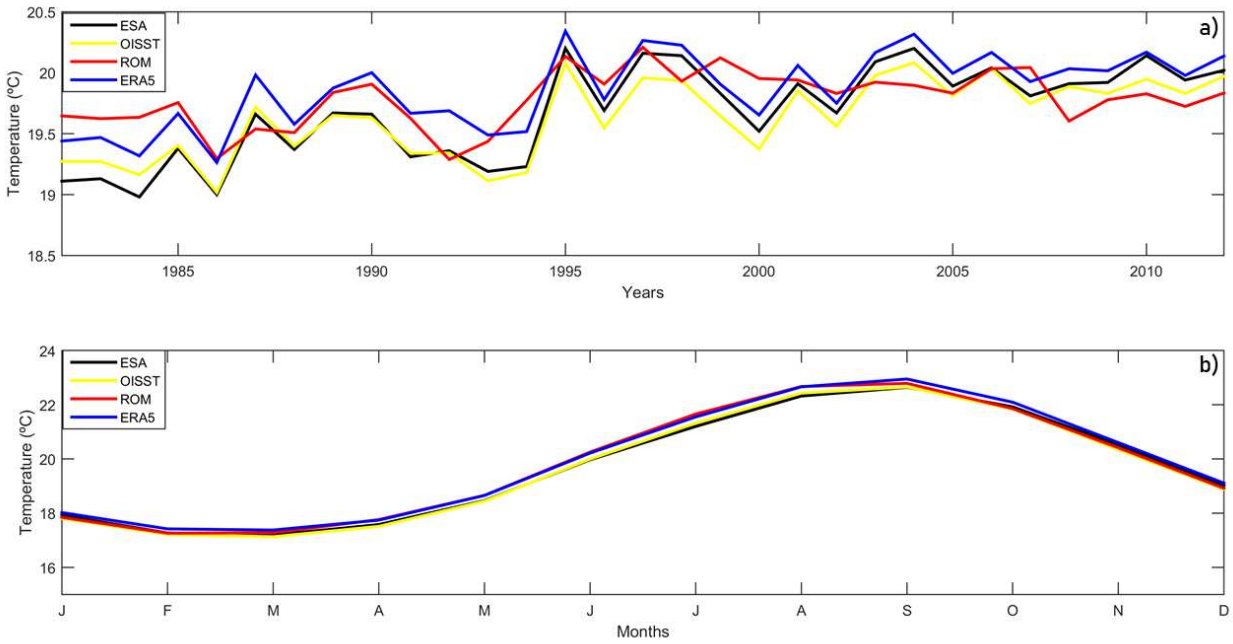

Fig. 3.3. a) Times series of yearly mean (a) and seasonal cycle (b) (1982-2012) SST (ºC) averaged over the domain.

The interannual variability and the seasonal cycle of the spatially averaged SST were evaluated using OISST, ERA5 and ESA data sets (Fig. 3.3). ERA5 and ESA were added to the analysis to account for uncertainty on SST observation-derived data. The time series of yearly spatially averaged ROM_P0 SST for the period 1980-2012 shows warm and cold biases ranging from +0.59 to -0.28 ºC compared to OISST (Fig. 3.3a), being mostly within the observation data sets spread range.

Fig. 3.3b shows the seasonal cycle of ROM_P0 SST compared to OISST, ERA5 and ESA. Minimum (maximum) temperatures are reached in February (September), being the amplitude of the seasonal cycle 5.4ºC for ESA and 5.5ºC for ERA5, OISST and ROM_P0.

Wind stress is the main driver of the CCUS (Fischer et al. 2019); erroneous intensities or directions of wind stress can have a strong impact on the seasonal upwelling system. To assess the ability of ROM_P0 reproducing the CCUS we analyze the seasonal wind stress intensity and direction compared to ERA5, MPI-ESM-LR, MPI-ESM-MR and CMIP5 during 1980-2012 period (Fig. 3.4). In DJF, when the anticyclonic circulation is weaker, the mean ERA5 wind stress intensity increases to north and south from 34ºN where a zonal band with minimum values is located. Moreover, low wind stress values extend along the coasts of the Iberian Peninsula and NW Africa, increasing gradually to the south of the Canary islands (Fig. 3.4a). ROM_P0 overestimates the ERA5 wind stress due to an overestimation of the Azores high during the winter months (Fig. 3.4b). In both MPI-ESM runs (Figs. 3.4c and 3.4d) this overestimation is even larger. On the contrary, the CMIP5 ensemble mean underestimates the strength but shows a spatial pattern closer to the wind stress depicted by ERA5 (Fig. 3.4e). Despite the larger scale differences, ROM_P0 adequately represents the spatial pattern induced by coast in the wind stress because of its high horizontal resolution.

In JJA, the Azores high strengthens and migrates to the NW, where ERA5 shows the lower intensities of wind stress (Fig. 3.4f). In ERA5, the wind stress increases to the south showing the largest values in the coastal strip from Cape Ghir to the south, and downwind from Canary Islands. By the Iberian and NW African coastlines the wind direction is along the coast, i.e. upwelling favourable. As in winter, MPI-ESMs strongly overestimate the wind stress field strength (Figs. 3.4h and 3.4i), while CMIP5 underestimates it, but both properly reproduce the wind stress field directions (Fig. 3.4j). Improving on the GCMs performance, ROM_P0 reproduces the JJA wind stress field remarkably well, including smaller scale features such as the local maximum off Cape Ghir, the Madeira and Canary Islands shadowing effect, the wind intensification in the passage between Canary Islands and Africa or the coastal weakening effect (Fig. 3.4g).

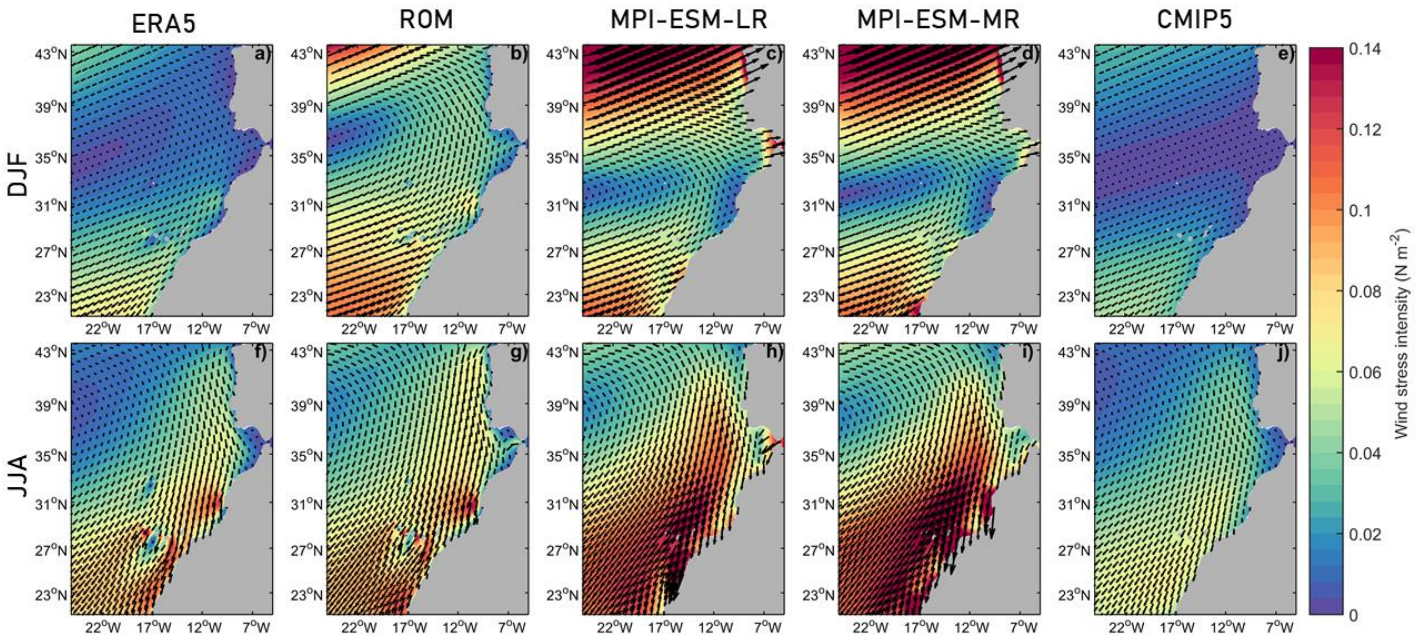

Fig. 3.4. a) Wind stress intensity and direction for the winter (upper row) and summer (lower row) months. It is shown ERA5 (a, f), ROM (b, g), MPI-ESM-LR (c, h), MPI-ESM-MR (d, i) and CMIP5 (e, j).

3.3.2 Latitudinal variability over the coastal band

The CCUS is a dynamically complex system with a large spatial and seasonal variability. Here, we will assess SST, wind and T2m variability focusing on the coastal band as the upwelling front is located within a few degrees offshore from the shelf break (Pelegrí and Bennazzouz, 2015), supplementing the analysis of the previous section.

The coastal cold SST is a key indicator to determinate the intensity of the upwelling system. The seasonal cycle of ROM_P0 was compared with the seasonal cycle of OISST over the coastal band (the mask is shown in Fig. 3.1a with red lines) and with the GCMs (MPI-ESM-LR, MPI-ESM-MR and CMIP5 ensemble). ROM_P0 performs better than GCMs with biases smaller than 0.5ºC in winter. It is also evident the effect of the coarse resolution in GCMs, especially in MPI-ESM-LR and CMIP5 (Fig. 3.5a-d).

In summer boreal months, when the Canary upwelling intensifies, ROM_P0 shows very small warm biases north of the Strait of Gibraltar and cold biases in the region of the NW African coast (Fig. 3.5e). Remarkably at 25ºN ROM cold bias extends uniformly offshore. MPI-ESM-LR shows the largest warm biases (up to 3.0ºC) in Cape Ghir and the Gulf of Cádiz. MPI-ESM-

MR and CMIP5 present cold biases in the Gulf of Cádiz and Cape Bojador (2.0ºC) and warm biases in Cape Ghir and Cape Blanc (Fig 3.5g and 3.5h).

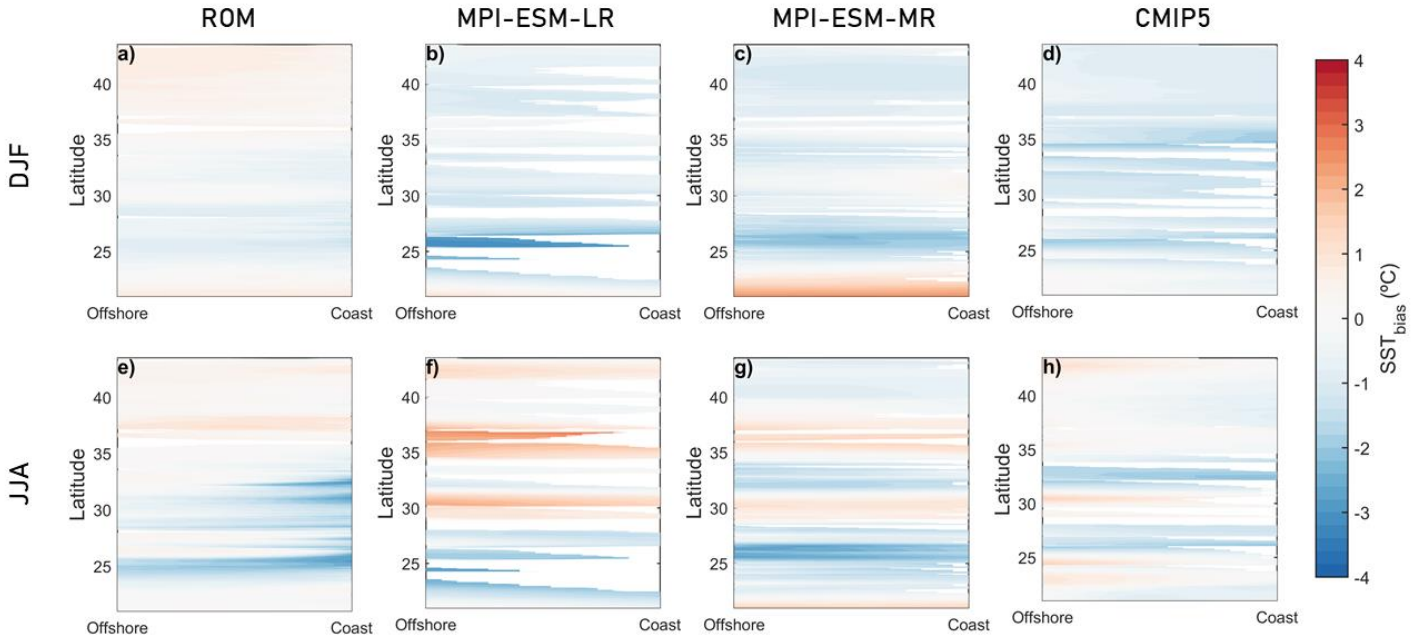

Fig. 3.5. SST (ºC) biases in the closest grid-points to the coast (red line Fig.1a; 100km from Coast to Offshore), between ROM (a, e), MPI-ESM-LR (b, f), MPI-ESM-MR (c, g) and CMIP5 (d, h) with OISST, in DJF (upper row) and JJA (lower row).

From these results it could be concluded that ROM_P0 magnifies in summer the upwelling in the zone of weak permanent upwelling located between 25°N and 33°N (Cropper et al., 2014; Gómez-Letona et al. 2017). To clarify the role of the high resolution in this issue we compared the ROM_P0 biases with respect to OISST, ERA5 and ESA in the grid points that are closer to the coast (Fig. 3.6). In DJF ROM_P0 biases are similar for the three datasets, with cold biases smaller than 1.0ºC along the African coast. From Cape Ghir to Cape Blanc, the biases with ESA are notably smaller (Fig. 3.6a). In JJA, the differences in the biases increase, being close to 0.5ºC in Cape Ghir and Cape Bojador for ESA and reaching the 4.0ºC for ERA5 at those locations (Fig. 3.6b). In general, ROM_P0 differences with ESA are smaller than with OISST and ERA5 along the African coast. The reason for these discrepancies can be related to the OISST and ERA5 resolution, which does not allow for a clear representation of the SST coastal pattern of the upwelling.

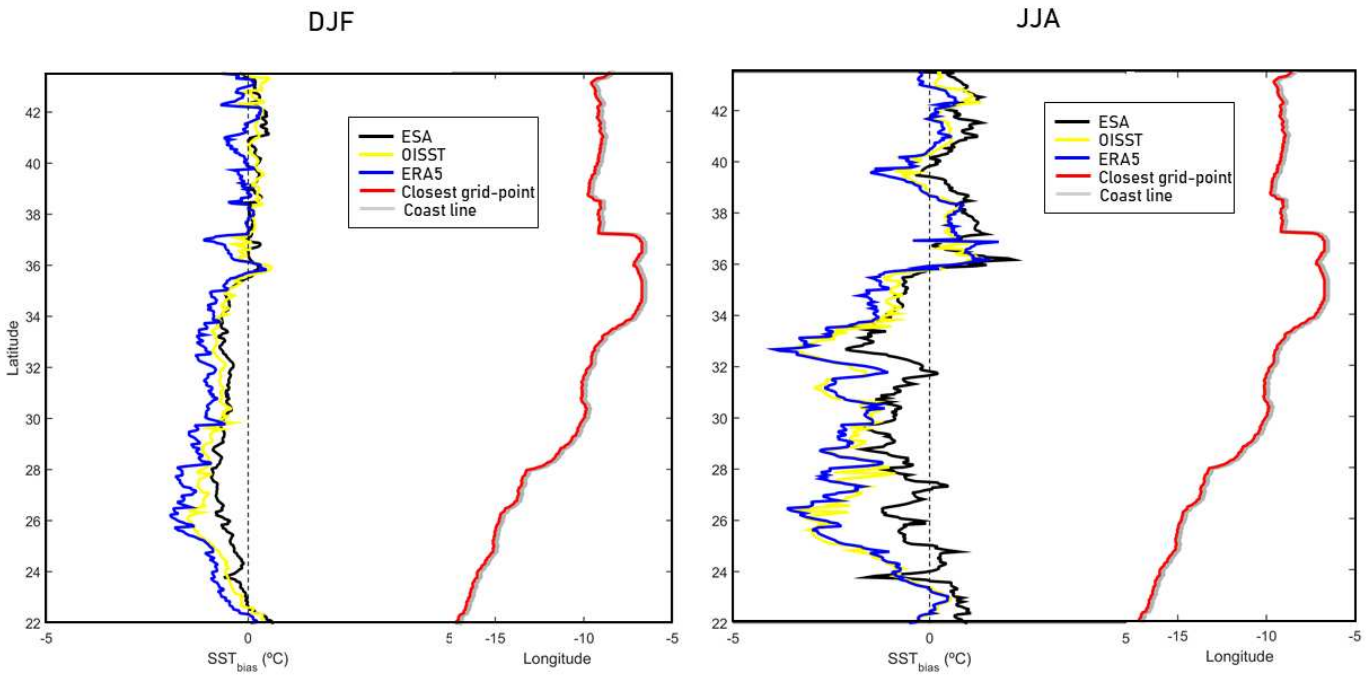

Fig. 3.6. ROM_P0 SST (ºC) biases in the closest grid-point to coast with OISST, ESA and ERA5, in DJF (a) and JJA (b).

The coastal wind stress was assessed through UI (Fig. 3.7) in order to quantify the upwelling intensity from Ekman transport. Positive (negative) *UI* corresponds to upwelling (downwelling) conditions. In DJF (Fig. 3.7a), ERA5 presents nearly neutral conditions along the coasts of the Iberian Peninsula. From the Gulf of Cádiz to Cape Ghir ERA5-based *UI* is positive increasing towards the south, where from Cape Bojador to Cape Blanc the upwelling becomes intense. This latitudinal variability is well represented by ROM_P0 and CORDEX, highlighting higher values in ROM_P0 for Cape Ghir and in southern regions and weaker in CORDEX for the region between the Gulf of Cádiz to Cape Blanc. CMIP5 also represents reasonably well the latitudinal variability, although it is smoother and with a general tendency to underestimate the upwelling index.

Table 4. Latitudinal coefficient of determination for *UI* averaged over the closest grid-points to coast in DJF and JJA, comparing ERA5 with ROM, MPI-ESM-LR, MPI-ESM-MR, CMIP5 and CORDEX

	WINTER	SUMMER
ROM_P0	0.96	0.94
MPI-ESM-LR	0.90	0.71
MPI-ESM-MR	0.92	0.72
CMIP5	0.96	0.92
CORDEX	0.98	0.98

In JJA, ERA5-based *UI* shows upwelling conditions along the Iberian coast and a clear intensification of the upwelling by the NW African coast, appearing a local maximum between Cape Beddouza and Cape Ghir (30.5ºN-32.5ºN). ROM_P0 and CORDEX present the same latitudinal pattern as ERA5, while CMIP5 reproduces the latitudinal variability, but with lower values of the *UI* and MPI-ESMs show different local maxima. In general, CORDEX shows a slightly better performance than ROM_P0 and CMIP5, with MPI-ESMs having the worst coefficients of determination (Table 4).

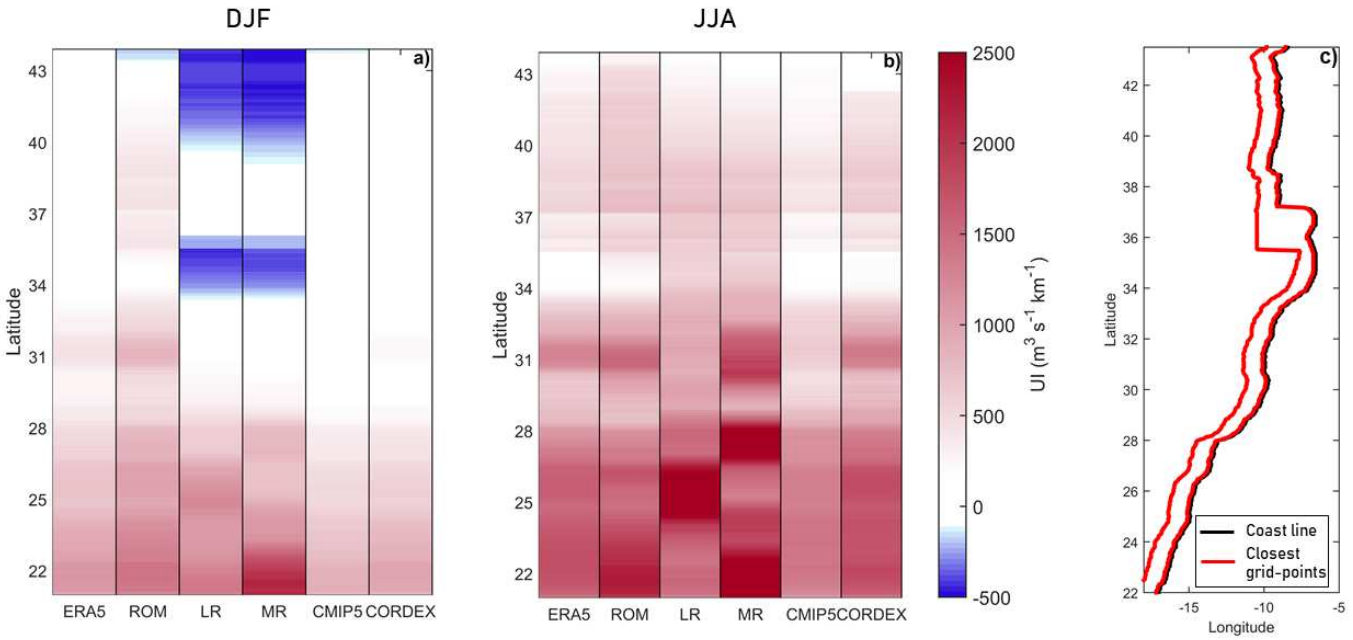

Fig. 3.7. *UI* (m^3 s^{-1} km^{-1}) averaged over the closest grid-points to the coast (c), for DJF (a) and JJA (b).

The T2m land-sea difference lies in the ground of Bakun's (1990) hypothesis of change in upwelling systems under global warming. The land-sea gradient simulated by ROM_P0 is validated against ERA5 and compared with MPI-ESM-LR, MPI-ESM-MR, CMIP5 and CORDEX simulations. For each latitude, we calculate the difference between the 2m air temperature zonally averaged over 100 km inshore (bounded by the red line, land) and zonally averaged over 100 km offshore (bounded by the blue line, ocean) as shown in the Fig. 11c.

Table 5. Latitudinal coefficient of determination for T2m land-sea differences averaged over the closest grid-points to coast in DJF and JJA, comparing ERA5 with ROM_P0, MPI-ESM-LR, MPI-ESM-MR, CMIP5 and CORDEX

	WINTER	SUMMER
ROM_P0	0.85	0.77
MPI-ESM-LR	0.71	0.30
MPI-ESM-MR	0.64	0.34
CMIP5	0.71	0.30
CORDEX	0.94	0.76

ERA5 T2m land-sea differences present mostly negative values in DJF, changing sign in the southern part from 21ºN to 23ºN (Cape Blanc). CORDEX reproduces accurately the latitudinal variability, while ROM_P0 and CMIP5 fail in simulating the sign change in the southernmost region. The MPI-ESMs do not reproduce properly the latitudinal variability and show too low values of the T2m land-sea difference (around 0.5ºC).

In JJA the insolation increases and the land becomes warmer than the sea, so T2m land-sea differences are mostly positive (Fig. 3.8b). ERA5 presents a high latitudinal variability, with two regions showing the largest positive differences (Cape Ghir and from Cape Bojador to Cape Blanc). ROM_P0 and CORDEX again reproduce well the T2m land-sea differences. CMIP5 does not reproduce properly the T2m land-sea differences latitudinal pattern, showing a spurious maximum in the Gulf of Cádiz, and the MPI-ESMs showed very low values compared to those of ERA5. CORDEX and ROM_P0 show a better performance, especially

in summer when CMIP5 and MPI-ESMs present a rather low coefficient of determination (Table 5).

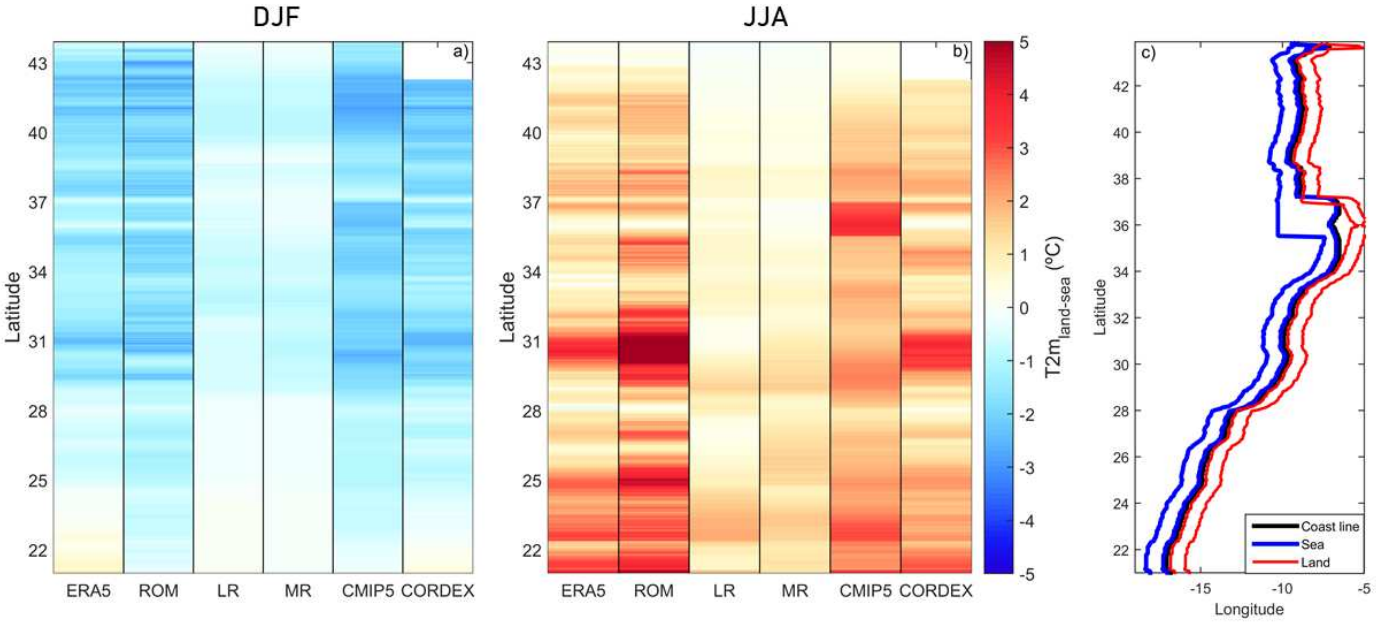

Fig. 3.8. Along-shore land (c; blue) – sea (c; red) temperature difference (ºC) for DJF (a) and JJA (b). It is assessed ROM_P0 with ERA5 and compared with MPI-ESM-LR, MPI-ESM-MR, CMIP5 and CORDEX.

3.3.3 Thermal Vertical Structure

The cross-shelf thermal vertical structure is commonly used to characterize coastal upwelling. The thermal vertical structure of the upper 200 m simulated by ROM_P0 was compared to SODA and GLORYS reanalysis and to in-situ data from WOD18. We choose a cross-shelf transect at Cape Ghir (31.5ºN). All observations used from WOD18 were taken between 1980 and 2012, and the isotherms were plotted as a qualitative reference (Fig 3.9a, b).

At Cape Ghir WOD18 presents a clear thermal stratification, more evident in summer, with isotherms sloping up to the coast and a temperature range between 14ºC and 22ºC. In summer the upwelling front outcrops in the surface near 10.3º W (see 17ºC isotherm), while it is relaxed in winter with the 17ºC isotherm outcropping more to the east by the coast (Fig. 3.9a, b). The cross-shelf structure and seasonality is properly represented by GLORYS and SODA reanalysis, but ROM_P0 is more accurate in the representation of the vertical gradients and the isotherm sloping by the coast (Fig. 3.9c-h).

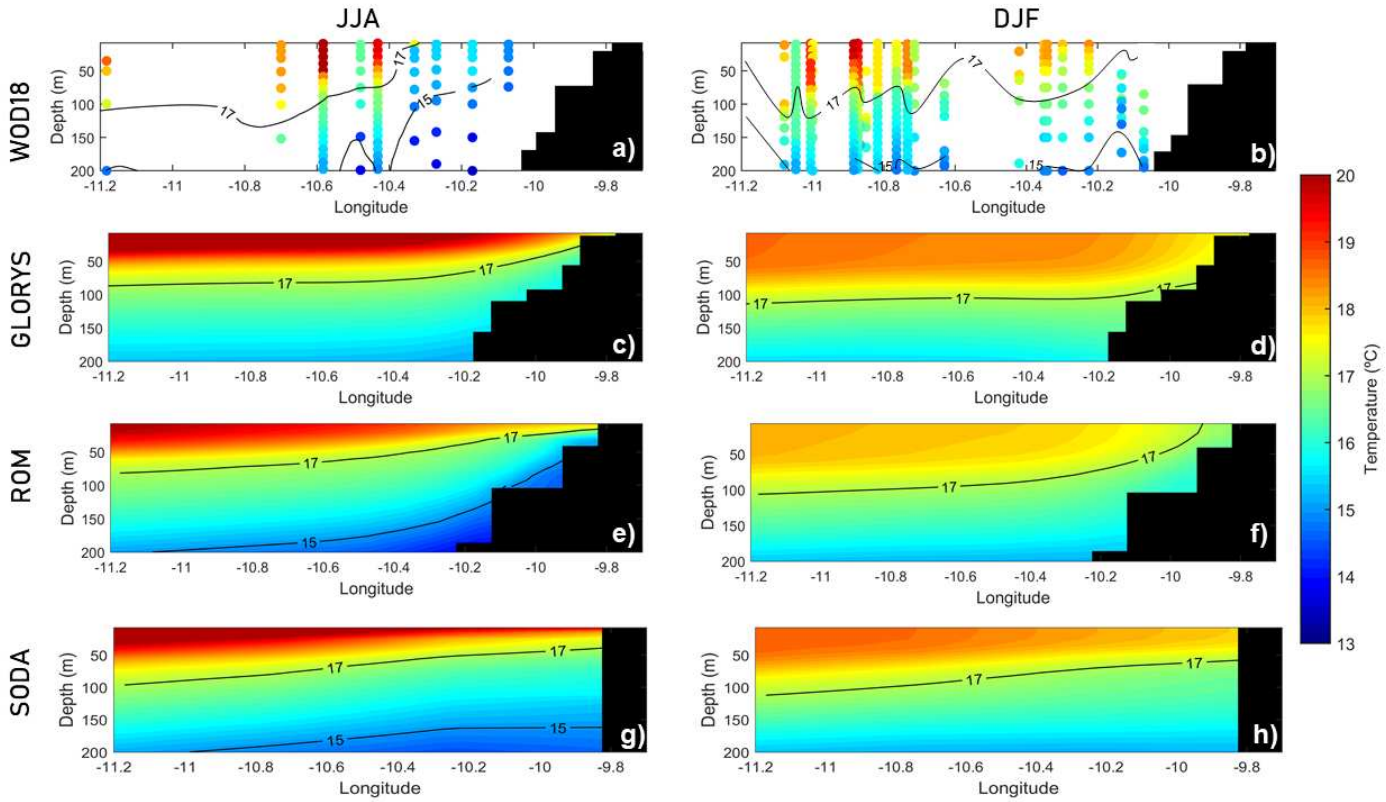

Fig. 3.9. Temperature (ºC) transect for JJA (left) and DJF (right) in Cape Ghir (1980-2012) for WOD18 (a, b), GLORYS (c, d), ROM_P0 (e, f) and SODA (g, h).

3.3.4 Upwelling filaments

The MPIOM high horizontal resolution in the central region of the CCUS allows marginally the representation of the mesoscale variability because the climatological first baroclinic Rossby radius of deformation is around 30 km in this area (Chelton et al. 1998). Upwelling filaments are elongated mesoscale structures of upwelled water extending offshore in the upper surface layer (Brink 1983). Alvarez-Salgado et al. (2007) and Lovecchio et al. (2018) highlighted the relevant contribution of upwelling filaments to offshore organic carbon in the CCUS. The most prominent filaments in the CCUS are located at Cape Ghir, Cape Juby, Cape Bojador and Cape Blanc. Cape Ghir filament, one of the largest and existing nearly all year round (Hagen et al. 1996), exports large amounts of organic material into the open ocean (García-Muñoz et al. 2005; Pelegrí et al. 2005, 2006). To assess ROM_P0 skills in reproducing these relevant mesoscale features we use two filament events in August 2006 and August 2009, the latter studied in detail by Sangrá (2015) and Sangrá et al. (2015). We compare the observed

MODIS Aqua SST with ROM_P0 and GLORYS output averaged for 21st to 28th August 2006 and 13th to 20th August 2009 (Fig. 3.10).

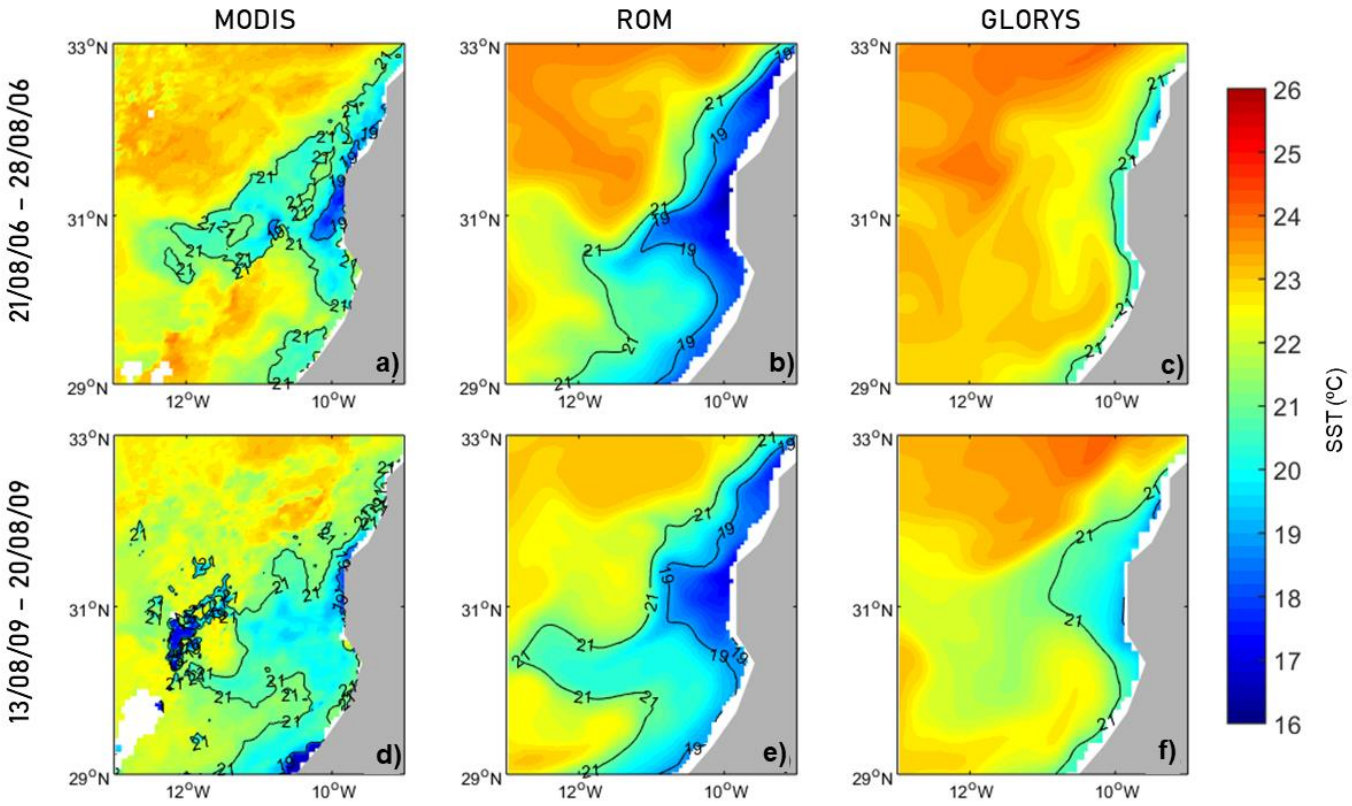

Fig. 3.10. Averaged SST (ºC) in 21-28 August of 2006 (upper row) and 13-20 August of 2009 (lower row) for MODIS Aqua (a, d), ROM (b, e) and GLORYS (c, f).

As described by Sangrá et al. (2015), ROM_P0 reproduces the filament cold core, with SST below 19ºC and a broader cool embracing region with temperatures between 19ºC and 21ºC. ROM_P0 reproduces properly both filament events, quite accurately the offshore extension of the embracing region and a overextended cold core, while GLORYS filament is excessively limited to the coast.

3.4 Discussion

When Bakun (1990) formulated his hypothesis highlighting that under global warming the increase in ocean-land temperature contrast may oppose the general tendency for ocean-basin scale circulation to slow down, the enormous uncertainty about the evolution of coastal ocean upwellings under global climate change conditions was evidenced. Additionally, the importance of the mesoscale in the decadal changes of the CCUS is widely acknowledged (e.

g. Relvas et al. 2009), as it is the role of the mesoscale in transporting nutrients and phytoplankton (e.g. Gruber et al. 2011). Since then many attempts have been done to get rid of such uncertainty and to deepen the knowledge about the behaviour of such fundamental marine ecosystems under global warming conditions, and different observational and model products have been used to resolve the different scales relevant for these questions. The study of the upwelling systems in the CMIP5 simulations (e. g. Oyarzun and Brierley et al. 2018) allowed identifying the climate change drivers and the main limitations of the GCMs to reproduce the mesoscale processes in the EBUSs (Garcia-Reyes et al. 2015; Bindoff et al. 2019). These local and mesoscale features may have greater impact on EBUSs than large-scale wind patterns (Renault et al. 2016; Xiu et al. 2018). The difficulties found in the representation of the CCUS by global models can be significantly resolved with the help of high resolution RCSMs (e. g. Xiu et al. 2018). In this work, the use of ROM_P0 in the CCUS region allows us to represent the fine-scale atmosphere-ocean feedback, reproducing the spatial and temporal structure needed in the regional climates (Li et al. 2012; Sein et al. 2015). Moreover, ROM_P0 configuration allows a high resolution in the region of interest maintaining a global ocean domain (Soares et al. 2018; Parras-Berrocal et al. 2020).

The provided climate assessment shows that ROM_P0 reproduces the basin scale climate and the seasonal signal affecting the CCUS (section 3.3.1) better than the GCMs (MPI-ESMs and CMIP5) and is in good agreement with OISST and ERA5. ROM_P0 presents also good skills in reproducing the interannual variability of the basin scale SST when compared to ERA5, OISST and ESA data sets (Fig. 3.3). However, in winter ROM_P0 has a warm bias in the northwest corner of the domain (Fig. 3.2a). We have also identified an overestimation of the Azores high in winter, originating a wrong wind stress field representation along the West Iberian coast (Fig. 3.4b). Parras-Berrocal et al. (2020) attributed those differences to the role played by the deficiencies of ROM_P0 to simulate the ocean circulation in the North Atlantic, with a cold bias centred east of Flemish Cap. Other studies stand out the difficulties of the ocean models to simulate the Gulf Stream in winter (Eden and Greatbatch 2003; Bryan et al. 2007) and Cabos et al. (2020) detected those deficiencies not only in the ocean models, but also in the Climate Forecasting System Reanalysis. However, according to our results the impact of those winter basin-scale inaccuracies on the CCUS seems to be quite limited, as they impact mostly in the West Iberian coast during the no upwelling season.

ROM_P0 also presents a cold bias compared to OISST along the NW African coast in summer, when the upwelling intensifies (Figs. 3.2 and 3.5). Mason et al. (2011) and Santana-Falcón et al. (2020) found a similar cold bias in their ocean regional models over the CCUS, attributing it to the warm bias in SST forcing data set identified by Dufois et al. (2012) in a number of modelling studies in the world EBUS. According to Dufois et al. (2012) the cause of the SST warm coastal bias in monthly Pathfinder data during summer was a flagging method based on an OISST reference test, which is explained by strong coastal SST gradients in these regions, which cannot be satisfactorily represented by the large scale OISST product. This drawback of OISST can partly explain the strong cold bias in ROM_P0 with respect to this observational product. Indeed, when we compared ROM_P0 SST with a higher resolution dataset (ESA) the cold bias was notably reduced (Fig. 3.6), demonstrating the importance of the high resolution in mesoscale regions as the CCUS.

This high ocean resolution is key for the representation of the CCUS mesoscale, which is determined by the accuracy in the representation of the coastal wind stress field and the land-ocean temperature contrast and characterized by the cross shelf thermal structure and the generation of events such as upwelling filaments.

ROM_P0 properly distinguishes the three main CCUS sub-regions (e.g. Aristegui et al. 2009, Crooper et al. 2014; Gomez-Letona et al. 2017) from the UI (Fig. 3.7): from 21ºN to 26ºN (permanent upwelling zone), from 26ºN to 33ºN (weak permanent upwelling zone) and from 33ºN to 43ºN (seasonal upwelling zone), although in part of the West Iberian coast ROM_P0 produces a nearly year-round upwelling (Fig. 3.7) as a consequence of the misrepresentation of the wind field in that area as previously discussed. Despite this fact, ROM_P0 performs better than the MPI-ESMs and the CMIP5 ensemble, and slightly worse than the AFRICA-CORDEX ensemble in terms of the *UI* (which is calculated from the wind stress). It must be taken into account that, although AFRICA-CORDEX models have lower horizontal resolution than ROM atmosphere (0.44º vs 0.22º) their west and north boundaries, forced by ERA-Interim, are pretty close to the CCUS and that the SST is also prescribed from ERA-Interim. The *UI* values along the Iberian Peninsula simulated by ROM_P0 are similar to other studies, with a localised downwelling by the Galician coasts (-200 m^3 s^{-1} km^{-1}) in winter and weak upwelling (500 m^3 s^{-1} km^{-1}) in the summer months (Pardo et al. 2011; Sousa et al. 2017a). The upwelling in the African coast also is in the range obtained by different studies (Pardo et al.

2011; Sousa et al. 2017b), with year-round permanent upwelling (from 600 m^3 s^{-1} km^{-1} to 1000 m^3 s^{-1} km^{-1}) in winter, increasing to 1500 m^3 s^{-1} km^{-1} in the African coastline.

The T2m land-sea difference and its latitudinal variability is relevant for CCUS representation as Bakun hypothesis is based on the global warming induced changes in the T2m land-sea differences. Several authors (Sydeman et al. 2014; Wang et al. 2015) supported Bakun's proposition, but remains unclear the relationship between coastal wind intensification and global warming (García-Reyes et al. 2015). Our results have shown a good performance of ROM_P0 representing the T2m land-sea contrast variability in CCUS as compared to ERA5. The latitudinal variability of the land sea temperature contrast is strongly reduced in the GCMs, indicating that global models have difficulties to represent the land-sea thermal differences in coastal regions (Ning et al. 2014; Roxy et al. 2015; Ward et al. 2020). ROM_P0 does not reproduce the sign change of T2m land-sea difference in Cape Blanc, while it is properly captured by AFRICA-CORDEX. In JJA, ROM_P0 overestimates the T2m land-sea differences in Cape Ghir as a consequence of a strong warming in the Atlas mountains.

Therefore, the ROM_P0 improvement over the GCMs and good performance as compared to AFRICA-CORDEX shows the impact of the higher resolution and coupling for CCUS climate modelling. Coming to details, we have identified the Cape Ghir as an intense upwelling location both in DJF as JJA, and as a place where upwelling filaments are a nearly permanent mesoscale feature. ROM_P0 properly reproduces the summer increase in ocean thermal stratification in the upper 100 m at Cape Ghir and the increase in the slope of the isotherms in the immediate proximity to the coast (Fig. 3.9), comparing well with WOD18 hydrographic data and with GLORYS reanalysis. The improvement over SODA is remarkable, especially over the shelf where the high resolution plays a key role.

The mesoscale events play an important factor over the CCUS, where only organic carbon export by filaments in the subtropical northeast Atlantic contributes to the 63% of the annual primary production associated with the coastal upwelling (Santana-Falcón et al. 2016, 2020). ROM_P0 reproduces the two selected events in Cape Ghir, exporting the water masses from coast to 150 km offshore (Fig. 3.10). Quite often limited area models are used for reproducing these events with the difficulties of dealing with the open boundary conditions. This is even more important when considering the biogeochemical relevance of the upwelling filament dynamics. Troupin et al. (2012) and Santana-Falcón et al. (2020) approached the study of upwelling filaments using nested domains and a one-way offline coupling. However, when the

focus is on the basin-scale, approaches accounting for the influence of the mesoscale on the larger scale are needed. Lovecchio et al. (2017, 2018) used such an approach by means of a telescopic curvilinear grid with strong refinement in the NW African coast, being able to highlight the key role of mesoscale processes in the offshore transport of organic carbon and concluding that a great part of this flux out of the upwelling regions is not accounted for in coarse global models. Here, we present a model approach capable of reproducing the large-scale climate signal accounting for the relevant upwelling mesoscale dynamics, which is of uttermost importance to assess the future evolution of CCUS and its socio-economic consequences under climate change scenarios.

3.5 Conclusions

In the present work, we assess the ability of the atmosphere-ocean regionally coupled model ROM_P0 to represent the large-scale climate and mesoscale processes involved in the CCUS dynamics, and compare it to two MPI-ESMs configurations and ensembles of CMIP5 GCMs and AFRICA-CORDEX RCMs. Our findings can be summarized as follows:

- ROM_P0 shows a better performance than the MPI-ESMs and CMIP5 models in representing the larger-scale wind stress and SST fields, although a relatively overestimation of the Azores high in winter affects slightly the CCUS over the West Iberian coast. Besides, ROM_P0 reproduces adequately the seasonal and interannual variability of the ERA5, ESA and OISST.

- High resolution is key to reproduce the latitudinal variability of the CCUS, as ROM_P0 represents the observed coastal SST with higher accuracy than the GCMs. Moreover, ROM_P0 successfully reproduces the coastal UI as well as the T2m land-sea differences, highlighting the impact of the higher resolution against the GCMs with a performance comparable to AFRICA-CORDEX.

- The mesoscale processes in the CCUS are well simulated by ROM_P0, which is able to transfer the coastal upwelling waters to the open ocean in a realistic way. Thus, it successfully represents two coastal upwelling filaments off Cape Ghir, which are not accounted for in most global models.

In conclusion, ROM_P0 is a powerful atmosphere-ocean model system able to reproduce with accuracy the CCUS, performing better than the GCMs. The improvement is related to a much higher horizontal resolution, which allows a better simulation of the dominant mesoscale coastal dynamics. The results here give ground to the future use of ROM_P0 to gain a deeper insight into the CCUS by the end of 21st century.

CHAPTER 4:

Climate change in the Canary current upwelling system: The role of ocean stratification and wind

The contents of this chapter is in preparation to submit to an international journal:

Vázquez R., Parras-Berrocal I.M., Cabos W., Sein D.V., Mañanes R., Bolado-Penagos M., Izquierdo A. (2023) Climate change in the Canary current upwelling system: The role of ocean stratification and wind

4.1 Introduction

Canary Current Upwelling System (CCUS) is one of the four large Eastern Boundary Upwelling Systems (EBUSs) in the world, which is driven by the equatorward alongshore winds. The upwelled cold and nutrient-rich waters do not only fuel the biological activity near the coast, but also in open ocean as shelf and slope waters are transported offshore by active mesoscale structures (e.g. filaments, fronts, eddies) (Pelegrí et al., 2005; Álvarez-Salgado, 2007; Sangrà, 2015).

The CCUS extends from the coast of West Africa at 12ºN to the northern tip of the Iberian Peninsula at 43ºN and constitutes the eastern boundary of the North Atlantic subtropical gyre (Pelegrí and Peña-Izquierdo 2015). The CCUS is divided mainly into four different sub-regions, the Mauritania-Senegalese upwelling region (12ºN-19ºN), the permanent upwelling region (21ºN-26ºN; PUR), the weak permanent upwelling region (26ºN- 33ºN; WPUR) and the Iberian upwelling region (IUR), dominated by a high seasonal variability with upwelling favourable winds in summer and downwelling winds during winter months (35ºN-43ºN; Arístegui et al. 2009; Cropper et al. 2014; Gómez-Letona et al. 2017).

Since the major mechanisms underpinning EBUSs originate from large-scale atmosphere-ocean coupling (García-Reyes et al. 2015), magnitude and timing of the EBUSs are sensitive and highly vulnerable to climate variability (Macías et al. 2012). Several studies based on historical datasets analysis (Bakun et al. 2010; Narayan et al. 2010; Gutierrez et al. 2011; Santos et al. 2012; Barton et al. 2013; Crooper et al. 2014; Sydeman et al. 2014; Bakun et al. 2015; Varela et al. 2015) have striven to reveal the EBUSs response under climate change showing contradictory results mainly due to the short duration of most observational time series (Garcia-Reyes et al. 2015) and methodological inconsistencies (considering only the upwelling season or annually averaged wind trends; Sydeman et al. 2014).

Wang et al. (2015) analyzed the upwelling response to climate change with 22 CMIP5 (Coupled Model Intercomparison Project) Global Climate models (GCMs), finding in the CCUS, a robust relationship between the increase of the land-sea temperature contrast and the upwelling intensity in the twenty-first century (Bakun's hypothesis; Bakun, 1990). However, Rykaczewski et al. (2015) and later Sousa et al. (2017a) suggested that the alongshore winds may be more sensitive to the intensity and position of the Azores high rather than to changes in the continental thermal low pressure systems. Along with wind changes, there are reports on

upper ocean warming during the last century (Levitus et al. 2000; Levitus et al. 2005), increasing the water stratification and reducing the upward nutrient-rich transport to the surface (Di Lorenzo et al. 2005; García-Reyes et al. 2015; Brady et al. 2019). In the north Atlantic, this increase in the upper ocean stratification is associated with a weakening in the Atlantic Meridional Overturning Circulation (AMOC; Levang and Smitch, 2020), which may reduce the Canary Current flow (Fischer et al. 2019). Thus, ocean stratification due to global warming may play a key role where deeper upwelled water might be less connected with the wind stress (Sousa et al. 2020), becoming the main driver of changes in EBUS during the 21st century (e.g. Oyarzun and Brierley, 2019 in the Humboldt upwelling system). Therefore, the CCUS future behavior is still uncertain and both stratification and wind changes may be complementary or competitive (Bonino et al. 2019).

The coarse spatial resolution (around 1 x 1º) of GCMs from CMIP5 is not enough to resolve the latitudinal variability and to reproduce mesoscale features or detailed shelf dynamics of the upwelling systems (García-Reyes et al. 2015; Xiu et al. 2018; Varela et al. 2022). Regional climate system models (RCSMs) are able to account for mesoscale processes, which are masked by the GCMs (Sein et al. 2017; Bindoff et al. 2019; Vázquez et al. 2022). This ability to reproduce the mesoscale processes allows to assess the impact of climate change in a more realistic way, given the importance of the eddies and coastal filaments that enrich the oligotrophic open waters (Lovecchio et al. 2017; Lovecchio et al. 2018; Haligeorgis et al. 2021).

Our objective is to study the future impact of climate change on the three northern regions of the CCUS (Fig. 4.1) with a high resolution RCSM. We will aim:

- To understand the impact of climate change in the wind field, identifying the main driver of changes in the alongshore winds for the future.
- To assess the impact on the coastal upwelling of the ocean stratification changes due to global warming.

The paper is organized as follows: the model and methodology are described in section 4.2 and the results are presented in section 4.3. Finally, the discussion and conclusions are given in section 4.4.

4.2 Material and methods

4.2.1 ROM configuration

We use the RCSM, ROM (Sein et al. 2015), composed of a global ocean model (MPIOM) coupled to an atmospheric regional model (REMO) via OASIS3 (Valcke, 2013) coupler. ROM includes the lateral freshwater fluxes at the land surface through the Hydrological Discharge (HD) as part of REMO and the relevant carbon stocks of the atmosphere, ocean and sediments through the Hamburg Ocean Carbon Cycle (HAMOCC) as a MPIOM subsystem (Parras-Berrocal et al. 2020; Sein et al. 2020). The ROM model was previously assessed over the CCUS for a present climate in Vázquez et al. (2022).

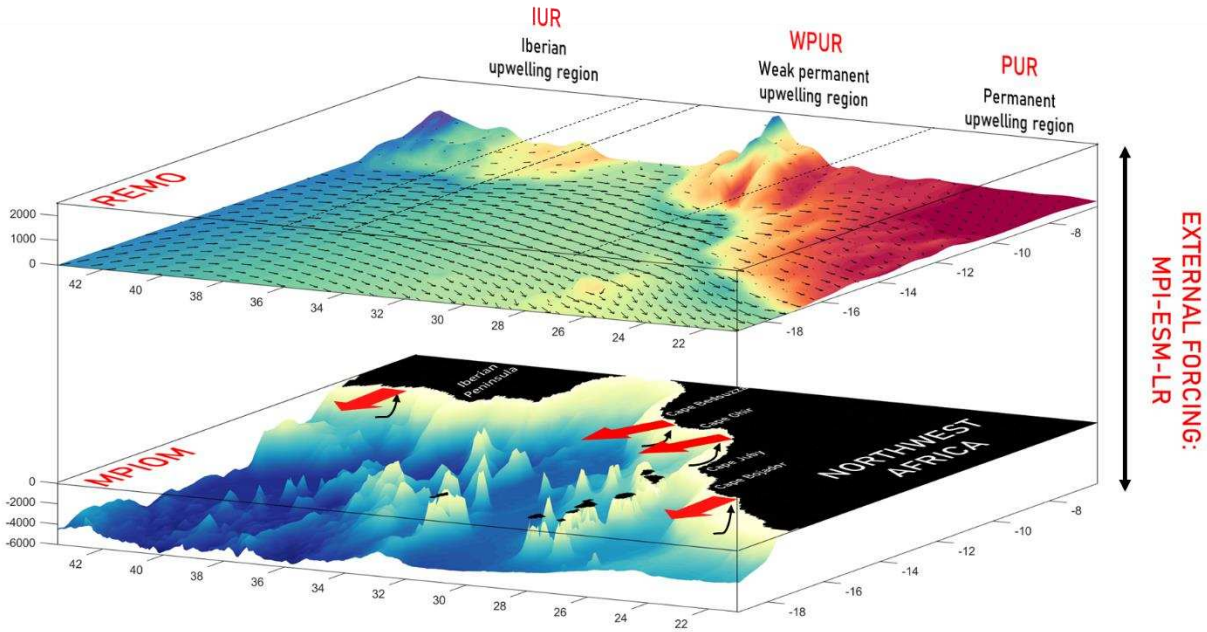

Fig. 4.1 ROM bathymetry (bottom), 2 m air temperature (T2m) and sea surface wind (top), for the CCUS with the three sub-regions studied: Iberian upwelling region (IUR; 35ºN-43ºN), weak permanent upwelling region (WPUR; 26ºN-33ºN) and permanent upwelling region (PUR; 21ºN-26ºN). It shows the conceptual upwelling mechanism (black arrows) generated by the Ekman transport (red arrows).

The oceanic component of ROM features a curvilinear grid with two poles, over North America and Northwestern Africa, yielding a grid size from 5 to 10 km in the CCUS. This resolution is high enough to study the frontal mesoscale processes associated to the upwelling (i.e. eddies and filaments) while maintaining a global domain (Vázquez et al. 2022). The model comprises 40 z-coordinate vertical levels with increasing level thickness towards the ocean bottom (Sein et al. 2015; Soares et al. 2019). REMO is integrated over a rotated regular grid with a horizontal resolution of 25 km and its domain includes the Eastern Tropical Pacific, the Mediterranean Sea regions and the CCUS in the North Atlantic, being the only model component of ROM run in regional configuration.

In this work, ROM is driven by the low resolution version (1.5º x 1.5º) of the Max Plank Institute – Earth System Model (MPI-ESM-LR) in two runs: First, a historical run from 1950 to 2005 and second, the climate projection from 2006 to 2099 under the Representative Concentration Pathway 8.5 (RCP 8.5) CMIP5 scenario.

4.2.2 Upwelling analysis

To investigate how the seasonality and intensity of the coastal upwelling may change in the future, we split the historical reference period (defined as 1976-2005) and the future climate (defined as 2070-2099) into winter (DJF, December, January and February) and summer (JJA, June, July and August) seasons. Additionally, trends for the whole period (1950-2099) were calculated. We use monthly data of near-surface air temperature (T2m), mean sea level pressure (MSLP), wind stress, seawater temperature and salinity.

The wind stress curl-driven was estimated from the wind field (*wE*; Jacox et al. 2018). *wE* gives an estimation of the vertical transport in the Ekman layer, where positive values are associated with upwelling (Ekman suction) and negative values with downwelling (Ekman pumping). It is calculated as follow:

$$wE = \frac{1}{\rho_0 f}\left[\frac{\partial \tau_y}{\partial x} - \frac{\partial \tau_x}{\partial y}\right] \quad \text{Eq. 4.1}$$

where τx, and τy are the zonal and meridional components of the wind stress, respectively; ρ_0 is the reference sea water density (1025 kg m^{-3}) and f is the Coriolis parameter. Moreover we calculated the wind-driven Ekman transport as follow:

$$Q_x = \frac{\tau_y}{f\rho_0} \quad \text{Eq. 4.2}$$

$$Q_y = -\frac{\tau_x}{f\rho_0} \quad \text{Eq. 4.3}$$

The coastal upwelling stratification is characterized through the Brunt-Väisälä frequency (N), where larger values indicate strong stratification, and values close to zero a well-mixed water column:

$$N^2 = \frac{g}{\rho_0}\frac{\partial \rho}{\partial z} \quad \text{Eq. 4.4}$$

where z is the depth, ρ the potential density and g is the gravitational acceleration.

Once analyzed the impact of the climate change in the wind pattern and the ocean stratification in an individual way, we use the source depth (Ds) to estimate the depth of the waters that reach the surface in the coastal upwelling region. Ds gives us further insight in the mechanisms that drive the coastal upwelling in the future, clarifying the role of the wind pattern and the coastal ocean stratification as complementary or competitive mechanisms. This parameter is defined in He and Mahadevan (2021) as follows:

$$Ds = Cs\left(\frac{UI}{N}\right)^{1/2} \quad \text{Eq. 4.5}$$

where $Cs = (4/Ce)^{1/2} = 8.16$ for $Ce = 0.06$, which is the efficiency factor used in Fox-Kemper and Ferrari (2008) and He and Mahadevan (2021). UI is the upwelling index (UI, Bakun et al.,

1973) based on the offshore wind-driven Ekman transport (***Q****;* Eq. 4.2 and 4.3) and is calculated as follows:

$$UI = -sin\left(\theta - \frac{\pi}{2}\right) Q_x + cos\left(\theta - \frac{\pi}{2}\right) Q_y \quad \text{Eq. 4.6}$$

and θ is the angle between the coastline and the equator.

4.3 Results

4.3.1 Climate change signal in the alongshore winds

To analyze the wind field in the CCUS and characterize future changes, we examined the Ekman transport and the wind stress curl-driven (*wE*) in the historical (1976-2005) and future (2070-2099) simulations and their differences for DJF and JJA. In DJF, the historical simulation presents higher *wE* in the African coast from Cape Ghir to Cape Blanc, with perpendicular Ekman transport to the shoreline (Fig. 4.2a). In the northern IUR (between 41ºN and 43ºN) are shown negative values (Ekman pumping), with parallel shore direction, resulting in downwelling winds. For the future, *wE* increases in the PUR and decreases in the whole IUR (Fig. 4.2b), suggesting a strengthening of upwelling/downwelling favourable winds in the PUR/IUR. In JJA, *wE* is intensified with upwelling favourable winds along the whole CCUS against DJF (Fig. 4.2c). However, in the future, *wE* increases in the IUR, reaching differences greater than 0.2 m s^{-1} in the northernmost region (Fig. 4.2d). From the Strait of Gibraltar to Cape Blanc *wE* decreases, indicating a coastal upwelling weakening over the end of 21st century.

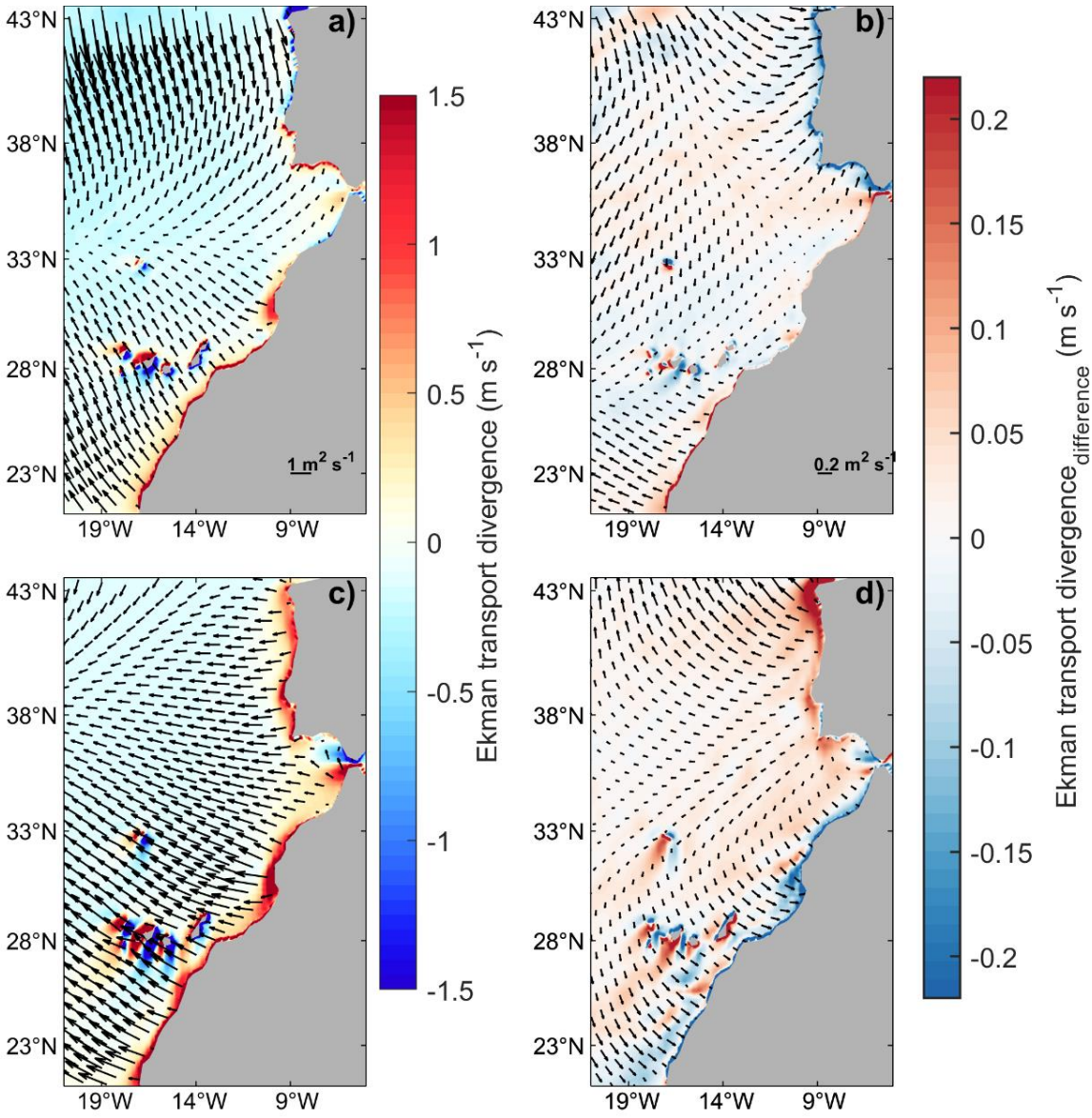

Fig. 4.2. Ekman transport divergence (*wE*; m s^{-1}) and Ekman transport (vector field; m^2 s^{-1}) averaged from 1976 to 2005 (a, c) and the difference (future minus historical) (b, d), for DJF (upper row) and JJA (lower row).

The *wE* trends from 1950 to 2099 calculated over the coastal band show a clear dipole structure from N to S that reverses seasonally. This pattern suggests an intensification of upwelling winds during the winter period over the African coast and a weakening at IUR (Fig. 4.3a). Instead in JJA, upwelling intensifies in IUR and weakens along the whole African coast, excepting the region around 26ºN, where positive trends are observed. The wE trends (both positive and negative) are intensified in the regions closest to the coast, where the upwelling is more effective and the high resolution of ROM plays a role.

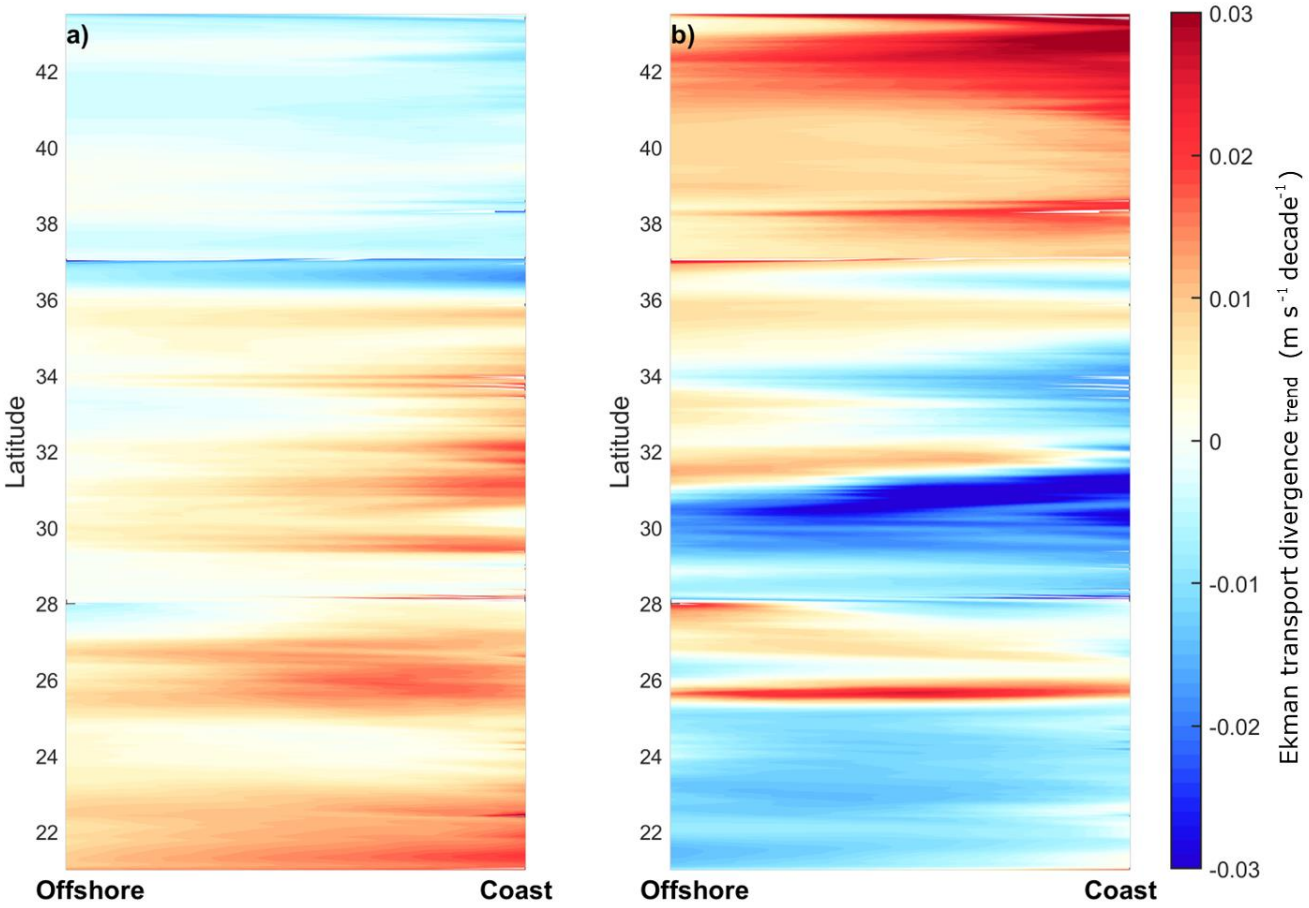

Fig. 4.3. Ekman transport divergence (*wE*) trend (m s^{-1} $decade^{-1}$) in the closest grid-points to the coast (within 100 km from the coast), from 1950 to 2099 for DJF (a) and JJA (b).

4.3.2 Drivers of climate change in the alongshore winds

In this section, we study the role of the main drivers of changes in the CCUS wind field under RCP8.5 through the analysis of T2m and MSLP.

For the reference period, in DJF, the T2m presents the minimum values (<10ºC) over the ocean in the northwest corner of the domain, with increasing temperature towards the equator. Other minima are also found over the Iberian Peninsula and the northernmost region of Africa (Fig. 4.4a), which are strongly influenced by the topography. T2m trends (Fig. 4.4b) are very low in the whole ocean domain, including the coastal regions. For land, the trends rise slightly in the western Iberian Peninsula, not more than 0.04ºC $decade^{-1}$, increasing progressively to the eastern of the Peninsula. In the African continent, the trends are larger reaching the 0.16ºC $decade^{-1}$ in the Atlas mountain chain. It is noticeable that the T2m land-sea differences (not

shown) increase considerably in the African upwelling regions, due to the larger T2m rise in the continent than in the ocean, but not in the Iberian Peninsula.

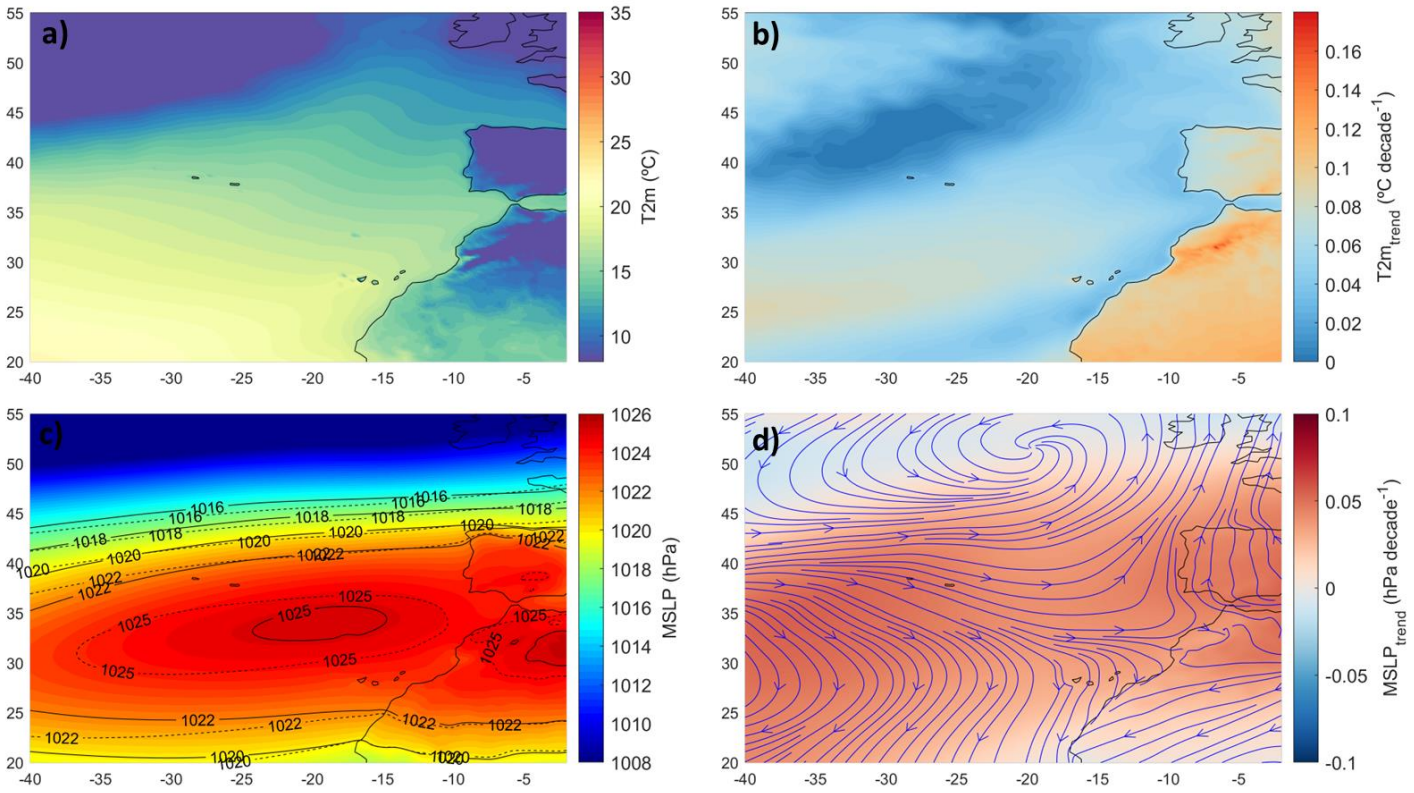

Fig. 4.4. T2m (a) for the historical simulation (1976-2005) and T2m trend (b) from 1950 to 2099 in DJF. MSLP (c) for the historical simulation (1976-2005) and MSLP trend (b) from 1950 to 2099 in DJF. In (c) the isobars are presented for both the historical (continuous black line) and RCP8.5 (dashed black line) simulations. In (d) anomalous wind trajectories (RCP8.5 - Historical) are shown over the MSLP trend.

In the MSLP field for DJF, the highest pressures are located around 35ºN, depicting the position of the Azores high in the historical simulation (continuous line of Fig. 4.4c), the major driver of the large-scale wind pattern in the CCUS. The high pressure region stretches zonally and intensifies in the future (dashed line of Fig. 4.4c). The MSLP trends show a bipolar pattern, with a reduction above 40ºN and an intensification in the region of the Azores high, including the Iberian Peninsula. The wind anomaly trajectory shows a relationship between MSLP intensification and the strengthening of winds, presenting northward direction anomalies over the IUR (intensification of the downwelling winds) and south direction anomalies in the PUR (intensification of the upwelling winds). Therefore, this intensification of the Azores high

seems to lead the changes in the wind field at the end of the 21st century against the increase of air temperatures for the winter months.

In JJA there is a notable rise of the T2m, strongly increased in the African continent with values higher than 35ºC (around 25ºC for the Iberian Peninsula) (Fig. 4.5a). The T2m trends over the ocean are below 0.1ºC decade^{-1} (Fig. 4.5b). However, the T2m over the Iberian Peninsula present trends over 0.2ºC decade^{-1}. Similar trends are found over the African continent, where the T2m increases more in the interior regions than in the coast, which is related to the regulatory effects of the ocean on these coastal regions.

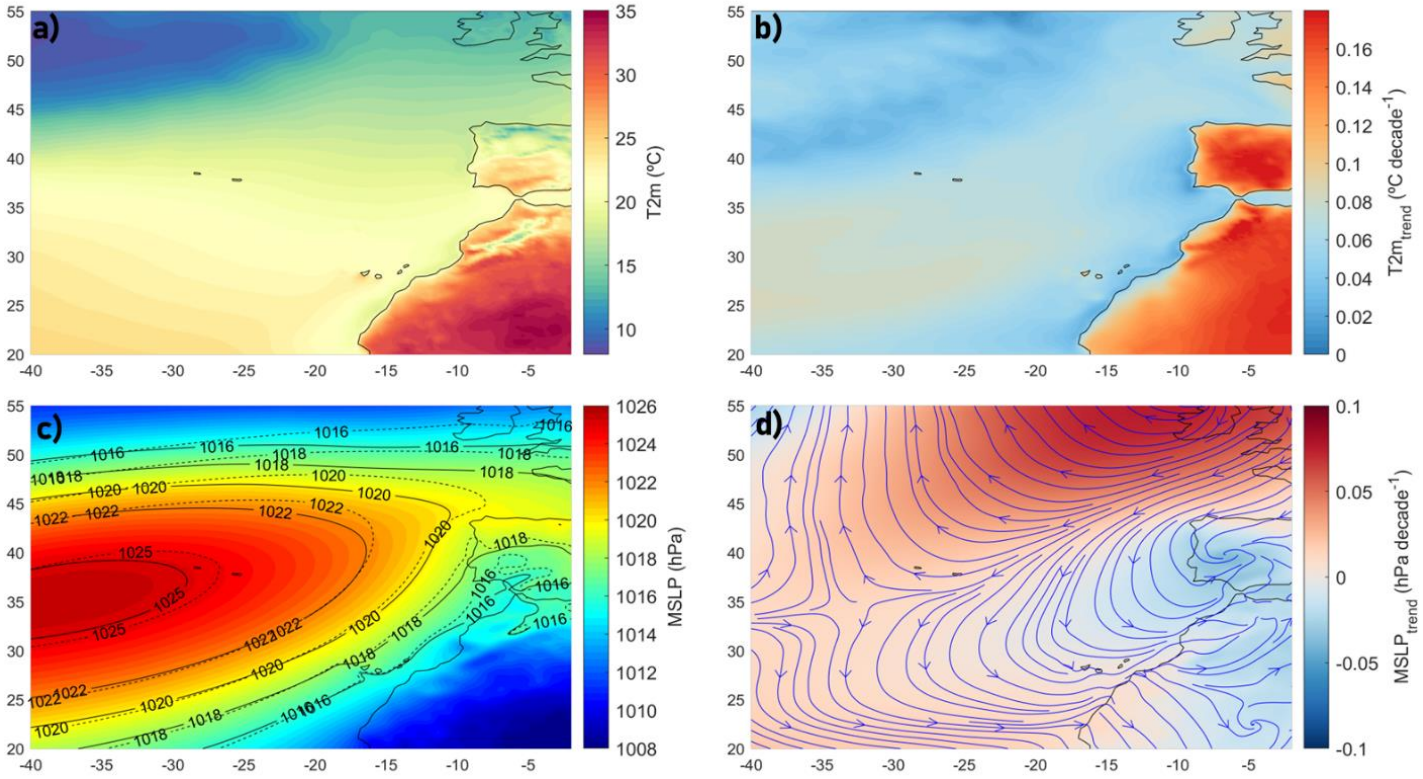

Fig. 4.5 As Fig. 4.4, but for JJA.

In MSLP for JJA (Fig. 4.5c) the highest pressures are located in the western region (Azores high), increasing the pressure gradient toward the Iberian Peninsula and the African coast. In MSLP trends is found a decrease of the MSLP from the Iberian Peninsula to the 20ºW (Iberian thermal low), along with a MSLP intensification centered over the British Isles (Fig. 4.5d).

The intensified thermal low of the Iberian Peninsula is associated with the thermal rise at the end of the 21st century as a consequence of global warming (Fig. 4.5b). Along with the lower pressures over the Iberian Peninsula it appears an anomalous high pressure over the British

Isles, which increases the pressure gradient between Ireland and the Iberian Peninsula, triggering the strengthening of the upwelling winds in the IUR.

4.3.3 Ocean stratification

In this section, we study the role of the ocean stratification as the main driver of change in the regions of the CCUS. Ocean stratification changes in the CCUS for DJF and JJA are evaluated with the help of the Brunt-Väisäla frequency. Brunt-Väisäla frequency is calculated within a 100 km wide band along the MSUR (the mask is shown in Fig. 4.6d) and averaged from surface to 150 m (the average depth associated with the ascent of water masses to the surface; Kämpf and Chapman, 2016).

In DJF, the Brunt-Väisälä frequency presents values lower than 0.005 s^{-1} throughout the CCUS (Fig. 4.6a). It increases slightly as the latitude decreases, reaching 0.008 s^{-1} at the PUR. In JJA, the increase in sea surface temperature leads to a significant enhancement of the Brunt-Väisälä frequency, which reaches values close to 0.01 s^{-1} (Fig. 4.6b). In this season, there are no significant changes with latitude

To assess ocean stratification in the future, we analyzed the differences between ROM_P2 and ROM_P1 (Fig. 4.6; black shading). In DJF, we found a large increase in the Brunt-Väisälä frequency for IUR (Fig. 4.6a). These differences are even stronger in the WPUR, indicating enhanced ocean stratification in the future (almost doubling the values of the Brunt-Väisälä frequency from the historical simulation). In PUR, the stratification remains similar to the present, with differences around 0 s^{-1}. In JJA, the differences between ROM_P2 and ROM_P1 present a similar pattern as in DJF but with lower differences, showinf an increase in ocean stratification in IUR, with the largest differences observed in WPUR (Fig. 4.6b). In PUR, the differences are larger than in DJF, but again, this is the region with the lowest differences between the future and historical period. In summary, ocean stratification increases are mainly found in the two northern regions, with practically no changes in PUR.

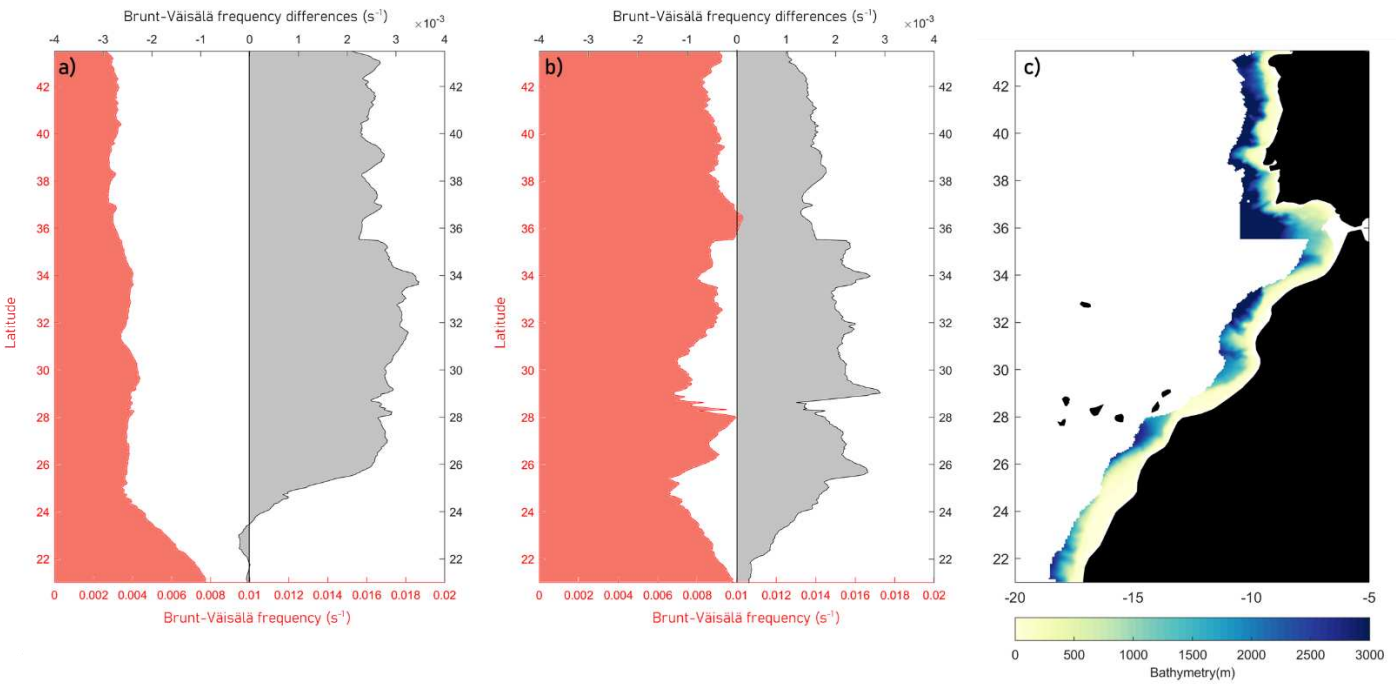

Fig. 4.6 Brunt-Väisälä frequency (s^{-1}) averaged from surface to 150 m in the closest grid points to coast for DJF (a) and JJA (b) for ROM_P1 (red shading; Historical) and the differences between ROM_P2 and ROM_P1 (black shading; RCP8.5 - Historical). The mask used is shown in the panel c.

A very important characteristic of the upwelling is the source water depth. The upwelling source water depth is calculated (see Eq. 4.5) taking into consideration both the action of the alongshore favourable winds and the ocean stratification. We calculate the upwelling source water depth in the historical simulation (ROM_P1) for DJF and JJA (Fig. 4.7 a, b).

In DJF, we found source depths of 0 m in the northern part of the IUR as a result of downwelling favourable winds (Fig. 4.7a). In the southern part of IUR and along the rest of the African coast, we detected source depths above 50 m, with the deepest values occurring in Cape Ghir and PUR (approximately 100 m). In JJA, the IUR presents source depths of around 70 m because downwelling favourable winds turn into upwelling favourable winds at the northern tip of the Iberian Peninsula (Fig. 4.7c). In the African regions, the source depth values remain similar to those in DJF. This is because, although the upwelling favourable winds increase in intensity, the ocean stratification is also enhanced, and the effects of these two opposing mechanisms maintain the same source depth throughout the seasons.

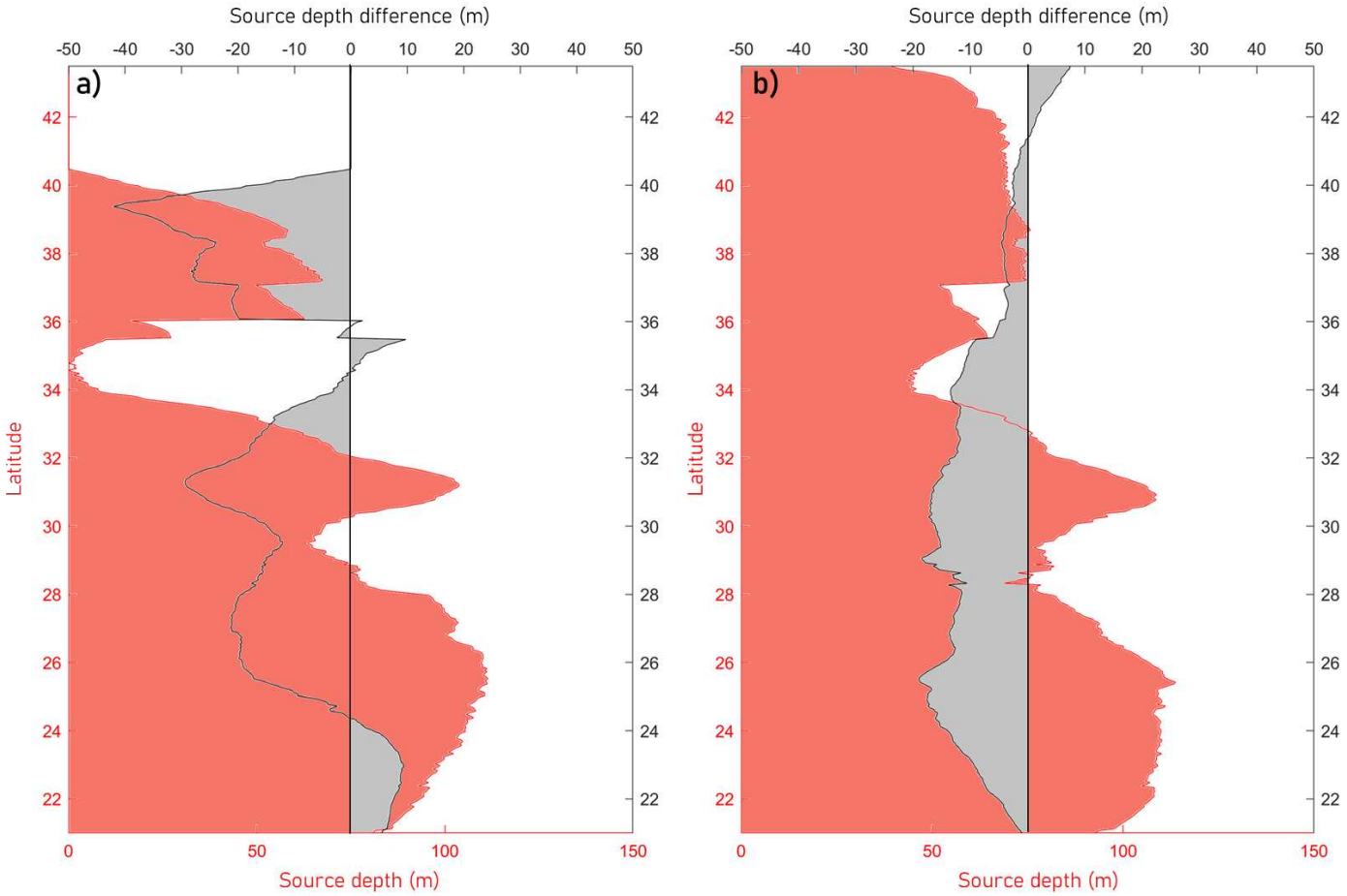

Fig. 4.7 Upwelling source water depth (m) in the closest grid points to coast (Fig. 4.6c) for DJF (a) and JJA (b), both for ROM_P1 (red shading; Historical) and the differences between ROM_P2 and ROM_P1 (black shading; RCP8.5 - Historical). The mask used is shown in Fig. 4.6c.

Differences in source water depth between ROM_P2 and ROM_P1 are shown in Figure 6.7 (depicted in black shading). In DJF, the difference between ROM_P2 and ROM_P1 presents a decrease in source depth that reaches -40 m in the southern IUR (Fig. 4.7a; black shading). This decrease is mainly driven by the weakening of the upwelling favorable winds found in section 4.3.1 and is aided by the enhanced ocean stratification. However, in WPUR, we detect a decrease in source depth (between -30 m and -20 m) associated mainly with the increase in ocean stratification, as we found a strengthening of the upwelling favorable winds in this region. Finally, in PUR, the intensification of the upwelling favorable winds is practically the only driver of change in source depth, since ocean stratification is not enhanced.

In JJA, we detected two main patterns (Fig. 4.7b; black shading): First, in the IUR, where the intensification of the upwelling favorable winds is competing with the enhanced ocean stratification, resulting in a source deepening of 8 m in the future. Second, in WPUR and northern PUR, where the upwelling favorable winds present a weakening in the future, which will be complemented by enhanced ocean stratification (Fig. 4.6b), reducing the source water depth to -20 m in the future.

4.4 Discussion and conclusions

Future climate change has important biological and socio-economic implications in the CCUS. These effects are associated with changes in the upwelling favourable winds and increasing ocean stratification (Garcia-Reyes et al. 2015). Here, we take advantage of the regional climate system model ROM to reach oceanic and atmospheric resolutions that allow us to achieve a regional view of the climate change impact in the CCUS. The projected coastal upwelling wind changes present a clearly differentiated seasonal cycle and marked latitudinal variations under the RCP8.5 scenario. The IUR shows a strengthening of the upwelling (downwelling) favourable winds in JJA (DJF), which is in accord with results reported in Sousa et al. (2017a) from a EURO-CORDEX multimodel study. Similar results were shown by Casabella et al. (2014) and Alvarez et al. (2017) in terms of upwelling intensity in the northwest of the Iberian Peninsula. Further south, our results show that the African coast is projected to experience a decrease in the upwelling favourable winds in the JJA and an increase in DJF. Sousa et al. (2017b) found similar results with the AFRICA-CORDEX ensemble model, confirming the clear seasonality of the change in the CCUS under global warming conditions found in this study.

These results were obtained by other authors (Garcia-Reyes et al. 2015; Rykaczewski et al. 2015; Wang et al. 2015; Sousa et al. 2017a; Sousa et al. 2017b; Aguirre et al. 2019; Sylla et al. 2019; Varela et al. 2022), who associated the upwelling winds increase with increasing summertime T2m land-sea differences (Bakun, 1990) or shifts in the positioning of the atmospheric high-pressure systems (Rykaczewski et al. 2015). However, we do not find a significant relationship between these mechanisms and the seasonal and latitudinal changes in upwelling wind intensity. We propose two mechanisms, one for each season studied: (1) In DJF, the intensification of the Azores high will increase the downwelling and upwelling winds in the IUR and PUR, respectively. (2) In JJA, the larger pressure gradient between the Iberian

Peninsula and the British Islands will strengthen the Iberian upwelling winds in the future. This larger MSLP gradient is associated with two responses to climate change: (a) the air temperature increase at the end of the 21st century will intensify the summer thermal low over the Iberian Peninsula (Fig. 4.5b and 4.5d), (b) the weakening of the AMOC in the future will temper the temperature rise over the North Atlantic, triggering an increase of pressures in the British Islands (Fig. 4.5; Haarsma et al. 2015).

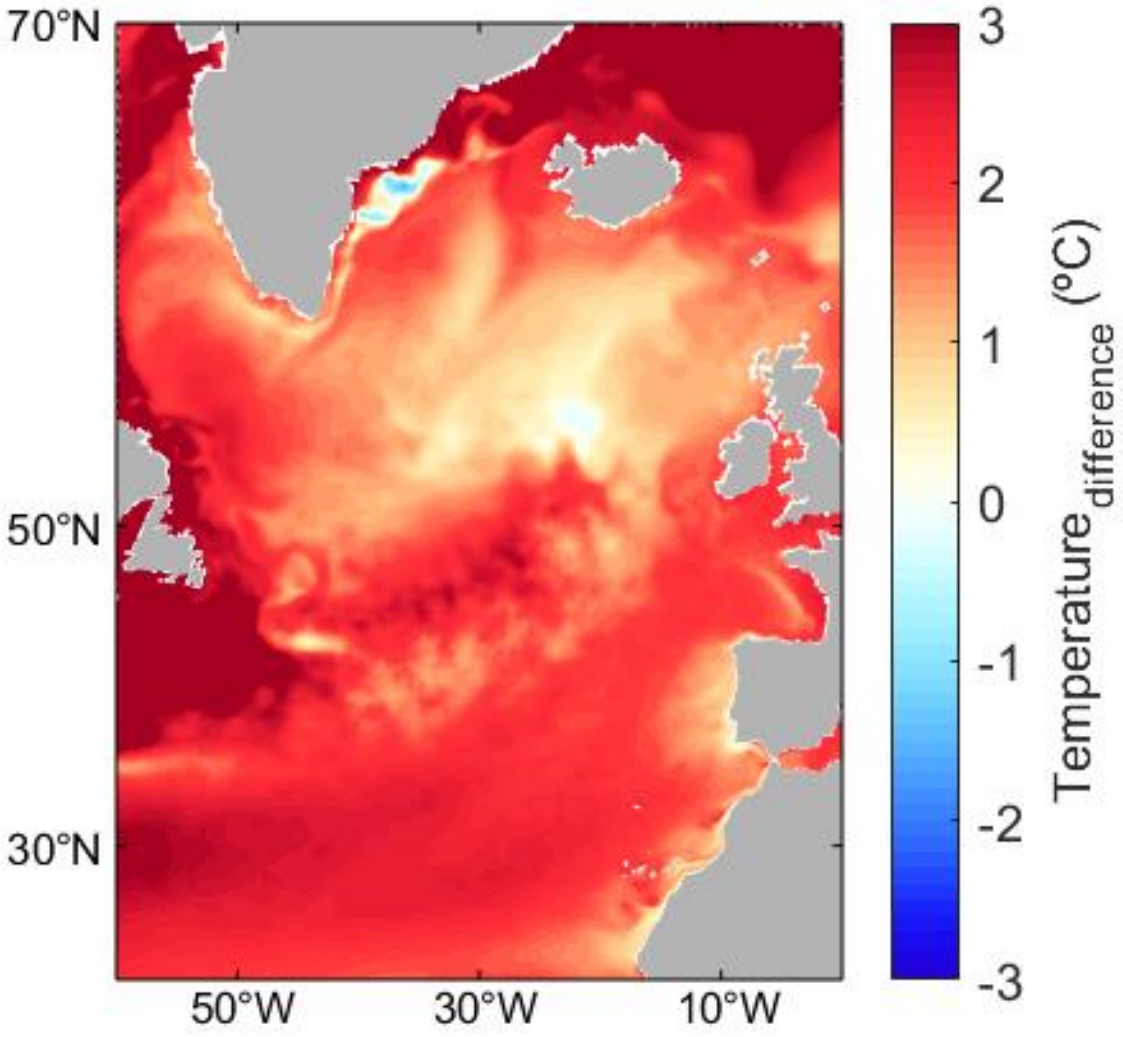

Fig. 4.8. Temperature difference between the future and historical simulation in 8 m for JJA.

First, the Iberian thermal low will be intensified in the future as a consequence of a more than evident temperature increase over the Iberian Peninsula in JJA (Fig. 4.5). This fact was reported by Miranda et al. (2013) with a RCM, and Soares et al. (2017) associated the upwelling wind intensification with Anticyclone-Thermal Low dipole enhanced in the future. Like those

studies, we find an intensification of the Iberian thermal low, but the MSLP increase over the British Islands is not associated with a greater influence of the Azores high in the northeast but with a weakening of the AMOC in the future. This fact was studied by Haarsma et al. (2015), who proposed that the surface waters will be less dense in the North Atlantic due to an intensification of the precipitation and enhanced Greenland mass loss in the future, which will reduce the sinking of deep water and will weaken the AMOC. Thus the weakening will temper the North Atlantic, containing a minimum of temperature over the northern North Atlantic (Fig. 4.8), decreasing the northward heat transport by the AMOC and increasing the pressures over the British Islands (de Vries et al. 2022). This fact in conjunction with the intensification of the thermal low in the Iberian Peninsula will be the driver of upwelling strengthening in the IUR in JJA.

In coastal upwellings an increased ocean stratification limits the depth from which water is upwelled, reducing the coming of nutrients to the euphotic zone (Chhak and Di Lorenzo 2007; Jacox and Edwards, 2011; Jacox et al. 2015). Our results show an increase of the ocean stratification in coastal regions, being more evident in the two northernmost regions both in DJF and JJA (Fig. 4.6). This is due to the fact that although the ocean stratification is associated with the ocean warming, the upper layers of the north Atlantic will present a freshening in the future. This freshening is limited to the upper 200 m, which will generate an increase of the stratification in the shallow regions as the coastal upwelling. This pattern is associated with a larger scale freshening in the Eastern North Atlantic (Fig. 4.9) as reported by Levang and Schmit (2019) in a study with CMIP5 models. The Canary current carries the freshening signal from the north to southern regions and it is separated from the coast in Cape Blanc to join with the north equatorial current (Stramma, 1984; Mason et al. 2011; Santana-Falcón et al. 2020), and does not carry practically the freshening to the PUR.

Therefore, in our study we found both changes in wind patterns and ocean stratification as possible drivers of changes in coastal upwelling under climate change conditions in the CCUS. However, both mechanisms have not been brought together to evaluate the effects of climate change on this vulnerable system. This fact is one of the main challenges for the scientific community and recent studies have attempted to evaluate the impact of climate change by combining both mechanisms using an ensemble of "Community Earth System Model (Chang et al. 2023; Jing et al. 2023) for the four EBUSs. However, these studies use latitudinal averages to evaluate a single upwelling system. Like previous studies (Sousa et al. 2017a; Sousa et al.

2017b), we advocate for the implementation of latitudinal studies to provide an accurate response to this important challenge. In fact, our study demonstrates the great latitudinal variability of the CCUS, showing different responses depending on the upwelling region within the CCUS.

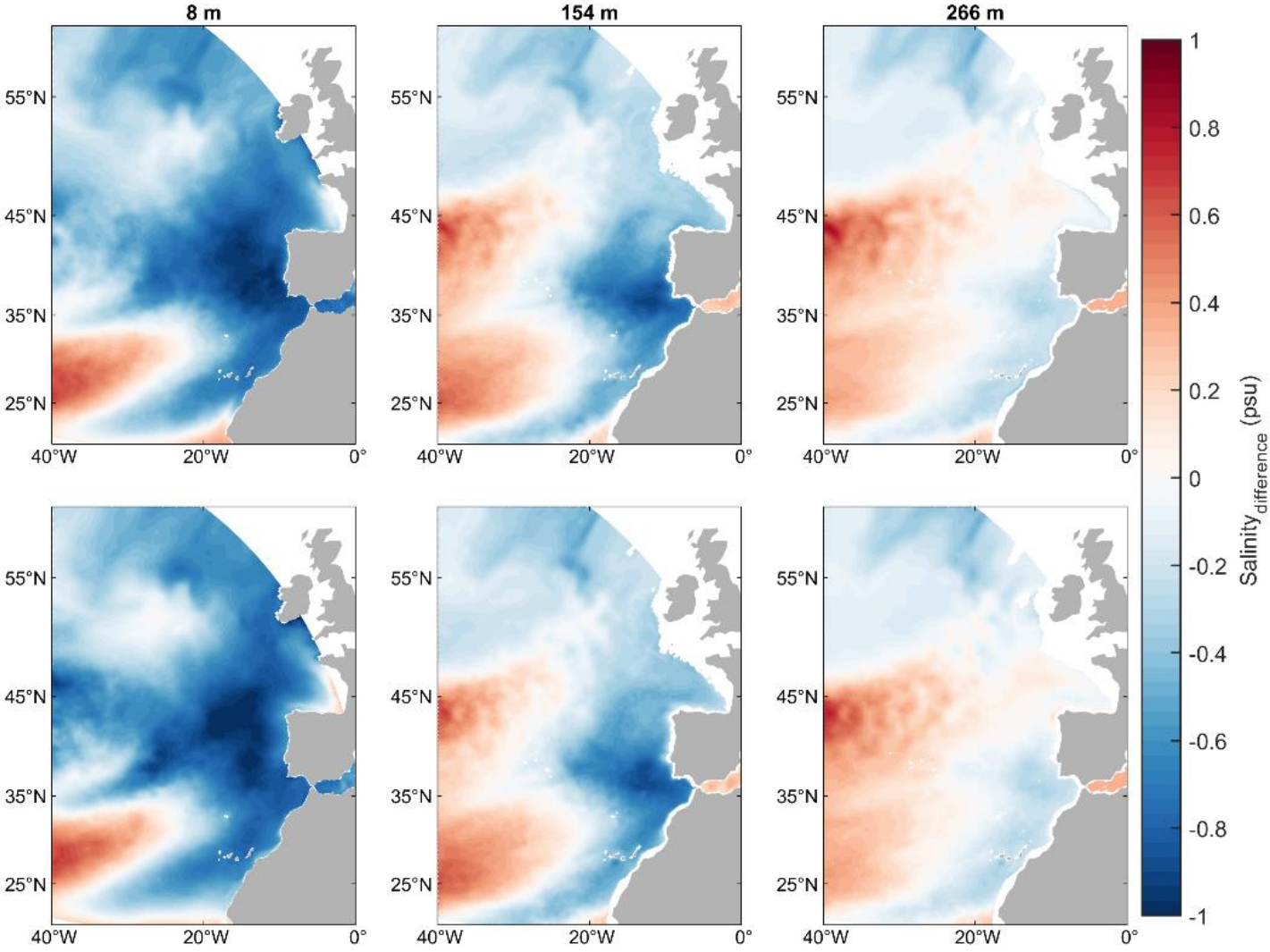

Fig. 4.9. Salinity difference between the future and historical simulation in three depths: 8 m, 154 m and 266 m for DJF (upper row) and JJA (lower row).

To address this challenge, we evaluated the joint action of wind and ocean stratification based on the upwelling source depth. Our results show that upwelling will be reduced in the southern region of the IUR and throughout the WPUR for DJF. This shallowing of the upwelling source depth in winter months is primarily associated with changes in ocean stratification (Fig. 4.10a), which will play a major role in the future, overlapping changes in wind patterns. These results are consistent with studies such as Oyarzun and Brierley (2019) in the Humboldt upwelling

system and Sousa et al. (2020) in the north of the Iberian Peninsula. However, in JJA in the north of the Iberian Peninsula, the upwelling source depth will be greater. In this sense, our results show a competitive role between improved ocean stratification and intensifying upwelling winds in the future (Fig. 4.10b). Jing et al. (2023) found an increase in upwelling source water depth due to a stronger wind effect overcoming the effect of enhanced ocean stratification for the CCUS, and Chang et al. (2023) reported an increase in vertical transport towards the surface in the CCUS associated with an increase in Ekman suction. However, in the rest of the CCUS regions, enhanced ocean stratification complements weakening upwelling winds, generating a shallower upwelling source depth.

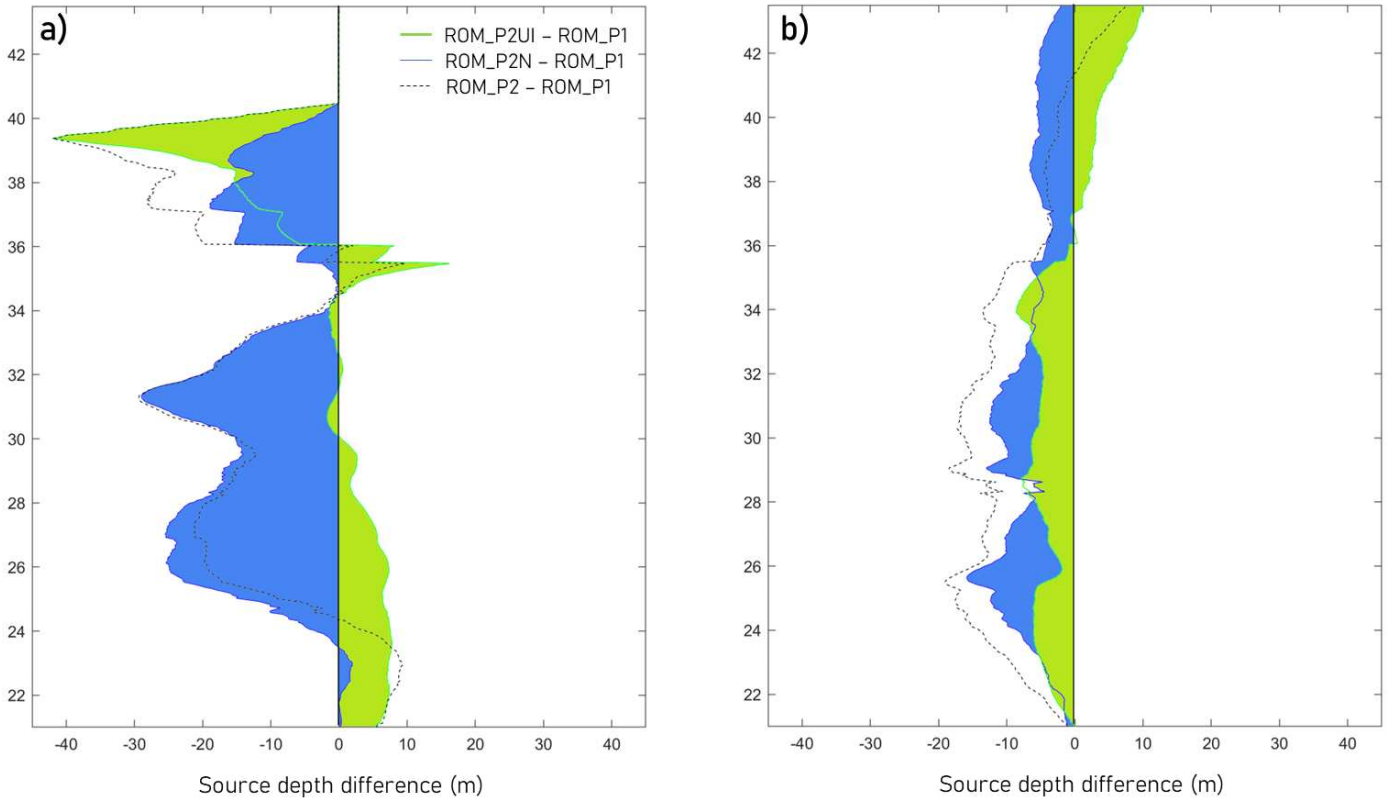

Fig. 4.10. Upwelling source water depth differences (m) in the closest grid points to coast (Fig. 4.6d) for DJF (a) and JJA (b) between ROM_P2UI (green shading), ROM_P2N (blue shading), ROM_P2 (dashed line) and ROM_P1. The mask used is shown in Fig. 4.6d. ROM_P2UI is calculated by maintaining the *N* of the historical simulation and the *UI* of the future (ROM_P2UI), and ROM_PN is calculated by maintaining the *UI* of the present and the *N* of the future (ROM_P2N).

Therefore, there is no dominant mechanism in the CCUS under climate change conditions, and both intensification and weakening depend on latitude, season, as well as the complementarity or competitiveness of wind patterns and ocean stratification.

CHAPTER 5:

Seasonality of coastal upwelling trends in the Mauritania-Senegalese region under RCP8.5 climate change scenario

The contents of this chapter have been submitted to Science of the Total Environment and it is under review:

Vázquez R., Parras-Berrocal I.M., Shunya K., Cabos W., Sein D.V., Izquierdo A. (2023) Seasonality of coastal upwelling trends in the Mauritania-Senegalese region under climate change scenarios. In preparation.

5.1 Introduction

The Canary Current Upwelling System (CCUS), one of the most important marine ecosystems in the world, constitutes one of the four large Eastern Boundary Upwelling Systems (EBUSs). EBUSs are driven by the equatorward alongshore winds that transport the surface waters offshore (Ekman dynamics), which in turn are replaced by cold and nutrient-rich waters from subsurface (Bakun 1990).

CCUS is located in the eastern branch of the North Atlantic subtropical gyre (Kämpf and Chapman, 2016), extending from the northern tip of the Iberian Peninsula (43ºN) to the southwest of Senegal (around 12ºN). Although the CCUS is well known for its coastal productive areas, it also plays a key role in the enrichment of the oligotrophic open ocean through the shedding of mesoscale structures as filaments and eddies, which contribute to the offshore transport of the upwelled coastal waters (Lovecchio et al. 2017). In terms of seasonality and intensity, the CCUS is divided into four regions: Iberian upwelling region (35ºN-43ºN), weak permanent upwelling region (26ºN-33ºN), permanent upwelling region (21ºN-26ºN) and the southernmost Mauritania-Senegalese upwelling region (12ºN-19ºN; MSUR).

The MSUR, unlike the rest of the CCUS, is not only influenced by the Azores high pressure centre, but it is also highly dependent on the latitudinal migration of the Intertropical Convergence Zone (ITCZ) (Sylla et al. 2019). In winter, when the ITCZ reaches its southernmost position, the strong northeastern equatorward trade winds cause upwelling in the coast of Guinea, Senegal and Mauritania (12ºN-19ºN). However, in summer, the ITCZ shifts to the north, weakening the winds in the whole region. As a result the coastal upwelling is reduced, even reversing to downwelling in the Senegalese region (Cropper et al. 2014) due to the appearance of the onshore monsoonal winds (Gomez-Letona et al 2017). Therefore, the MSUR presents a large seasonal and latitudinal variability clearly defined by the migration of the ITCZ (Pardo et al. 2011; Cropper et al. 2014; Benazzouz et al. 2015) and divided by Cap Vert (~15ºN), with year-round upwelling favourable winds in the northern MSUR and downwelling favourable winds during the summer months in the southern MSUR.

The future behavior of the EBUSs under climate change has been analyzed in a number of studies under different hypothesis and yielding different outcomes. As early as 1990, Bakun proposed that an increased warming over the continent in comparison to the ocean would result

in a strengthening in upwelling favourable winds. Rykaczewski et al. (2015) proposed that the changes in the upwelling favourable winds would be mostly related to shifts in the position and timing of the high pressure cells rather than changes in the continental thermal low pressure systems. Sylla et al. (2019) bore out this hypothesis for the MSUR, where they found a strong relationship between changes in the upwelling and shifts in the Azores high along with an influence of the Sahara thermal low expansion in the northern MSUR. However, the wind is not the only driver of change at the end of the 21st century and Oyarzun and Brierley (2019) and Sousa et al. (2020) found that global warming could cause an increase in the ocean stratification that will disconnect the wind stress from the deeper waters.

However, the coarse spatial resolution (below 1º x 1º) of GCMs comprised in CMIP5 is not enough to resolve the latitudinal EBUS variability and to reproduce their mesoscale features or detailed shelf dynamics (García-Reyes et al. 2015; Xiu et al. 2018; Varela et al. 2022). Thus, there is still uncertainty about what is the main driver of future change in the MSUR, and the relative role played by the ocean stratification and wind. Although the models from High Resolution Model Intercomparison project (HighResMIP, Haarsma et al. 2016) present an opportunity for nearshore analysis (Varela et al. 2022; Sylla et al. 2022) they still have a resolution coarser than 25 km. In fact, recent studies (García-Reyes et al. 2015; Wang et al. 2015; Sein et al. 2017; Gómez-Letona et al. 2017; Bindoff et al. 2019; Vázquez et al. 2022) showed the need for much higher horizontal resolution for the representation of mesoscale processes in the upwelling systems that are partly masked in the current GCMs. Considering the increased upper-ocean stratification and decreased nutrient supply, exploring the response of ecosystems to intensified upwelling and ocean surface warming would require a more detailed modeling framework for a better representation of the relevant physical processes. These processes can be reproduced by Regional Climate Systems Models (RCSMs) (Xiu et al. 2018; Vázquez et al. 2022).

The MSUR is considered to be the most productive region in the CCUS, according to Sylla et al. (2019). However, the attempt to evaluate the effects of climate change has triggered a significant amount of uncertainty due to the coarse resolution of GCMs. Therefore, this study aims to investigate the evolution of the MSUR under the RCP8.5 scenario with a RCSM that is capable of reproducing the relevant mesoscale processes in the other three CCUS regions with a high confidence in a present climate (Vázquez et al. 2022).

The objectives of this study can be summarized as follows:

- First, to validate the representation of the main variables in the MSUR in a present time.

- Second, to assess the projected climate change signal in the MSUR under the RCP8.5 scenario, analyzing both the action of the wind pattern and the ocean stratification under the global warming conditions.

The paper is organized as follows: the model, data sets and methodology are described in section 5.2, the model validation and the results are presented in section 5.3 and 5.4, respectively. Finally, the discussion is presented in the section 5.5 and conclusions in section 5.6.

5.2 Methodology

5.2.1 Model setup

In this study we use the RCSM ROM (Sein et al. 2015), which comprises the REgional atmosphere MOdel REMO (e.g. Jacob, 2001) with horizontal resolution of 25 km with a rotated grid coupled to the global ocean-sea ice-marine biogeochemistry model MPIOM/HAMOCC (Marsland et al. 2003) via the OASIS3 coupler (Valke, 2013). Moreover, ROM includes the Hydrological Discharge model (Hagemann and Dümenil-Gates, 1998, 2001) and a dynamic/thermodynamic sea ice model (Hibler, 1979).

MPIOM is discretized on an orthogonal curvilinear Arakawa C-grid, with two grid poles over North America and northwestern Africa that allows a high resolution in the CCUS while maintaining a global domain (Vázquez et al. 2022). In the MSUR, the MPIOM resolution ranges from 9 km (northernmost region) to 15 km in the southernmost region (Fig. 5.1). The ocean model has 40 vertical levels with increasing level thickness towards the ocean bottom (Sein et al. 2015; Vázquez et al. 2022). The ocean spin-up was done according to the procedure described in Sein et al. (2015). MPIOM is started with climatological temperature and salinity data (Levitus et al. 1998). Subsequently, it is integrated six times through the 1958–2002 period forced by ERA-40 and one more time by ERA-Interim reanalysis (1979–2012) and with 60 min coupling timestep.

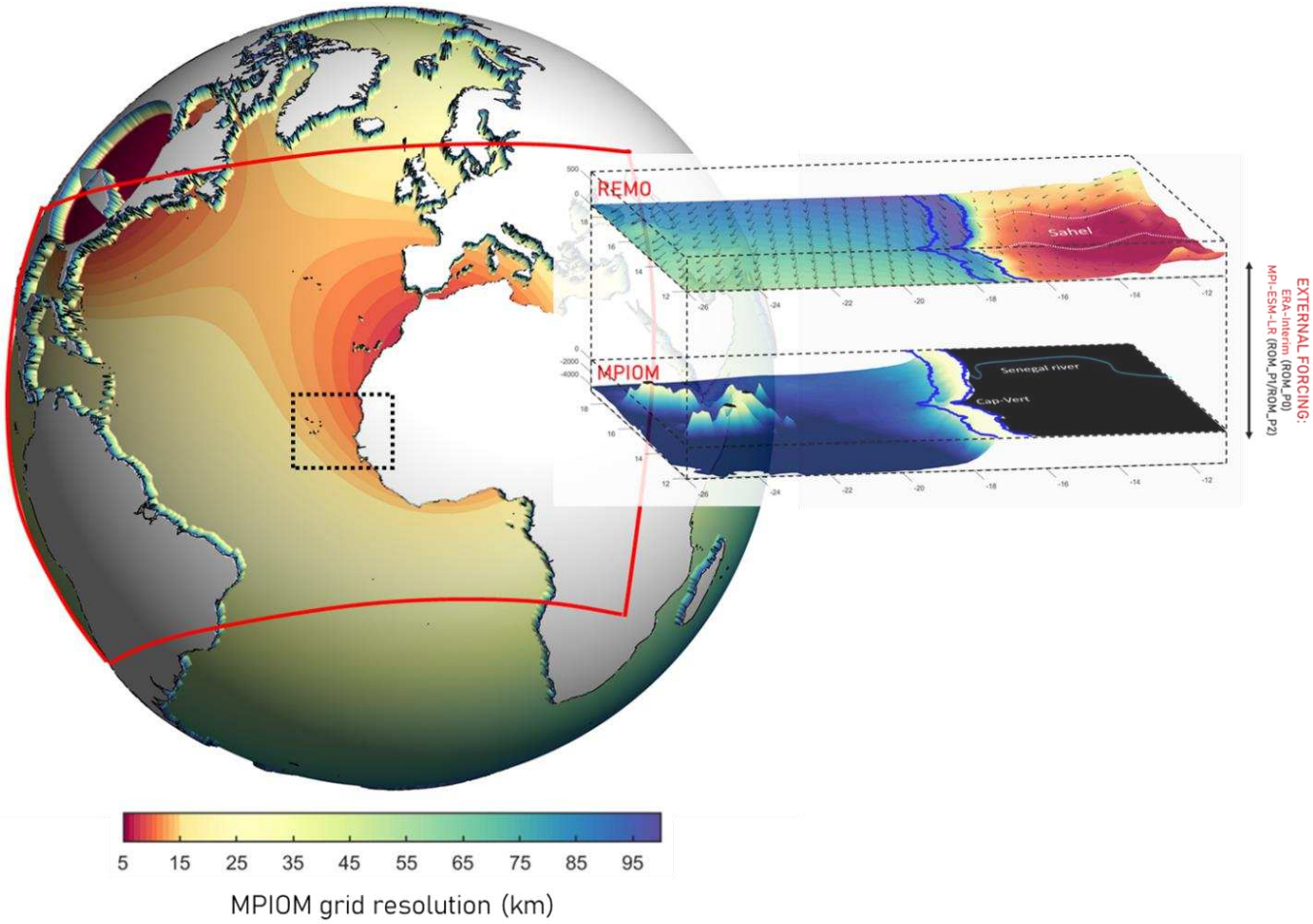

Fig. 5.1 MPI-OM grid resolution (km) and REMO domain (red line). The black box represents the MSUR domain (12ºN-19ºN). The overlaid figure outlines the MSUR domain with the external forcing used in the work and the mask used for the upwelling index calculation (blue lines). It is also outlined the 2 m air temperature, the wind field, the bathymetry and topography of ROM. The Sahel region was located following Ikazaki (2015).

In this work we use two different global sources to provide lateral boundary conditions for REMO and to force MPIOM outside the coupling region: ERA-Interim (Dee et al. 2011) and MPI-ESM-LR (Giorgetta et al. 2013). In the region covered by REMO (Fig. 5.1) the atmosphere and the ocean interact while prescribed atmospheric forcing drives the rest of the global ocean, outside the coupled domain. A 30 year-long experiment forced by ERA-Interim (ROM_P0) was used to evaluate the ability of ROM to simulate the present climate (1980-2012) in the MSUR. Then, in order to evaluate the impact of climate change in the MSUR, we run ROM model forced by MPI-ESM-LR (about 1.5º ocean and 2º atmospheric resolution) for two periods: the first, extends from 1950 to 2005 (ROM_P1) is the historical run and the

second, which extends from 2006 to 2099 represents the future climate under the Representative Concentration Pathway 8.5 (RCP 8.5) CMIP5 scenario (ROM_P2).

5.2.2 Validation strategy and climate change evaluation

To evaluate the ROM_P0 performance in the MSUR, we focus on the wind field over the coastal band from which we build an upwelling index (Eq. 3). We also evaluate the main drivers involved in the changes of upwelling winds over the MSUR: Azores high and the ITCZ. The validation is carried out against ERA5 reanalysis (Hersbach et al. 2020), which presents a constant spatial resolution of 31 km.

The upwelling index (*UI*, Bakun et al. 1973) is based on the offshore wind-driven Ekman transport (***Q***) and is calculated as follows:

$$Q_x = \frac{\tau_y}{f\rho_0} \quad \text{Eq. 5.1}$$

$$Q_y = -\frac{\tau_x}{f\rho_0} \quad \text{Eq. 5.2}$$

$$UI = -sin\left(\theta - \frac{\pi}{2}\right) Q_x + cos\left(\theta - \frac{\pi}{2}\right) Q_y \quad \text{Eq. 5.3}$$

where Q_x, Q_y and τ_x, τ_y are the zonal and meridional components of the horizontal Ekman transport and the wind stress vector, respectively; ρ_0 is the reference sea water density (1025 kg m^{-3}); f is the Coriolis parameter and θ is the angle between the coastline and the equator. The UI is estimated within a 100 km wide band along the MSUR (mask in Fig. 5.1; Benazzouz et al. 2014; Lovecchio et al. 2017; Bonino et al. 2019) and it is expressed as the oceanward flow of surface waters per km of coastline (m^3 s^{-1} km^{-1}; Pardo et al. 2011). The Azores high and the ITCZ position are assessed from the mean sea level pressure (MSLP) and wind fields.

In order to assess the future change in seasonality and intensity of the coastal upwelling we use the whole historical (1950-2005) and RCP8.5 (2006-2099) simulated periods to calculate the *UI*, near-surface air temperature (T2m) and MSLP trends. Also, we calculate the wind change as the difference between the time-averaged ROM_P2 (2070-2099) and ROM_P1 (1976-2005) outputs. Moreover, the coastal stratification is characterized in both periods through the Brunt-Väisälä frequency (*N*), where larger values indicate strong stratification, and values close to zero a well-mixed water column:

$$N^2 = \frac{g}{\rho_0}\frac{\partial \rho}{\partial z} \quad \text{Eq. 5.5}$$

where z is the depth, ρ the potential density and g is the gravitational acceleration.

We also use the source depth (*Ds*) to estimate the depth of the waters that reach the surface in the coastal upwelling region. *Ds* gives us further insight into the properties of upwelled waters and the mechanisms that drive the coastal upwelling in the future, as a combined effect of the changes in wind stress and coastal ocean stratification. This parameter is defined in He and Mahadevan (2021) as follows:

$$Ds = Cs\ \left(\frac{UI}{N}\right)^{1/2} \quad \text{Eq. 5.6}$$

where $Cs = (4/Ce)^{1/2} = 8.16$ for $Ce = 0.06$, which is the efficiency factor used in Fox-Kemper and Ferrari (2008) and He and Mahadevan (2021).

5.3 Evaluation

5.3.1 Alongshore winds

In terms of the *UI*, the MSUR is divided in two parts: The northern MSUR extends from the south of Cape Blanc (19ºN) to Cap Vert (15ºN), where the *UI* is positive year-round, with peaks in April and May (Fig. 5.2a). The southern MSUR is located to the south of 15ºN, where the coastal ocean is under downwelling favourable winds from July to September, as the ITCZ reaches its northernmost position in summer.

ROM reproduces well the seasonal cycle of the *UI* (Fig. 5.2b), presenting the same seasonal and spatial pattern as ERA5, with the northward migration of the ITCZ in the summer period. ERA5 presents larger *UI* values than ROM_P0 in the northern MSUR from April to May. In summer, ROM_P0 presents a downwelling more extended to the north and intense than ERA5 (-200 $m^3\ s^{-1}\ km^{-1}$). These discrepancies may be partially explained by the higher horizontal resolution of ROM against ERA5. In this context, Vázquez et al. (2022) found significant differences in the ERA5 reanalysis at points closest to the coast in the CCUS, when compared to a higher-resolution observational dataset, demonstrating the importance of high resolution to reproduce the mesoscale processes in the upwelling regions. Nevertheless, both the

latitudinal and seasonal correlations between ERA5 and ROM_P0 winds are higher than 0.94, confirming the good performance of ROM in reproducing the coastal wind field.

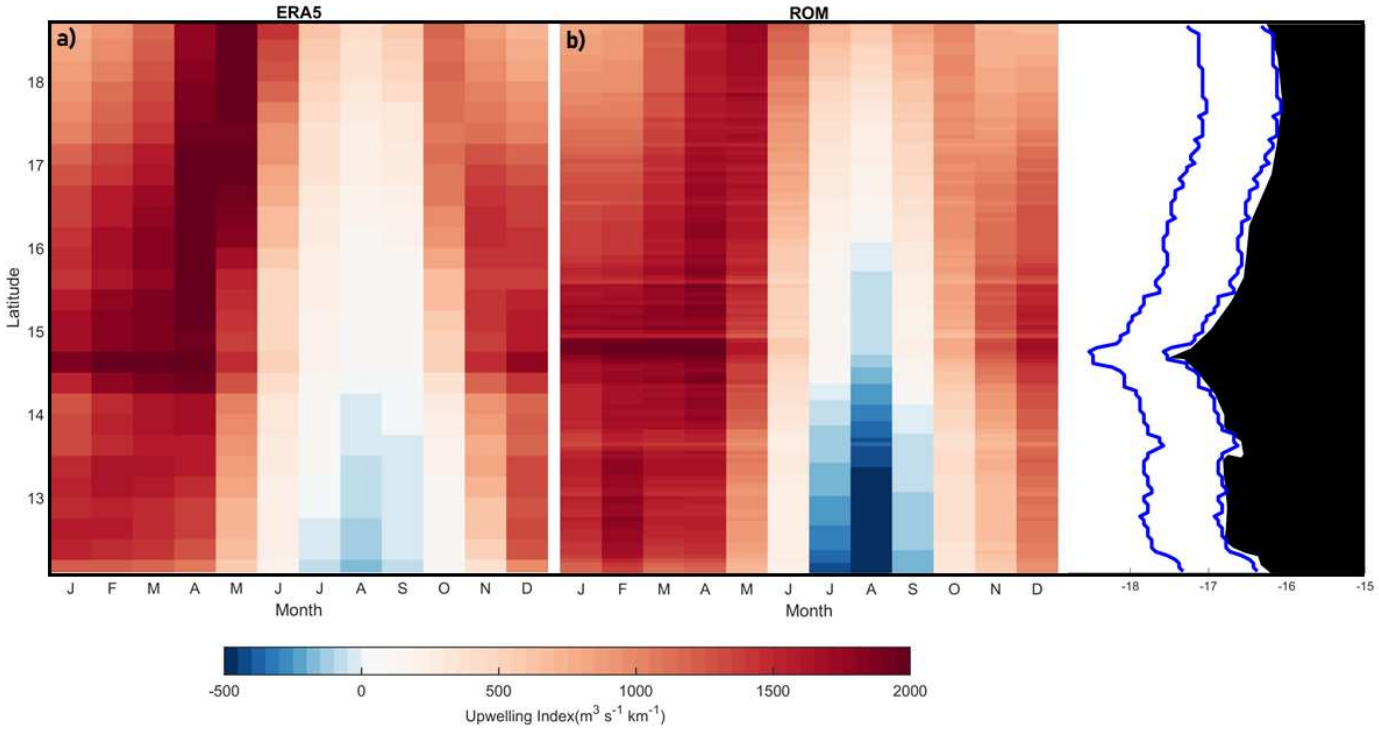

Fig. 5.2 Seasonal cycle of the *UI* (m^3 s^{-1} km^{-1}) averaged over the closest grid-points to the coast in ERA5 (a) and ROM_P0 (b).

5.3.2 Drivers of the alongshore winds

In this section we evaluate the drivers involved in the seasonal march of the alongshore favourable winds over the MSUR: The Azores high and the ITCZ. Both drivers present a seasonal north-south oscillation, since are part of the Hadley cell.

In April, the centre of the Azores high is located to the south of 35ºN in ERA5, reaching its annual southernmost and easternmost position (Fig. 5.3a). These conditions make April the month with the strongest upwelling favourable winds in the MSUR. Moreover, along with the southward shift of the Azores high, the ITCZ presents its southernmost position, which is identified by surface winds convergence and associated with a low pressure band (between 5ºS and 5ºN). As a result there are upwelling favourable winds both in the northern and southern MSUR.

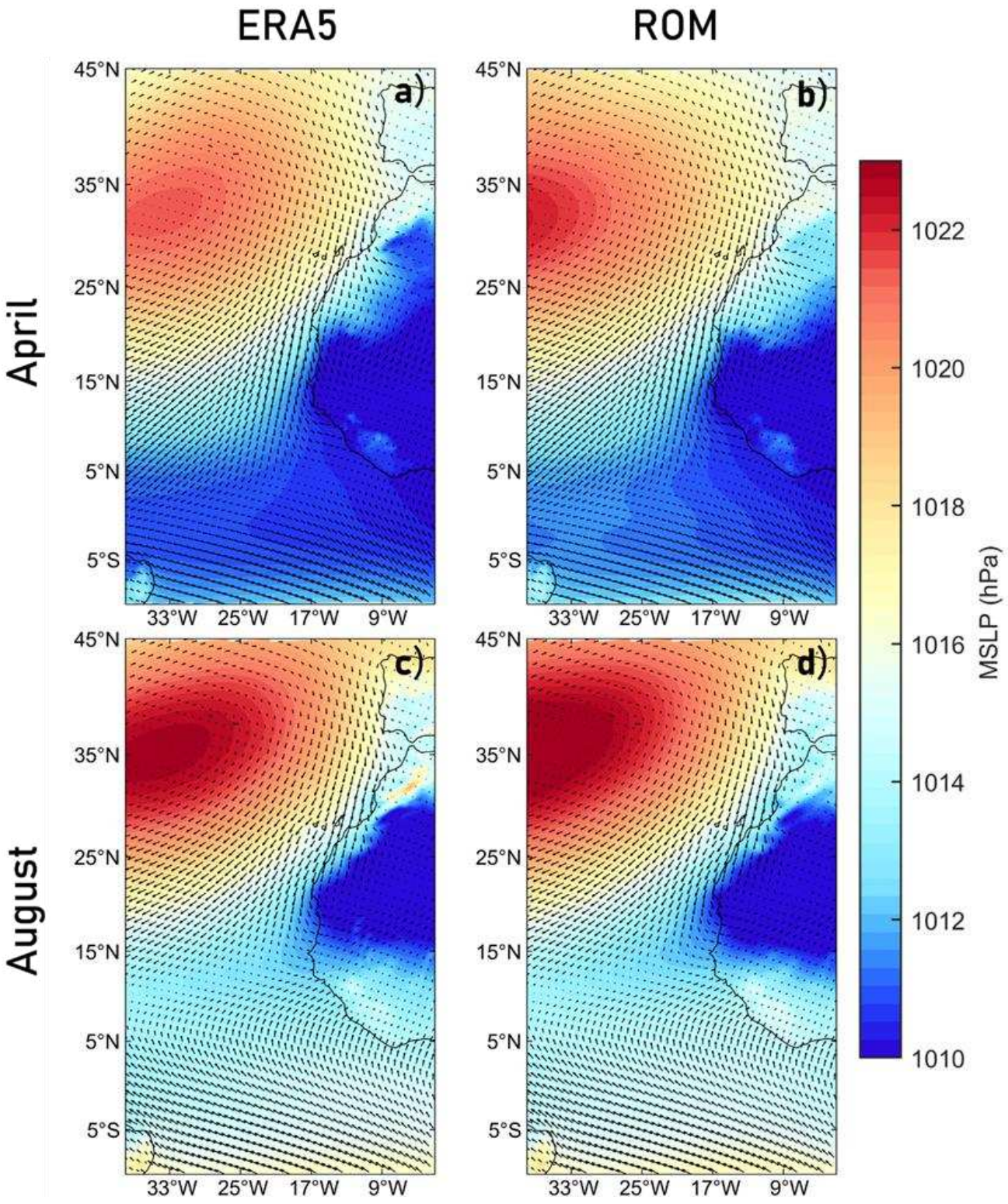

Fig. 5.3 Climatological mean sea level pressure (hPa) and wind field in April (top) and August (bottom) for ERA5 (a, c) and ROM_P0 (b, d) from 1980 to 2012.

During the summer season, the Azores high and ITCZ migrate to the north being centered at 35ºN and 13ºN, respectively (Fig. 5.3c). This fact make August the month with the weakest upwelling favourable winds in MSUR in the year, with downwelling favourable winds in the southern MSUR. ROM_P0 reproduces well the seasonality of the MSLP field, representing the northward migration of the trade winds belt (Fig. 5.3d). Therefore, we can conclude that ROM is able to reproduce the main drivers of the wind field and its seasonality in the MSUR.

5.4 MSUR under global warming

With the objective to investigate possible seasonality changes in the MSUR for the future, we calculate the monthly *UI* trends (1950-2099) along the coast (Fig. 5.4). In January positive *UI* trends are found in the whole MSUR (Fig. 5.4a) with maximum values between 13ºN and 15ºN (20 m^3 s^{-1} km^{-1} $decade^{-1}$), due to a future strengthening of the upwelling favourable winds. From February to April (Fig. 5.4b-d) positive trends are found through all the northern MSUR, but the trends turn negative in the southern MSUR reflecting a weakening of the upwelling favourable winds (-20 m^3 s^{-1} km^{-1} $decade^{-1}$). In May (Fig. 5.4e) the *UI* trend is nearly zero in all MSUR. From June to September (Fig. 5.4f-i), the *UI* trends indicate a future intensification of the upwelling favourable winds for the northern MSUR and a weakening of the downwelling favourable winds in the southern MSUR (Fig. 5.2). In November-December (Fig. 5.4k-l), the trends are similar to January, positive in the whole region except for the southernmost latitudes.

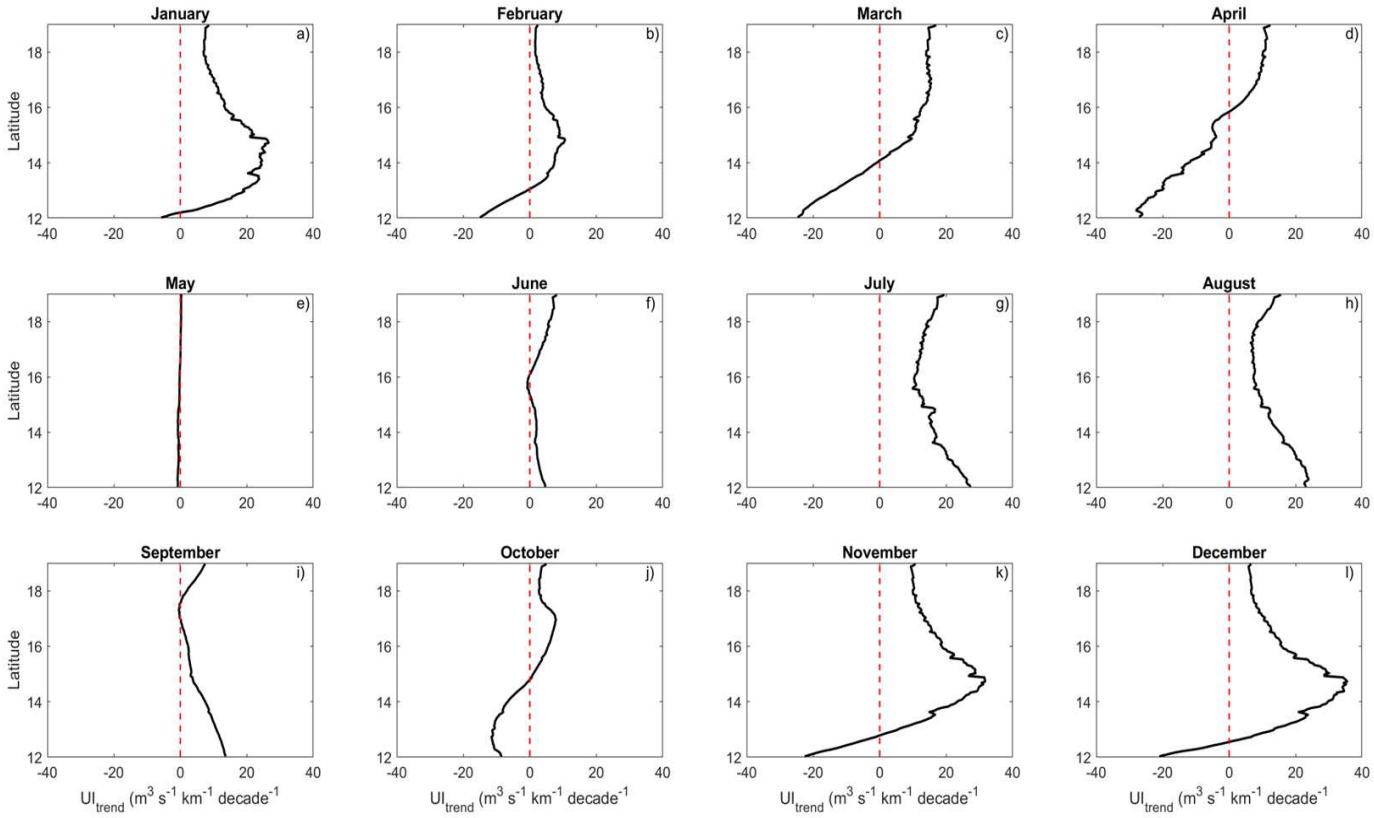

Fig. 5.4 Monthly linear trends of *UI* ($m^3\ s^{-1}\ km^{-1}$ $decade^{-2}$) averaged over the closest grid points to the coast from 1950 to 2099.

On the basis of the *UI* trend latitudinal pattern we divide the year in three periods: (Period 1) January, November and December with positive trends over most of the region, with maximum values around 15º N and negative trends in the southernmost region; (Period 2) March and April with bipolar *UI* trends: positive north of 15ºN and negative to the south; and (Period 3) June, July, August and September with positive *UI* trends in the whole domain. February, May and October were removed from the analysis because they behave as transition months between periods with clearly defined latitudinal trends.

Along with the *UI*, we assessed the MSLP and T2m trends over the same period. In Period 1, when positive *UI* trends (Fig. 5.5a; black line) can be found in practically the whole coastal region with maximum values around Cap Vert, the T2m shows a remarkable local increase in the southern Sahel, around 12N-14ºN, while the Azores high intensifies (Fig. 5.5c). These conditions strengthen the upwelling favourable winds over the whole MSUR. Moreover, the local increase of T2m in the southern region of Sahel reduces the continental low pressures, generating a cyclonic circulation anomaly around 15 ºN and 12ºW. This mechanism further intensifies the upwelling favourable winds in practically the whole domain, excepting 12ºN,

where the wind anomaly turns onshore, weakening the upwelling winds in the southernmost region (Fig. 5.5c; see with detail in Fig. 5.10a).

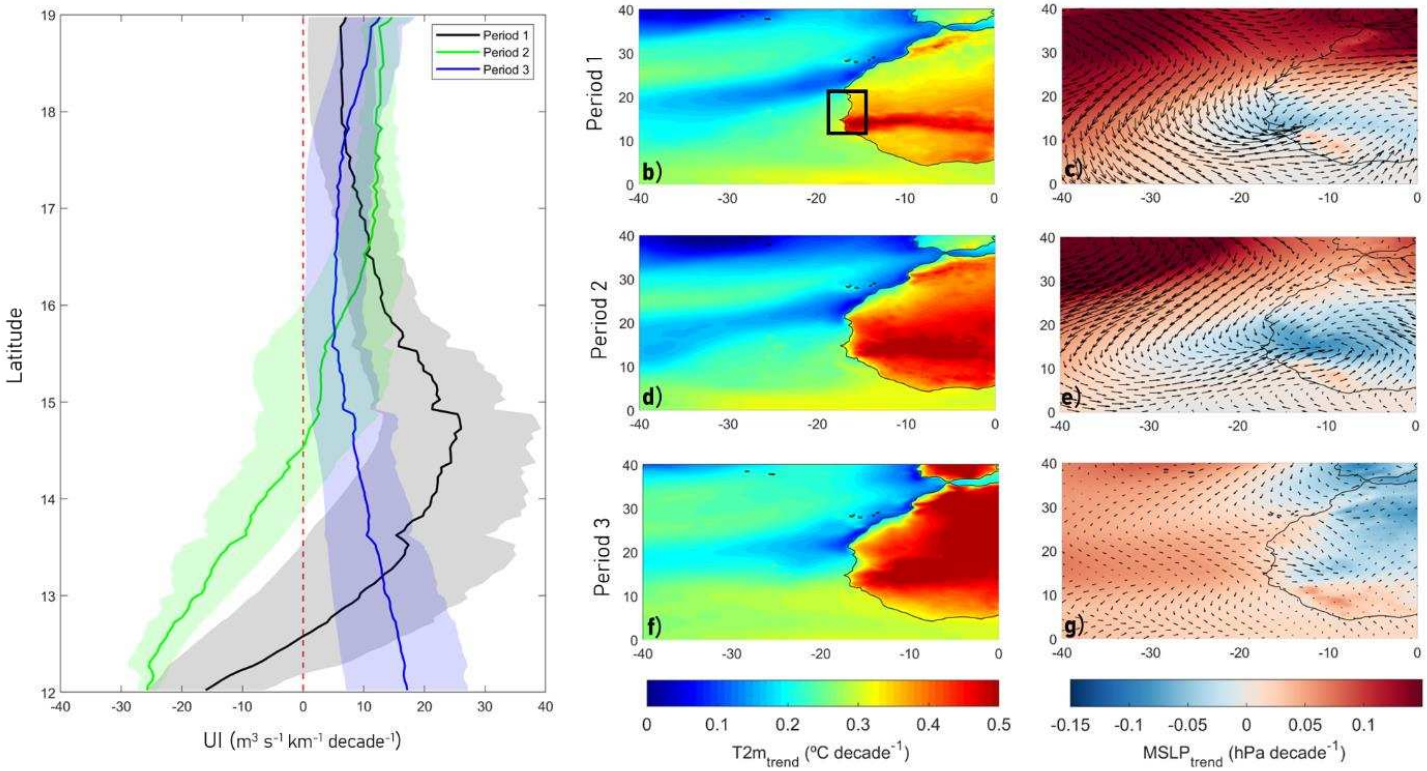

Fig. 5.5 *UI* trends (a) averaged over the closest grid points to the coast from 1950 to 2099 for each period. T2m (b,d,f) and MSLP (c,e,g) trends averaged from 1950 to 2099 for each period. Wind differences between the last 30 years of ROM_P2 (2070-2099) and ROM_P1 (1976-2005) are represented over the MSLP trends for each period. The black box (b) represents the MSUR (12ºN-19ºN).

Period 2, similarly to Period 1, presents an increase in the MSLP at the Azores high. As the T2m increase over land is generally stronger than in Period 1, the decrease in MSLP is stretched out over the African continent (Fig. 5.5d-e). Therefore, the cyclonic circulation anomaly presents its core north of 15ºN and further east than in the Period 1, contributing to the intensification of the upwelling favourable winds (along with the Azores high intensification) over the northern MSUR and to a weakening of the upwelling favourable winds in the southern MSUR (Fig. 5.5a; green line). Finally, Period 3 is dominated by the Sahara thermal low in summer, presenting a drastic increase of the T2m (0.5ºC decade^{-1}) in the African continent (Fig. 5.5f-g). Unlike the rest of periods, the Azores high does not present changes in intensity. The Saharan thermal low is located far away from the coastal region, so that the wind anomaly

results with southeastern direction, stimulating slightly the upwelling winds in the northern MSUR and weakening the downwelling winds in the southern MSUR.

Ocean stratification changes in the MSUR are evaluated with the help of the Brunt-Väisäla frequency. Brunt-Väisäla frequency is calculated within a 100 km wide band along the MSUR (the mask is shown in Fig. 5.6d) and averaged from surface to 150 m (the average depth associated with the ascent of water masses to the surface; Kämpf and Chapman, 2016). This analysis is realized for the three periods defined above.

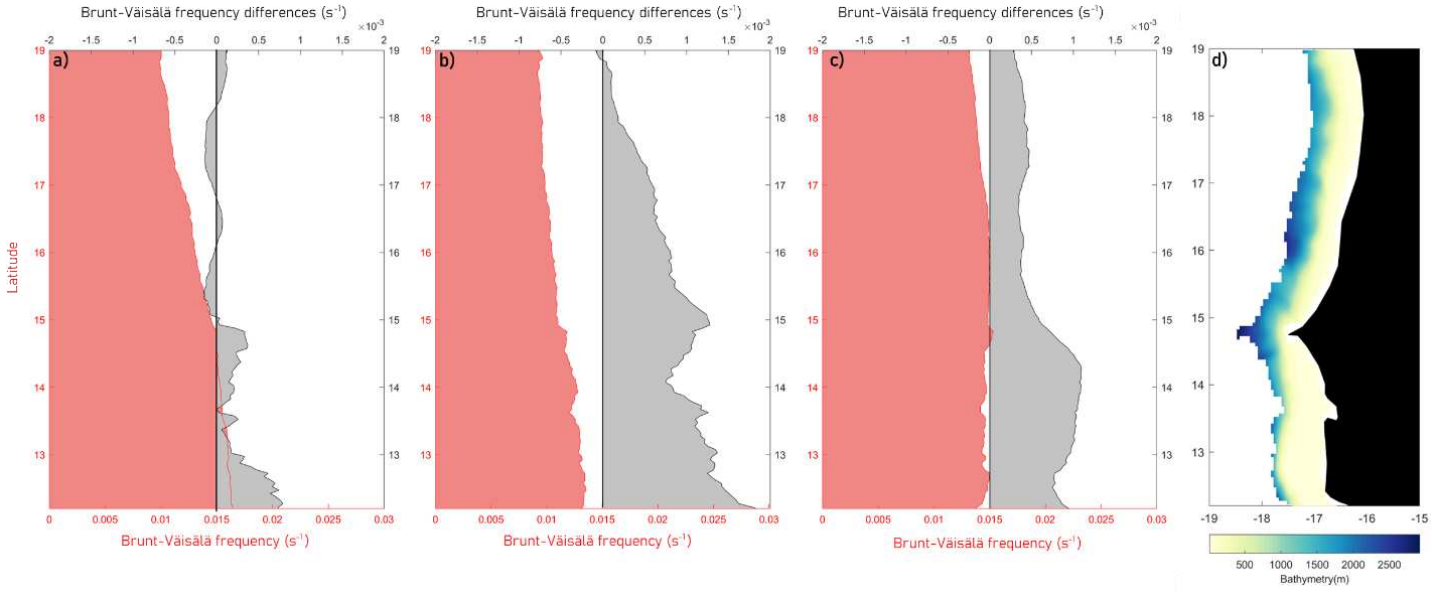

Fig. 5.6 Brunt-Väisälä frequency (s^{-1}) averaged from surface to 150 m in the closest grid points to coast for Period 1 (a), Period 2 (b) and Period 3 (c) for ROM_P1 (red shading; Historical) and the differences between ROM_P2 and ROM_P1 (black shading; RCP8.5 - Historical). The mask used is shown in the panel d.

For all periods the Brunt-Väisälä frequency is below 0.02 s^{-1} (Fig. 5.6a-c, red shading), with increasing values as latitude decreases. This is related to the influence of the warmer surface equatorial waters in the southern MSUR. The Period 3 presents the most stratified water column in the whole MSUR, associated with higher sea surface temperature in the summer season (Fig. 5.6c). Low values of the Brunt-Väisälä frequency are associated with a vertically homogeneous water column, in this case due to the coastal upwelling (strongest in Period 2).

In order to assess the changes in ocean stratification in the future we analyze the differences between ROM_P2 and ROM_P1 (Fig. 5.6; black shading). In Period 1, we found a slight decrease in the ocean stratification in some region of the northern MSUR (Fig. 5.6a). This

decrease is associated with a larger increase of the temperature in the sub-surface waters (50-70 m) than in the surface waters (Fig. 8a). In the Period 2 the ocean stratification increases in the whole MSUR, being more evident from 12ºN to 16ºN. In Period 3 the stratification changes are similar to Period 2.

A very important characteristic of the upwelling is the source water depth. The upwelling source water depth is calculated (see Eq. 5.5) taking into consideration both the action of the alongshore favourable winds and the ocean stratification. We calculate the upwelling source water depth in the historical simulation (ROM_P1) for the three periods defined above (Fig. 5.7 a, b, c).

For the historical simulation (ROM_P1), in Period 1 the upwelling source water depth is around 60 m in the whole MSUR, with slightly larger values in the northern MSUR (Fig. 5.7a). The upwelling source water is deeper in Period 2, ca. 80 m and slightly deeper (around 90 m) in northern than in southern MSUR (Fig. 5.7c). Deeper sources are mainly associated with the strengthening of the upwelling favourable winds in this period. In Period 3 the maximum source water depth (ca. 70 m) is found at northernmost MSUR, and then linearly decreases to Cap Vert (30 m). To the south of Cap Vert source depth is 0 m as the southern MSUR is dominated by downwelling favourable winds (Fig. 5.7e).

Differences in source water depth between ROM_P2 and ROM_P1 are shown in Fig. 5.7 (depicted in black shading). The upwelling source water is deeper in ROM_P2 during Period 1 (approximately 5 m), and decreases towards the southernmost region. In Period 2, deeper sources are found in the northern MSUR and shallower sources from Cap Vert to the southernmost MSUR. The upwelling source water depth does not significantly change in the entire MSUR during Period 3.

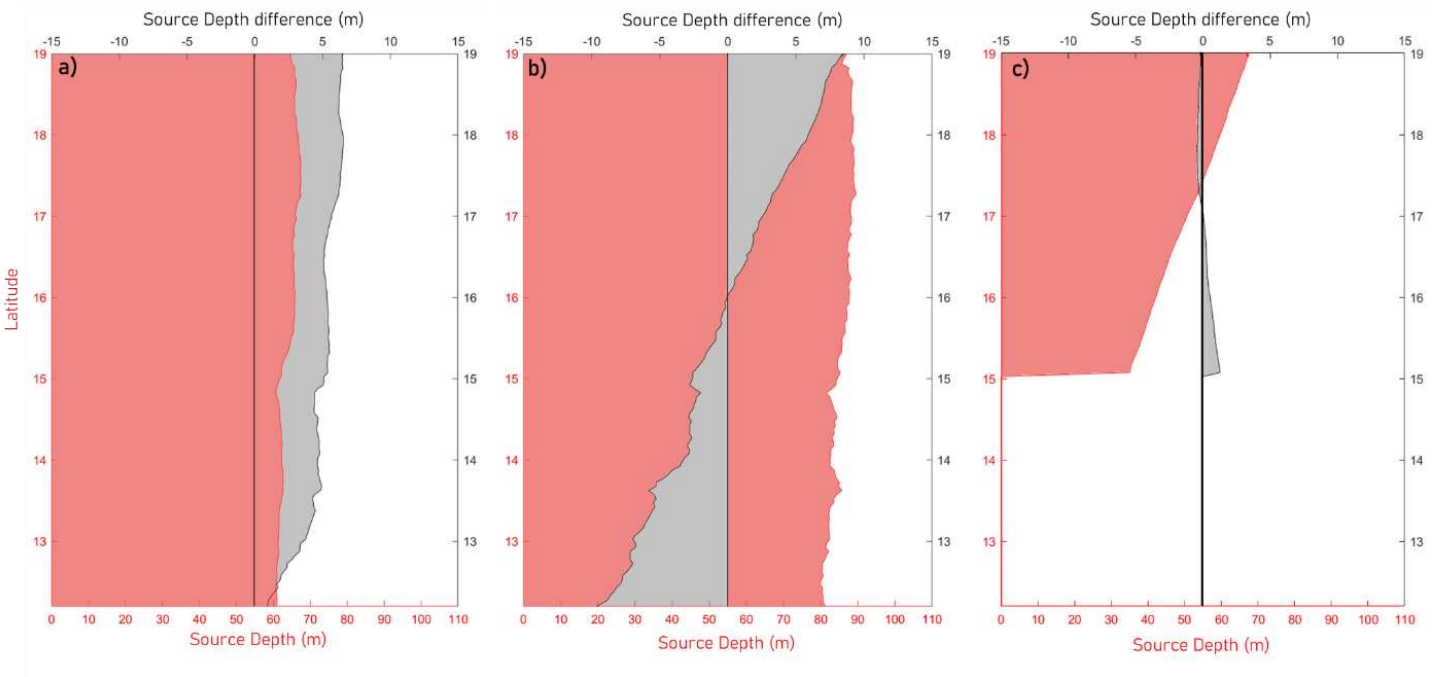

Fig. 5.7 Upwelling source water depth (m) in the closest grid points to coast (Fig. 5.6d) for Period 1 (a), Period 2 (b) and Period 3 (c) both for ROM_P1 (red shading; Historical) and the differences between ROM_P2 and ROM_P1 (black shading; RCP8.5 - Historical). The mask used is shown in Fig. 5.6d.

5.5 Discussion

The impact of climate change on upwelling systems has been a topic of interest over the last few decades. Both reanalysis and climate models have been used with the objective of understanding the impact of climate change on these important and vulnerable ecosystems. However, the spatial resolution of the GCMs used for global climate projections is insufficient to adequately reproduce the upwelling systems, resulting in uncertainty in future projections. Here, we take advantage of the ROM RCSM, which can reproduce the characteristics, variability, and associated mesoscale processes of the CCUS with high confidence (Vázquez et al. 2022). We investigate the future evolution of the MSUR under the RCP8.5 CMIP5 scenario using ROM.

To date, the efforts of the scientific community to evaluate the effect of climate change on EBUSs have focussed on two different responses: changes in wind patterns and changes in ocean stratification. Although both responses can provide useful information on the future of

these vulnerable ecosystems, obtaining a joint response from both mechanisms becomes essential. Recent studies have attempted to address the impact of climate change by combining both mechanisms using a large ensemble of the Community Earth System Model (Chang et al. 2023; Jing et al. 2023), conducting a joint study of the four main EBUSs. However, the large latitudinal and seasonal variability observed in our study, for a single region of the CCUS, indicates the difficulties of proposing a generic response for an entire upwelling system.

In fact, in this study we propose a monthly analysis of the *UI* trends to evaluate the effect of climate change on the MSUR, due to its large seasonal and latitudinal variability (Pardo et al. 2011; Cropper et al. 2014; Benazzouz et al. 2015). This analysis allowed us to find the causes of the changes in wind pattern throughout the year, identifying three periods with similar trends (Fig. 5.4). Sylla et al. (2019) proposed to evaluate the MSUR from November to May, as most studies associated with upwelling are only focused on the summer season, when the MSUR exhibits its weakest upwelling compared to other regions of the CCUS. They linked a weakening of the upwelling favourable winds in the southern MSUR (from Cap Vert to 12ºN), to shift of the Azores High (Rykaczewski's hypothesis).

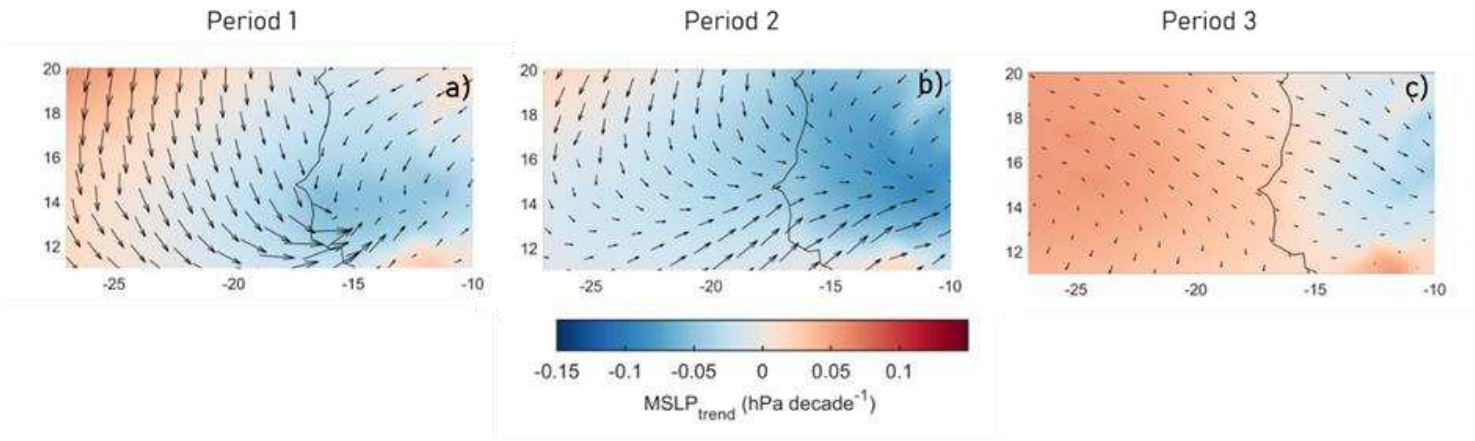

Fig. 5.8 MSLP trends averaged from 1950 to 2099 for each period. Wind differences between the last 30 years of ROM_P2 (2070-2099) and ROM_P1 (1976-2005) are represented over the MSLP trends for each period. The domain is represented in the Fig. 5b with a black box.

Our results in two out of the three annual periods are in agreement with this hypothesis for the MSUR. We detected an intensification of the Azores high (Rykaczewski et al. 2015; Sousa et al. 2017; Sousa et al. 2017b; Aguirre et al. 2019; Sylla et al. 2019; Varela et al. 2022), which strengths the upwelling favourable winds in the Periods 1 and 2. However, our monthly *UI* trends analysis suggests that other processes also affect the change in upwelling favourable winds in MSUR: during Period 1 the upwelling is influenced by a strong T2m local increase over the southern region of Sahel that can be explained by a southward expansion of the Sahara desert (e.g., Cook and Vizy, 2015; Zhou, 2016). In this context, we find that the local T2m changes have a remarkable impact on the upwelling favourable winds, since unlike Period 2, the T2m increase close to coast in the Period 1 enhances the upwelling favourable winds in the southern MSUR (see with detail in Fig. 5.8). During the summer months (Period 3), there are not significant changes in position or intensity of the Azores high. Nevertheless, we detected an evident increase in the T2m land-sea differences associated to an intensification of the Saharan thermal low that leads to a southeastern wind anomaly (e.g., Bakun 1990), which reinforce slightly the upwelling favourable winds over the northern MSUR and weakens the downwelling favourable winds in the southern MSUR.

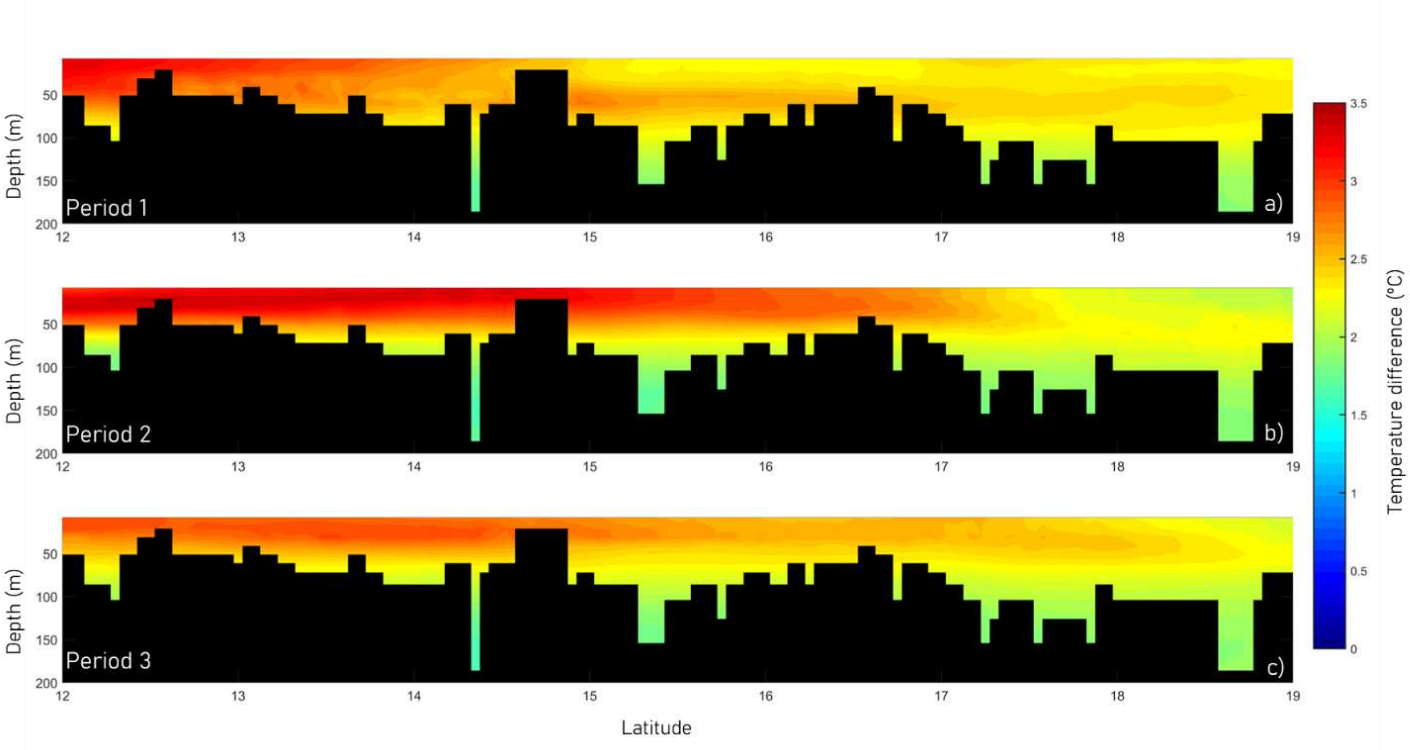

Fig. 5.9 Temperature differences between ROM_P2 and ROM_P1 averaged from surface to the maximum depth in the closest grid points to coast (Mask in Fig. 5.6d) for Period 1 (a), Period 2 (b) and Period 3 (c).

Oyarzún and Bradley (2019) found a hampering in the ascent of deeper water masses towards the surface in the Benguela upwelling, associated with an increase in the stratification of the upper layers of the water column, and Sousa et al. (2020) proposed the same hypothesis for the northern region of the Iberian upwelling. We found an enhanced ocean stratification in Period 2 (spring), very similar to the summer period (Period 3), associated with an increase in temperature in the ocean surface layers (Fig. 5.9). This pattern may be associated with a shorter and warmer spring seasons at the end of the century found in most CMIP5 models (Wang et al. 2021), resulting in an amplified summer throughout the year, except for the winter months (Period 1).

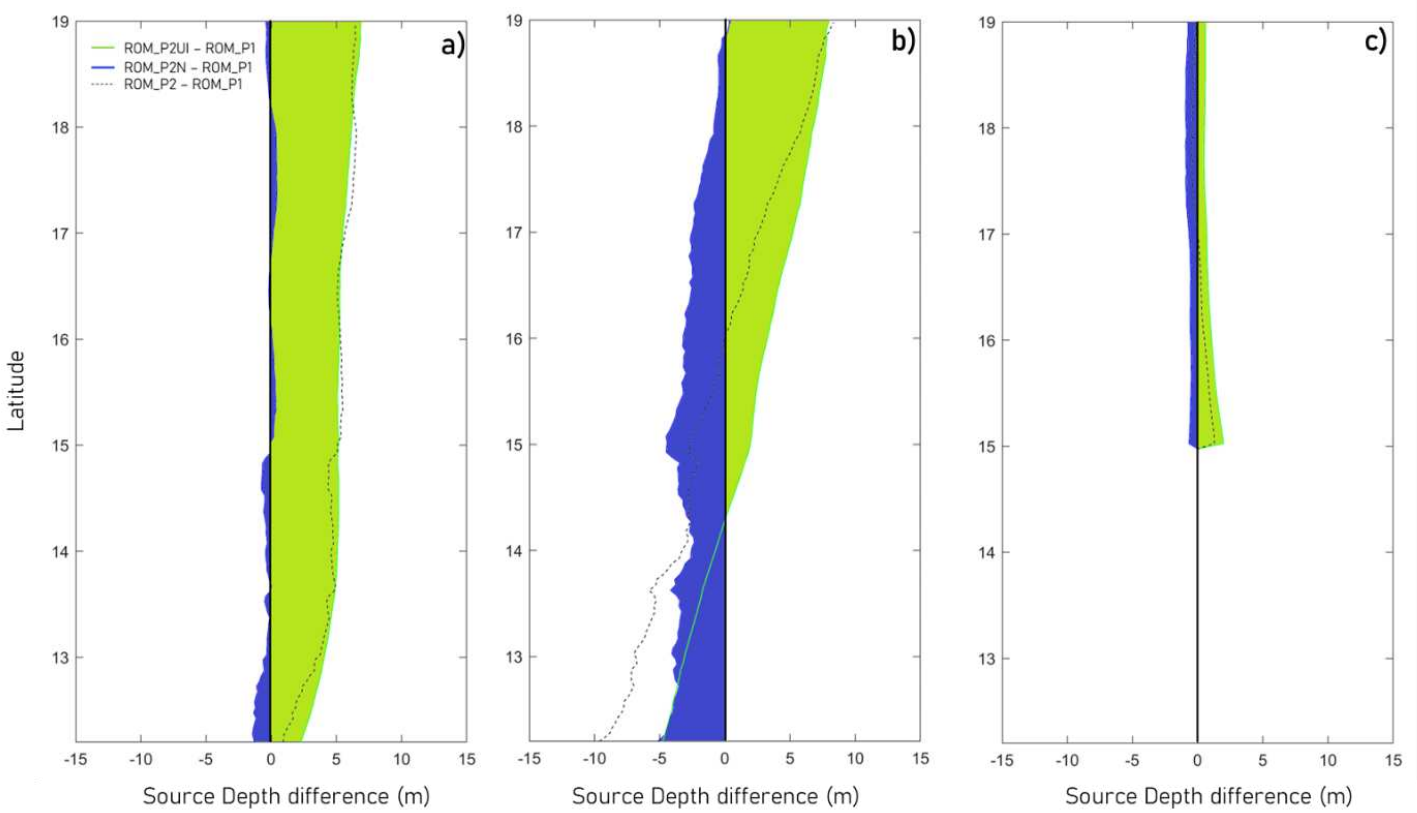

Fig. 5.10. Upwelling source water depth differences (m) in the closest grid points to coast (Fig. 5.6d) for Period 1 (a), Period 2 (b) and Period 3 (c) between ROM_P2UI (green shading), ROM_P2N (blue shading), ROM_P2 (dashed line) and ROM_P1. The mask used is shown in Fig. 5.6d. ROM_P2UI is calculated by maintaining the *N* of the historical simulation and the *UI* of the future (ROM_P2UI), and ROM_PN is calculated by maintaining the *UI* of the present and the *N* of the future (ROM_P2N).

The combined effect of wind patterns and ocean stratification was evaluated through the upwelling source water depth. In this regard, we found water that upwells from greater depths in Period 1 for the whole MSUR and in the northern MSUR for Period 2, mainly associated with the increase of *UI,* with practically no differences when only the effect of stratification was present (Fig. 5.10a). This result is contrary to what some authors have proposed in the EBUSs (Garcia-Reyes et al. 2015; Oyarzún and Brierley, 2019; Abrahams et al. 2019; Sousa et al. 2020). However, Jing et al. (2023) found an increase in the upwelling source water depth due to a stronger wind effect overcoming the effect of enhanced ocean stratification for the CCUS, and Chang et al. (2023) reported an increase in vertical transport towards the surface in the CCUS associated with an increase in Ekman suction. Nevertheless, in the southern MSUR, we found that the upwelling source water depth will be shallower for Period 2, where the decrease in *UI* along with the enhanced ocean stratification contribute to this shallowing of the upwelling source water depth (Fig. 5.10b), highlighting the need to evaluate upwelling systems both latitudinally and monthly.

Finally, although the changes in the ocean stratification seem not to lead the changes in much of the MSUR, the ocean temperature increase is more than evident. This fact may affect to the species that inhabit in the MSUR, modifying the distribution of species, migrations and fisheries (Menge and Menge, 2013; Y. Wang et al., 2015, D. Wang et al., 2015).

5.6 Conclusions

The objective of this work is to assess the MSUR under the RCP8.5 scenario, clarifying the effects of the climate change on the wind pattern and ocean stratification, as well as to explore the main mechanisms responsible for these changes. To this end, we take advantage of ROM RCSM, which presents a high horizontal resolution in MSUR. Our findings can be summarized as follows:

- ROM reproduces well the seasonality of the alongshore favourable winds in a present time, as well as the main drivers of the wind patterns: Azores high and ITCZ.

- Under the RCP8.5 scenario, we found three responses of the wind pattern to climate change depending on seasonality: Intensification of favourable upwelling winds in the all MSUR (January-November-December; Period 1); strengthening of upwelling

favourable winds in the northern MSUR and weakening in the southern MSUR (March-April; Period 2); weak intensification of upwelling favourable winds in the northern MSUR and weakening of downwelling favourable winds in the southern MSUR (June-July-August-September; Period 3).

- These responses of the wind pattern to climate change are associated with an intensification of the Azores High in Periods 1 and 2, but with the particularity that Period 1 presents a local increase in the T2m in the southern Sahel region. The wind pattern found under RCP8.5 scenario in Period 3, it is associated with a drastic increase in the T2m field throughout the African continent.

- Ocean stratification will be enhanced in the MSUR under global warming conditions, primarily during Period 2, associated with a surface temperature increase.

- Finally, the combined effect of changes associated with the wind pattern and ocean stratification in MSUR reveal a deepening of the upwelling source water depth during Period 1 and in the northern MSUR for Period 2, and a shallowing of the upwelling source water depth in the southern MSUR during Period 2.

CHAPTER 6:

General discussion

6.1. General discussion

The main goal of this thesis is to evaluate the impact of the climate change on the Canary Current Upwelling System (CCUS) and identify the main mechanisms responsible. To date attempts of the scientific community to clarify the effects of the climate change on Eastern Boundary Upwelling Systems (EBUSs) have left significant uncertainty, mainly due to the coarser resolution of the current Global Climate Models (GCMs). In this work, we take advantage from a Regional Climate System Model ROM, which offers high horizontal resolution in the CCUS.

The CCUS is one of the four major EBUSs in the world, highly productive coastal ocean areas where cold water upwells by the action of favourable winds, generating highly productive ecosystem and commercially important fisheries. However, the importance of the CCUS is not only bounded to the immediately regions to coast, hence the mesoscale processes as eddies, filaments and fronts have an impact in the ocean productivity, transporting the upwelled water properties to oligotrophic open waters. Therefore, for a proper representation of the coastal upwelling, the models must join both the ability to reproduce the larger-scale pattern (e.g. Azores high) and the local processes close to coast. Therefore, a high resolution atmosphere-ocean feedback is needed to represent properly these complex ecosystems.

The RCSM, ROM, presents a good opportunity to resolve the coastal dynamic with ocean high resolution in the CCUS (5 km), maintaining a global domain. ROM is able to reproduce the larger scale with a high confidence with the observational and reanalysis datasets in a present time. ROM showed the seasonal and latitudinal variability of the CCUS, improving the GCMs used for the comparison (MPI-ESM and CMIP5 ensemble). Moreover, ROM was able to reproduce the seasonal changes of the main mechanisms in the CCUS (Azores high and ITCZ) in a good agreement with ERA5, proving that is a good tool to reproduce the larger-scale dynamics which generate the CCUS.

As for the processes generated in the coastal upwelling regions, we evaluated the ROM performances in the coastal band (100 km). ROM was able to represent from the coastal wind stress the seasonal variability in the CCUS, getting to differentiate the regions which is divided the CCUS (e.g. Aristegui et al. 2009, Crooper et al. 2014; Gomez-Letona et al. 2017): Iberian upwelling region (IUR), weak permanent upwelling region (WPUR), permanent upwelling region (PUR) and Mauritania-Senegalese upwelling region (MSUR). ROM reproduced well the alongshore favourable winds in the coastal band, better than the GCMs and in a comparable

way with the RCMs, proving that is a powerful tool to reproduce the main drivers of the coastal upwelling in the CCUS. Moreover, ROM was able to represent some of the mesoscale events (Cape Ghir filaments), which play an important factor over the CCUS, where only organic carbon export by filaments in the subtropical northeast Atlantic contributes to the 63% of the annual primary production associated with the coastal upwelling (Santana-Falcón et al. 2016, 2020).

Concluded the first step with the evaluation in a present time, and being shown the ROM's ability to reproduce the CCUS, we used the ROM outputs forced by MPI-ESM-LR to evaluate the impact of the climate change. At the moment, the main hypotheses of change in the CCUS are focused on the wind pattern: (1) Air over land will warm more rapidly than air over the ocean, and resultant deepening of the continental thermal low-pressure systems will increase the cross-shore pressure gradients that drive upwelling favorable winds (Bakun, 1990). (2) Changes in the upwelling winds would be mostly related to shifts in the position and timing of the high pressure cells (Azores high in the CCUS) rather than changes in the continental thermal low pressure systems (Rykaczewski et al. 2015).

Nevertheless, other studies revealed the role of the ocean stratification in the future of the coastal upwelling, finding a drastic increase in the stratification of the upper layers in the water column due to the global warming, hampering the outcrop of the deeper water to surface and being the main mechanism of change at the end of 21st century (Oyarzún and Brierley, 2019; Sousa et al. 2020).

In this thesis, we find that the climate change response in the CCUS is subject to the large latitudinal variability and that the previous hypothesis can be complementary in some regions of the CCUS. Consequently, we will divide the different response of the climate change from the four regions of the CCUS.

6.1.1 Iberian upwelling region (IUR)

The Iberian upwelling is mainly influenced by the Azores high seasonality. The Azores high is located in the easternmost position in winter, generating downwelling favourable winds in the northern tip of the Iberian Peninsula. The increase in intensity and the westward migration of the Azores high turns to upwelling favourable winds in summer. This seasonality will be intensified under global warming conditions. Our study reveals an intensification of the downwelling favourable winds in winter, whilst in summer will be the upwelling favourable winds which will be enhanced. Therefore, the mechanisms of change in the IUR will depend

on the seasonality of the upwelling. In winter, the main driver of the changes will be the Azores high, which will be increased not only in intensity but also in longitudinal extension at the end of century, enhancing the downwelling favourable winds.

In summer, the larger pressure gradient between the Iberian Peninsula and the British Islands will strengthen the Iberian upwelling winds in the future. This larger MSLP gradient is associated with two responses to climate change: (a) the air temperature increase at the end of the 21st century will intensify the summer thermal low over the Iberian Peninsula (b) the weakening of the AMOC in the future will temper the temperature rise over the North Atlantic, triggering an increase of pressures in the British Islands (Haarsma et al. 2015). The join action of the two mechanisms will increase the pressure gradient between the Iberian peninsula and the British islands, increasing the intensity of the upwelling favourable winds.

Along with the alongshore favourable winds, the ocean stratification is the other relevant topic in this thesis. Our results show an increase of the ocean stratification in the IUR, which present the greater stratification in the CCUS for the future along with the WPUR, both in DJF and JJA. This pattern is associated with a larger scale freshening in the Eastern North Atlantic as reported by Levang and Schmit (2020) in a study with CMIP5 models. This freshening is transported through the Canary current from the north Atlantic region, associated with an amplification of the water cycle and enhanced Greenland mass loss in the future. The decrease in salinity is only found in the upper layers of the water column (upper 100 m), increasing the stratification between the surface and deeper waters. Our results show a mechanism complementary between the decrease of the upwelling favourable winds and the enhanced ocean stratification in DJF, reducing the source depth of the coastal upwelling in the southern IUR to -40 m. In JJA, we found an opposite role, where the intensification of the upwelling favourable wind will be counteracted with the enhanced ocean stratification, found similar results with Sousa et al. (2020). Therefore, this fact would generate a competitive mechanism in the summer months over the IUR, where the intensification of the upwelling favourable winds would be competing with the enhanced ocean stratification

6.1.2 Weak permanent upwelling region (WPUR)

As well as the previous region, the seasonal changes of the Azores high play a key role in the upwelling seasonality. However, this region presents year-round upwelling favourable winds, pointing out the Cape Ghir region as one of the most productive in the CCUS. The WPUR present a notably increase of the upwelling favourable winds during the summer (Pardo et al.

2011). These seasonal differences will be reduced in the future, since the upwelling favourable winds will be intensified in the future and reduced in summer. This pattern is completely opposite to the previous region, but the mechanisms are related to each other. In winter, the intensification of the Azores high will strengthen the wind intensity, generating an increase of the upwelling favourable winds in the WPUR. In summer, the cyclonic circulation anomaly over the Iberian Peninsula will result to winds with northeastward direction, reducing slightly the upwelling favourable winds in the future.

As in the previous region, the ocean stratification will play a key role in the WPUR. This enhanced ocean stratification is also related to the north Atlantic freshening. WPUR presents the greatest differences in the Brunt-Väisälä frequency, being those differences more evident in DJF. In this season, the enhanced ocean stratification will be become the main mechanism of change in the future, as reported Oyarzun and Brierley (2019) in the Humboldt current upwelling system. Although the upwelling favourable winds will be intensified in this region, the enhanced ocean stratification will hamper the outcrop of the deeper waters to surface, shallowing the source depth in 20 m. In JJA, the weakening of the upwelling favourable winds and the increase of the ocean stratification will aggravate the upwell of the deeper waters to surface, reducing the coastal upwelling, acting as complementary mechanisms.

6.1.3 Permanent upwelling region (PUR)

The permanent upwelling region presents the strongest upwelling favourable winds in the whole CCUS along with the northern region of the MSUR. This region presents upwelling favourable winds during year-round, with higher intensity in the summer months (due to the higher intensity of the Azores high). Under global warming conditions, the PUR presents a similar pattern than the WPUR in terms of trends. In winter, the intensification of the Azores high in the future will generate an increase of the upwelling favourable winds. In summer, PUR presents northwestward wind anomalies, which triggers a slight weakening of the upwelling favourable winds. To difference with the previous region, PUR presents a higher increase of the upwelling favourable winds during the winter months. This fact generates a difference lesser between the winter and summer season, decreasing the seasonality in the PUR.

In the PUR the drop in density is practically homogenous upper 200 m of the water column, showing a slight increase of the ocean stratification in the future. This is due to the fact that the Canary current, carrying the freshening signal from the north, presents a lower influence in the

PUR, since it is separated from the coast in Cape Blanc to join with the north equatorial current (Stramma, 1984; Mason et al. 2011; Santana-Falcón et al. 2020). Therefore, in the PUR the ocean stratification will not play such a key role as in IUR and WPUR, and the upwelling favourable wind will drive the changes associated with the global warming.

6.1.4 Mauritania-Senegalese upwelling region (MSUR)

The climate change impact on the MSUR is highly dependent on the latitude and season. Contrastingly, we found a more refined pattern of change when calculated monthly *UI* trends. We identify the two sub-regions in MSUR, mainly defined by the north migration of the ITCZ around 15ºN in summer (Pardo et al. 2011; Cropper et al. 2014; Benazzouz et al. 2015). The monthly analysis allows us to identify three periods, mainly defined by the *UI* trends, first November to January with a strengthening of the upwelling intensity in practically the whole MSUR (maximum in 15ºN), excepting the southernmost region (12ºN). Second, March and April present a similar pattern as the previous period, but with negative *UI* trends extended to from 12ºN to 15ºN. Finally, from June to September, when the ITCZ is located about 15ºN and the downwelling-inducing winds dominate the southern region. In this period, we found a strengthening of the upwelling-inducing winds in the northern region and a weakening of downwelling favourable winds in the southern region.

Our results in two out three of the studied periods show mechanisms close to this hypothesis for the MSUR. We detected an intensification of the Azores high, which strengths the upwelling favourable winds, in the Periods 1 and 2. Similar results were reported by Sylla et al. (2019), who found a northward migration of the Azores high along with an extension of the Saharan heat low (from November to May). However, our monthly *UI* trends analysis suggests that other mechanism also affects the upwelling winds in MSUR: during Period 1 the upwelling is affected by a strong T2m local increase over the Sahel region that can be explained by the desert amplification (e.g., Cook and Vizy, 2015; Zhou, 2016). In this context, we find that the local T2m changes have a high impact on the upwelling winds, since the south location of the T2m increase in the Period 1 enhances the upwelling winds in part of the MSUR southern sub-region, which is not found in the Period 2.

In the Period 2 the intensification of the Azores high causes an increase in the upwelling winds in the northern region, but to difference with the Period 1, the effects of the T2m increase are extended to the interior of the African continent, as effect of the intensification of the Saharan

thermal low. This generates a weakening of the upwelling winds in the southern region, as reported Sylla et al. (2019), due to a northward displacement of the anomalous wind circulation.

During the summer months (Period 3), there are not significant changes in position or intensity of the Azores high. Nevertheless, we detected an evident increase in the T2m land-sea differences associated to an intensification of the Saharan thermal low that leads to a southeastern wind anomaly (e.g., Bakun 1990), which reinforce slightly the upwelling winds over the northern region and weakens the downwelling winds in the southern.

The influence of climate change on the upwelling systems is not only limited to the wind field, but projected changes can have important consequences in economic and biological terms (Demarcq, 2009; Gruber, 2011; Rykaczewski et al., 2015). Oyarzún and Bradley (2019) found a hampering in the ascent of deeper water masses towards the surface in the Benguela upwelling, associated with an increase in the stratification of the upper layers of the water column, and Sousa et al. (2020) proposed the same hypothesis for the northern region of the Iberian upwelling. We found an enhanced ocean stratification in Period 2 (spring), very similar to the summer period (Period 3), associated with an increase in temperature in the ocean surface layers. This pattern may be associated with a shorter and warmer spring seasons at the end of the century found in most CMIP5 models (Wang et al. 2021), resulting in an amplified summer throughout the year, except for the winter months (Period 1).

The combined effect of wind patterns and ocean stratification was evaluated through the upwelling source water depth. In this regard, we found water that upwells from greater depths in Period 1 for the whole MSUR and in the northern MSUR for Period 2, mainly associated with the intensification of the upwelling favourable winds. This result is contrary to what some authors have proposed in the EBUSs (Garcia-Reyes et al. 2015; Oyarzún and Brierley, 2019; Abrahams et al. 2019; Sousa et al. 2020). However, Jing et al. (2023) found an increase in the upwelling source water depth due to a stronger wind effect overcoming the effect of enhanced ocean stratification for the CCUS, and Chang et al. (2023) reported an increase in vertical transport towards the surface in the CCUS associated with an increase in Ekman suction. Nevertheless, in the southern MSUR, we found that the upwelling source water depth will be shallower for Period 2, where the decrease in upwelling favourable winds along with the enhanced ocean stratification contribute to this shallowing of the upwelling source water depth, highlighting the need to evaluate upwelling systems both latitudinally and monthly.

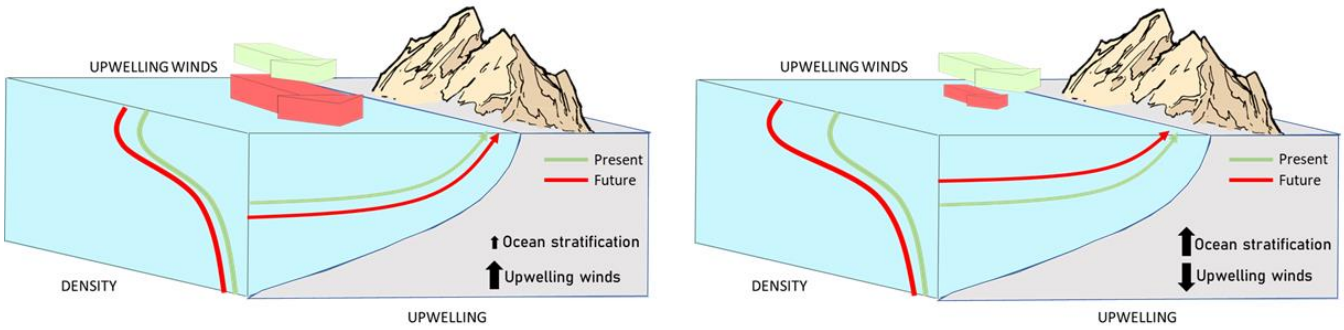

Fig. 6.1 Schematic representation of our suggested impact of climate change on coastal upwelling in the CCUS. We show a competitive mechanism as an increase of the upwelling favourable winds along with an enhanced ocean stratification (left) and a complementary mechanism as a decrease of the upwelling favourable winds along with an enhanced ocean stratification (right).

Finally, although the changes in the ocean stratification seem not to lead the changes in much of the MSUR, the ocean temperature increase is more than evident. This fact may affect to the species that inhabit in the MSUR, modifying the distribution of species, migrations and fisheries (Menge and Menge, 2013; Y. Wang et al., 2015, D. Wang et al., 2015).

CHAPTER 7:

Conclusions

7.1 Conclusions

- The RCSM, ROM, is able to reproduce both the larger-scale and mesoscale processes involved in the CCUS with a high confidence.

- ROM shows a better performance than the MPI-ESMs and CMIP5 models in representing the larger-scale wind stress and SST fields. ROM reproduces adequately the seasonal and interannual variability of the ERA5, ESA and OISST.

- High resolution is key to reproduce the latitudinal variability of the CCUS, as ROM_P0 represents the observed coastal SST with higher accuracy than the GCMs. Moreover, ROM_P0 successfully reproduces the coastal *UI* as well as the T2m land-sea differences, highlighting the impact of the higher resolution against the GCMs with a performance comparable to AFRICA-CORDEX.

- The mesoscale processes in the CCUS are well simulated by ROM, which is able to transfer the coastal upwelling waters to the open ocean in a realistic way. Thus, it successfully represents two coastal upwelling filaments off Cape Ghir, which are not accounted for in most global models.

- ROM is a powerful atmosphere-ocean model system able to reproduce with accuracy the CCUS, performing better than the GCMs. The improvement is related to a much higher horizontal resolution, which allows a better simulation of the dominant mesoscale coastal dynamics. The results here give ground to the future use of ROM_P0 to gain a deeper insight into the CCUS by the end of 21st century.

- The projected coastal upwelling wind changes present a clearly differentiated seasonal cycle and marked latitudinal variations under the RCP8.5 scenario. The IUR shows a strengthening of the upwelling favourable winds in JJA and the African coast is projected to experience a decrease in the upwelling favourable winds in the JJA and an increase in DJF

- In winter, the intensification of the Azores high will drive the changes in the alongshore favourable winds in IUR, WPUR and PUR

- In summer, the higher pressure gradient between the Iberian Peninsula and the British Islands will strengthen the Iberian upwelling winds in the future. In turn, the higher gradient is associated with two responses to climate change: (a) the air temperature increase at the end of the 21st century will intensify the thermal low over the Iberian Peninsula. (b) the weakening of the AMOC in the future will temper the temperature rise over the North Atlantic, triggering an increase of pressures in the British Islands.

- The increase in ocean stratification in the IUR will compete against the strengthening of the upwelling favourable winds in JJA and those two mechanisms will be complementary in DJF. In WPUR the enhanced ocean stratification will become the main driver of change in DJF under RCP8.5 scenario. In PUR, the upwelling favourable winds will be the main mechanism associated with the climate change at the end of the 21st century, since the ocean stratification is not so enhanced as in the two northern regions.

- The enhanced ocean stratification in IUR and WPUR is related to a freshening in the upper layers of the north Atlantic, due to an intensification of the precipitation and enhanced Greenland mass loss in the future

- Under the RCP8.5 scenario, we found three responses of the wind pattern to climate change depending on seasonality in the MSUR: Intensification of favourable upwelling winds in the all MSUR (January-November-December; Period 1); strengthening of upwelling favourable winds in the northern MSUR and weakening in the southern MSUR (March-April; Period 2); weak intensification of upwelling favourable winds in the northern MSUR and weakening of downwelling favourable winds in the southern MSUR (June-July-August-September; Period 3).

- These responses of the wind pattern to climate change in MSUR are associated with an intensification of the Azores High in Periods 1 and 2, but with the particularity that

Period 1 presents a local increase in the T2m in the southern Sahel region. The wind pattern found under RCP8.5 scenario in Period 3, it is associated with a drastic increase in the T2m field throughout the African continent.

- Ocean stratification will be enhanced in the MSUR under global warming conditions, primarily during Period 2, associated with a surface temperature increase.

- Finally, the combined effect of changes associated with the wind pattern and ocean stratification in MSUR reveal a deepening of the upwelling source water depth during Period 1 and in the northern MSUR for Period 2, and a shallowing of the upwelling source water depth in the southern MSUR during Period 2.

7.2 Conclusiones

- El modelo regionalmente acoplado atmósfera-océano ROM es capaz de representar tanto la larga escala como los procesos meso-escalares involucrados en la CCUS con una alta confianza.

- ROM mejora a los modelos MPI-ESMs y CMIP5 en la representación de los campos de la tensión tangencial del viento en superficie y de la SST de larga escala, aunque sobreestima el alto de las Azores en los meses de invierno, afectando débilmente el norte del afloramiento Ibérico. A pesar de ello, ROM reproduce adecuadamente la variabilidad estacional e interanual de ERA5, ESA y OISST en las tres regiones norte de la CCUS.

- La alta resolución es clave para reproducir la variabilidad latitudinal de la CCUS, ya que ROM representa la SST costera observada con mayor exactitud que los GCMs. Además, ROM reproduce exitosamente el UI costero, así como las diferencias T2m tierra-océano, destacando el impacto de la mayor resolución frente a los GCMs y con una actuación comparable a los modelos de AFRICA-CORDEX.

- Los procesos meso-escalares en la CCUS son bien simulados por ROM, el cuál es capaz de transferir las propiedades de las aguas afloradas costeras hacia el océano abierto de una manera realista. Así, ROM representa de manera exitosa dos eventos de filamentos costeros en Cabo Ghir, los cuales no son capaces de reproducir la mayoría de modelos globales.

- Por lo tanto, ROM es un poderoso sistema de modelo atmósfera-océano capaz de reproducir con un buen detalle las 3 regiones más al norte de la CCUS, actuando mejor que los GCMs. La mejora es relacionada a una mayor resolución horizontal, la cual permite una mejor simulación de la dinámica costera dominante en la CCUS.

- La proyección futura del afloramiento costero, en las 3 regiones más al norte de la CCUS, presenta cambios estacionales y latitudinales en el campo de vientos bajo el

escenario de cambio climático RCP8.5. La región Ibérica muestra un fortalecimiento de los vientos favorables de afloramiento (hundimiento) en verano (invierno) y las regiones WPUR y PUR están proyectadas a experimentar un descenso de los vientos favorables de afloramiento en verano y un incremento en invierno

- En invierno, la intensificación del alto de las Azores impulsará un incremento de los vientos favorables de hundimiento/afloramiento en las regiones IUR/PUR.

- En verano, un mayor gradiente de presiones entre la Península Ibérica y las islas Británicas fortalecerá el afloramiento ibérico a finales de siglo. Este mayor gradiente está asociado a dos respuestas al cambio climático: 1) El incremento de la temperatura del aire superficial a finales del siglo XXI intensificará la baja térmica de la Península Ibérica. 2) El debilitamiento de la AMOC en el futuro atemperará el aumento de temperatura sobre el Atlántico norte, desencadenando un incremento de presiones en las Islas Británicas.

- El incremento de la estratificación en la IUR competirá frente al fortalecimiento de los vientos favorables de afloramiento en JJA y esos mecanismos serán complementarios en DJF. En WPUR la mayor estratificación oceánica se convertirá en el principal conductor de cambio en DJF bajos el escenario RCP8.5. En PUR, las menor influencia de la estratificación oceánica convertirá a los vientos favorables de afloramiento en el principal mecanismo de cambio asociado con el calentamiento global a finales del siglo XXI

- Esta mayor estratificación en IUR y WPUR está relacionada con un descenso en la salinidad de las capas superficiales del Atlántico norte, como efecto de un incremento de las precipitaciones y una mayor pérdida de masa de Groenlandia

- La incrementada resolución en la costa noroccidental africana permite a ROM reproducir el UI representado por ERA5 en la región Mauritana-Senegalesa en el tiempo presente. Además, ROM es capaz de representar los principales mecanismos que afectan a la región sur del CCUS, el alto de las Azores y la zona de convergencia intertropical.

- Bajo scenario RCP8.5, nosotros encontramos tres respuestas diferentes del patrón de viento al cambio climático dependiendo de la estacionalidad en el MSUR: Intensificación de los vientos favorables de afloramiento en todo el MSUR (Enero-Noviembre-Diciembre; Periodo 1); fortalecimiento de los vientos favorables de afloramiento en el MSUR norte y debilitamiento en el MSUR sur (Marzo-Abril; Periodo 2); débil intensificación de los vientos favorables de afloramiento en el MSUR norte y debilitamiento de los vientos favorables de hundimiento en el MSUR sur (Junio-Julio-Septiembre; Periodo 3).

- Estas respuesta del patrón de viento al cambio climático están asociadas con una intensificación del Alto de las Azores en los Periodos 1 y 2, pero con la particularidad que el Periodo 1 presenta un incremento local de la T2m en el sur de la región de Sahel. El patrón de vientos encontrado bajo el escenario RCP8.5 en el Periodo 3 es asociado con un incremento drástico en la T2m en todo el continente Africano.

- La estratificación oceánica será mejorada en el MSUR bajo condiciones de calentamiento global, principalmente durante el Periodo 2, asociado con una incremento superficial de la temperatura.

- Finalmente, el efecto combinado de cambios asociados con el patrón de viento y la estratificación oceánica en el MSUR revelan una profundización de la profundidad fuente del afloramiento durante el Periodo 1 y en el MSUR norte para el Periodo 2, y una profundidad fuente del afloramiento más somera en el MSUR sur durante el Periodo 2.

CHAPTER 8:

Future research

8.1 Future research

The results of this PhD give response to the hypothesis and objectives posed at the beginning. Nevertheless, these results open and encourage new hypothesis and research lines. In this sense, we are going to enumerate the main lines to develop:

- To evaluate the climate change impact with ROM forced under the new climate change scenarios from CMIP6. This fact would allow to update the global warming conditions to the raised in the last reports of the IPCC.

- To study the CCUS from a biogeochemistry point of view. Once we have evaluated the main physical changes in the CCUS it would be interesting to analyze the effect of those changes in the nitrates, phosphates, chlorophyl, primary production.

- To evaluate the impact of the climate change in the export processes from the coastal band (eddies and filaments). In this sense, it appears the opportunity to study how the different filaments along the CCUS may be affected under global warming conditions and if these structures will be reduced in longitude, intensity or timing.

- To analyze the climate change mechanisms found in the thesis through a RCSM ensemble mean, which will give a higher robustness of the results. In this sense, although an only model, as ROM, can give useful information about the climate change impact in the CCUS, an ensemble mean would allow to obtain a model-independent more robust assessment.

References

References

Aguirre, C., Rojas, M., Garreaud, R.D., Rahn, D.A., (2019) Role of synoptic activity on projected changes in upwelling-favourable winds at the ocean's eastern boundaries. npj Clim. Atmos. Sci. 2 (1), 1–7. https://doi.org/10.1038/s41612-019-0101-9

Álvarez-Salgado XA, Arístegui J, Barton ED, Hansell DA (2007) Contribution of upwelling filaments to offshore carbon export in the subtropical Northeast Atlantic Ocean. Limnology and Oceanography, 52:1287-1292. https://doi.org/10.4319/lo.2007.52.3.1287

Arístegui J, Barton ED, Álvarez-Salgado XA, Santos AMP, Figueiras FG, Kifani S, Hernández-León S, Mason E, Machú E, Demarcq H (2009) Sub-regional ecosystem variability in the Canary Current upwelling. Prog Oceanogr. 83(1–4):33–48. http://dx.doi.org/10.1016/j.pocean.2009.07.031

Bakun A (1973) Coastal upwelling indices, West Coast of North America. 1946-71. US Department of Commerce, National Oceanic and Atmospheric Administration, National Marine Fisheries Service.

Bakun A (1990) Global climate change and intensification of coastal ocean upwelling. Science 247:198–201. https://doi.org/10.1126/science.247.4939.198

Bakun, A., Field, DB, Redondo-Rodríguez, A, Weeks, S (2010) Greenhouse gas, upwelling-favorable winds, and the future of coastal ocean upwelling ecosystems. Global Change Biology, 16: 1213-1228. https://doi.org/10.1111/j.1365-2486.2009.02094.x

Bakun, A., Black, B. A., Bograd, S. J., Garcia-Reyes, M., Miller, A. J., Rykaczewski, R. R., Sydeman, W. J. (2015) Anticipated effects of climate change on coastal upwelling ecosystems. Current Climate Change Reports, 1(2), 85-93. https://doi.org/10.1007/s40641-015-0008-4

Barton, E., Arıstegui, J., Tett, P., Canton, M., Garcıa-Braun, J., Hernandez-Leon, S., Nykjaer, L., Almeida, C., Almunia, J., Ballesteros, S., et al., (1998). The transition zone of the Canary Current upwelling region. Progress in Oceanography 41 (4), 455–504. https://doi.org/10.1016/S0079-6611(98)00023-8

Barton, E. D., Field, D. B., Roy, C. (2013) Canary current upwelling: more or less?. Progress in Oceanography, 116, 167-178. doi:10.1016/j.pocean.2013.07.007

Benazzouz A., (2014) Upwelling Côtier et Effet de la Dynamique Océanique à Méso-Échelle Sur la Variabilité Planctonique Dans le Système du Courant des Canaries (Ph.D. thesis). Hassan II Mohammedia-Casablanca University.

Benazzouz, A., Mordane, S., Orbi, A., Chagdali, M., Hilmi, K., Atillah, A., Pelegrí, J.L., Herv´e, D., (2014) An improved coastal upwelling index from sea surface temperature using satellite-based approach–the case of the Canary current upwelling system. Cont. Shelf Res. 81, 38–54. doi: 10.1016/j.csr.2014.03.012

Benazzouz, A., Demarcq, H., González-Nuevo, G., and de Vigo, C. O. (2015). Recent changes and trends of the upwelling intensity in the Canary Current Large Marine Ecosystem. Oceanogr. Biol. Features Canary Curr. Large Mar. Ecosyst. 115, 321–330. doi: 10.4060/ca7253en

Bindoff NL, Cheung WWL, Kairo JG, Arístegui J, Guinder VA, Hallberg R, Hilmi N, Jiao N, Karim MS, Levin L, O'Donoghue S, Purca Cuicapusa SR, Rinkevich B, Suga T, Tagliabue A, Williamson P (2019) Changing Ocean, Marine Ecosystems, and Dependent Communities. In: IPCC Special Report on the Ocean and Cryosphere in a Changing Climate [H.-O. Pörtner, D.C. Roberts, V. Masson-Delmotte, P. Zhai, M. Tignor, E. Poloczanska, K. Mintenbeck, A. Alegría, M. Nicolai, A. Okem, J. Petzold, B. Rama, N.M. Weyer (eds.)] Cambridge University Press, Cambridge, UK and New York, NY, USA, pp. 447-587. https://doi.org/10.1017/9781009157964.007.

Bonino G, Di Lorenzo E, Masina S, Iovino D (2019) Interannual to decadal variability within and across the major Eastern Boundary Upwelling Systems. Sci Rep 9:1-14. https://doi.org/10.1038/s41598-019-56514-8

Boyer TP, Baranova OK, Coleman C, Garcia HE, Grodsky A, Locarnini RA, Mishonov AV, Paver CR, Reagan J, Seidov D, Smolyar IV, Weathers K, Zweng MM (2019) World Ocean Database 2018. AV Mishonov Technical Editor, NOAA Atlas NESDIS 87.

Brady RX, Lovenduski NS, Alexander MA, Jacox M, Gruber N (2019) On the role of climate modes in modulating the air–sea co2 fluxes in eastern boundary upwelling systems. Biogeosciences 16:329–346. https://doi.org/10.5194/bg-16-329-2019

Brink, KH, (1983) The near-surface dynamics of coastal upwelling. Progr. Oceanogr 2:223-257. https://doi.org/10.1016/0079-6611(83)90009-5

Bryan FO, Hecht, MW, Smith RD (2007) Resolution convergence and sensitivity studies with North Atlantic circulation models. Part I: The western boundary current system. Ocean Model 16(3– 4):141–159. https://doi.org/10.1016/j.ocemod.2006.08.005

Cabos W, de la Vara A, Álvarez-García FJ, Sánchez E, Sieck K, Pérez-Sanz JI, Limareva N, Sein DV (2020) Impact of ocean-atmosphere coupling on regional climate: the Iberian Peninsula case. Clim Dyn 54:4441–4467. https://doi.org/10.1007/s00382-020-05238-x

Capet, A., Mason, E., Rossi, V., Troupin, C., Faugere, Y., Pujol, I., Pascual, A., (2014) Implications of refined altimetry on estimates of mesoscale activity and eddy-driven offshore transport in the Eastern Boundary Upwelling Systems. Geophysical Research Letters 41 (21), 7602–7610. https://doi.org/10.1002/2014GL061770

Carr, M.E., (2001) Estimation of potential productivity in Eastern Boundary Currents using remote sensing. Deep Sea Research Part II: Topical Studies in Oceanography 49 (1), 59–80. https://doi.org/10.1016/S0967-0645(01)00094-7

Carr, M.-E. and Kearns, E. J. (2003) Production regimes in four Eastern Boundary Current Systems, Deep-Sea Res. Pt. II, 50, 3199–3221, https://doi.org/10.1016/j.dsr2.2003.07.015

Casabella, N., Lorenzo, M.N., Taboada, J.J., (2014) Trends of the Galician upwelling in the context of climate change. J. Sea Res. 93, 23–27. https://doi.org/10.1016/j.seares.2014.01.013

Carton JA, Chepurin GA, Chen L (2018) SODA3: a new ocean climate reanalysis. J Clim 31:6967-6983. https://doi.org/10.1175/JCLI-D-18-0149.1

Chang, P., Xu, G., Kurian, J., Small R.J., Danabasoglu, G., Yeager, S., Castruccio, F., Zhang, Q., Rosenbloom, N., Chapman, P. (2023) Uncertain future of susainable fisheries environment in eastern boundary upwelling zones under climate change. Commun Earth Environ 4, 19. https://doi.org/10.1038/s43247-023-00681-0

Chhak,K., and Di Lorenzo, E.(2007). Decadal variations in the California Current upwelling cells. Geophys.Res.Lett. 34,L14604.doi:10.1029/2007GL030203

Chelton DB, deSzoeke RA, Schlax MG, El Naggar K, Siwertz N (1998) Geographical Variability of the First Baroclinic Rossby Radius of Deformation. J of Phys Ocean. 433-460. https://doi.org/10.1175/1520-0485(1998)028<0433:GVOTFB>2.0.CO;2

Christensen O, Drews M, Christensen J, Dethloff K, Ketelsen K, Hebestadt I, Rinke, A (2006) The HIRHAM Regional Climate Model, Version 5. Available online at: http://www.dmi.dk/fileadmin/Rapporter/TR/tr06-17.pdf

Cook, K. H., and Vizy, E. K. (2015). Detection and Analysis of an Amplified Warming of the Sahara Desert. Journal of Climate, 28(16), 6560-6580. https://doi.org/10.1175/Jcli-D-14-00230.1

Copernicus Climate Change Service (C3S) (2017) ERA5: Fifth generation of ECMWF atmospheric reanalyses of the global climate. Copernicus Climate Change Service Climate Data Store (CDS), date of access. https://cds.climate.copernicus.eu/cdsapp#!/home

Cropper TE, Hanna E, Bigg GR (2014) Spatial and temporal seasonal trends in coastal upwelling off Northwest Africa, 1981–2012. Deep Sea Res 86:94-111. https://doi.org/10.1016/j.dsr.2014.01.007

de la Vara, A., Cabos, W., Sein, D.V., Teichmann, C., Jacob, D. (2021) Impact of air–sea coupling on the climate change signal over the Iberian Peninsula. Clim Dyn 57, 2325–2349. https://doi.org/10.1007/s00382-021-05812-x

De Vries, H., Lenderink, G., Van der Wiel, K. and Van Meijgaard, E. (2022): Quantifying the role of the large-scale circulation on European summer precipitation change. Climate Dynamics, https://doi.org/10.1007/s00382-022-06250-z.

Dee DP, Uppala SM, Simmons AJ, Berrisford P, Poli P, Kobayashi S, Andrae U, Balmaseda MA, Balsamo G, Bauer P, Bechtold P, Beljaars ACM, van den Berg L, Bidlot J, Bormann N, Delsol C, Dragani R, Fuentes M, Geer AJ, Haimberger L, Healy SB, Hersbach H, Hólm EV, Isaksen L, Kallber P, Kohler M, Matricardi M, McNally AP, Monge-Sanz BM, Morcrett JJ, Park BK, Peubey C, de Rosnay P, Tavolato C, Thépaut JN, Vitart F (2011) The ERA-Interim reanalysis: configuration and performance of the data assimilation system. Q J Roy Meteor Soc 137:553–597. https://doi.org/10.1002/qj.828

Demarcq, H. (2009). Trends in primary production, sea surface temperature and wind in upwelling systems (1998-2007). Prog. Oceanogr. 83, 376–385. doi: 10.1016/j.pocean.2009.07.022

Drévillon M, Regnier C, Lellouche JM, Garric G, Bricaud C, Hernandez O (2018) CMEMS-GLO-QUID-001-030, 1.2 edn., E.U. Copernicus Marine Service Information [Online]. Available at: https://resources.marine.copernicus.eu/documents/QUID/CMEMS-GLO-QUID-001-030.pdf

Di Lorenzo E, Miller AJ, Schneider N, McWilliams JC (2005) The warming of the california current system: Dynamics and ecosystem implications. J of Phys Oceanogr 35:336–362. https://10.1175/JPO-2690.1

Dufois F, Penven P, Whittle CP, Veitch J (2012) On the warm nearshore bias in Pathfinder monthly SST products over Eastern Boundary Upwelling Systems. Ocean Model. 47, 113–118. https://doi.org/10.1016/j.ocemod.2012.01.007.

Dufresne JL, Foujols MA, Denvil S, Caubel A, Marti O, Aumont O, Balkanski Y, Bekki S, Bellenger H, Benshila R, Bony S, Bopp L, Braconnot P, Brockmann P, Cadule P, Cheruy F, Codron F, Cozic A, Cugnet D, de Noblet N, Duvel JP, Ethe´ C, Fairhead L, Fichefet T, Flavoni S, Friedlingstein P, Grandpeix JY, Guez L, Guilyardi E, Hauglustaine D, Hourdin F, Idelkadi A, Ghattas J, Joussaume S, Kageyama M, Krinner G, Labetoulle S, Lahellec A, Lefebvre MP, Lefevre FM, Levy C, Li ZX, Lloyd J, Lott F, Madec G, Mancip M, Marchand M, Masson S, Meurdesoif Y, Mignot J, Musat I, Parouty S, Polcher J, Rio C, Schulz M, Swingedouw D, Szopa S, Talandier C, Terray P, Viovy N, Vuichard N (2013) Climate change projections using the IPSL-CM5 Earth

System Model: from CMIP3 to CMIP5. Clim Dyn 40:2123–2165. https://doi.org/10.1007/s00382-012-1636-1

Eden C, Greatbatch RJ (2003) A damped decadal oscillation in the North Atlantic climate system. J Climate 16(24):4043–4060. https://10.1175/1520-0442(2003)0162.0.CO;2

Fischer G, Romero O, Toby E, Iversen M, Donner B, Mollenhauer G, Nowald N, Ruhland G, Klann M, Hamady B, Wefer G (2019) Changes in the Dust-Influenced Biological Carbon Pump in the Canary Current System: Implications From a Coastal and an Offshore Sediment Trap Record Off Cape Blanc, Mauritania. Global Biogeochem Cycles 33(8):1100–28. https://doi.org/10.1029/2019GB006194

Flato, G., Marotzke, J., Abiodun, B., Braconnot, P., Chou, S. C., Collins, W., Cox, P.,Driouech, F., Emori, S., Eyring, V., et al. (2014). Evaluation of climate models. In Climate change 2013: the physical science basis. Contribution of Working Group I to the Fifth Assessment Report of the Intergovernmental Panel on Climate Change, pages 741–866.Cambridge University Press. doi:10.1017/CBO9781107415324.020.

García-Muñoz M, Arístegui J, Pelegrí JL, Antoranz A, Ojeda A, Torres M (2005) Exchange of carbon by an upwelling filament off Cape Ghir (NW Africa). Journal of Marine Systems 54, 1–4: 83-95. https://doi.org/10.1016/j.jmarsys.2004.07.005

García-Reyes M, Sydeman WJ, Schoeman DS, Rykaczewski RR, Black BA, Smit AJ, Bograd SJ (2015) Under pressure: climate change, upwelling, and eastern boundary upwelling ecosystems. Front Mar Sci 2:109. https://10.3389/fmars.2015.00109

Gelaro, R., McCarty, W., Suárez, M. J., Todling, R., Molod, A., Takacs, L., Randles,C. A., Darmenov, A., Bosilovich, M. G., Reichle, R., et al. (2017). The modern-era retrospective analysis for research and applications, version 2 (MERRA-2).Journal of Climate,30(14):5419–5454. https://doi.org/10.1175/JCLI-D-16-0758.1

Giorgetta, MA, Jungclaus J, Reick CH, Legutke S, Bader J, Böttinger M, Brovkin V, Crueger T, Esch M, Fieg K, Glushak K, Gayler V, Haak H, Hollweg HD, Ilyina T, Kinne S, Kornblueh L, Matei D, Mauritsen T, Mikolajewicz U, Mueller W, Notz D, Pithan F, Raddatz T, Rast S, Redler R, Roeckner E, Schmidt H, Schnur R, Segschneider J, Six KD, Stockhause M, Timmreck C, Wegner J, Widmann H, Wieners KH, Claussen M,

Marotzke J, Stevens B (2013) Climate and carbon cycle changes from 1850 to 2100 in MPI-ESM simulations for the Coupled Model Intercomparison Project phase 5. J Adv Model Earth Sy 5:572–597. https://10.1002/jame.20038

Giorgi, F., Jones, C., Asrar, G. R. (2009). Addressing climate information needs at the regional level: the CORDEX framework. World Meteorological Organization (WMO) Bulletin, 58(3), 175. http://www.wmo.ch/.../index_en.html

Giorgi F, Coppola E, Solmon F, Mariotti L, Sylla MB, Bi X, Elguindi N, Diro GT, Nair V, Giuliani G, Cozzini S, Gu¨ttler I, O'Brien TA, Tawfik AB, Shalaby A, Zakey AS, Steiner AL, Stordal F, Sloan LC, Brankovic C (2012) RegCM4: model description and preliminary tests over multiple CORDEX domains. Clim Res 52:7–29. https://doi.org/10.3354/cr01018

Giorgi, F. (2019). Thirty years of regional climate modeling: where are we and where are we going next? Journal of Geophysical Research: Atmospheres, 124(11):5696–5723. https://doi.org/10.1029/2018JD030094

Gomez-Gesteira M, Moreira C, Alvarez I, Decastro M (2006) Ekman transport along the Galician coast (northwest Spain) calculated from forecasted winds. J Geophys Res 111. https://10.1029/2005jc003331

Gómez-Letona M, Ramos AG, Coca J, Arístegui J (2017) Trends in primary production in the Canary Current upwelling system a regional perspective comparing remote sensing models. Front Mar Sci 4:370. https://10.3389/fmars.2017.00370

Good SA, Martin MJ, Rayner NA (2013) EN4: quality-controlled ocean temperature and salinity profiles and monthly objective analyses with uncertainty estimates. J Geophys Res-Oceans 118 (12):6704-6716. https://10.1002/2013JC009067

Good SA, Embury O, Bulgin CE, Mittaz J (2019) ESA Sea Surface Temperature Climate Change Initiative (SST_cci): Level 4 Analysis Climate Data Record, version 2.0. Centre for Environmental Data Analysis, 22 August 2019. https://10.5285/aced40d7cb964f23a0fd3e85772f2d48

Gabric, A.J., Garcia, L., Van Camp, L., Nykjaer, L., Eifler, W., Schrimpf, W., (1993) Offshore export of shelf production in the Cape Blanc (Mauritania) giant filament as derived

from coastal zone color scanner imagery. Journal of Geophysical Research: Oceans 98 (C3), 4697–4712. https://doi.org/10.1029/92JC01714

Gruber N, Lachkar Z, Frenzel H, Marchesiello P, Münnich M, McWilliams JC, Nagai T, Plattner GK (2011) Eddy-induced reduction of biological production in eastern boundary upwelling systems. Nature Geosci. 4 (11), 787–792. https://doi.org/10.1038/ngeo1273

Gutiérrez, D., Bouloubassi, I., Sifeddine, A., Purca, S., Goubanova, K., Graco, M., ... & Ortlieb, L. (2011). Coastal cooling and increased productivity in the main upwelling zone off Peru since the mid-twentieth century. Geophysical Research Letters, 38(7). doi:10.1029/2010GL046324

Haarsma RJ, Selten FM, Drijfhout SS (2015) Decelerating Atlantic meridional overturning circulation main cause of future west European summer atmospheric circulation changes. Environ Res Lett. https:// doi. org/ 10. 1088/ 1748- 9326/ 10/9/ 094007

Hagemann S, Dumenil-Gates L (1998) A parameterization of the lateral waterflow for the global scale. Clim Dyn 14:17–31. https://10.1007/s003820050205

Hagemann S, Dumenil-Gates L (2001) Validation of the hydrological cycle of ECMWF and NCEP reanalysis using the MPI hydrological discharge model. J Geophys Res 106 (D2):1503–1510. https://10.1029/2000JD900568

Hagen E, Zülicke C, Feistel R (1996) Near-surface structures in the Cape Ghir filament off Morocco. Oceanol Acta 19: 577-598. https://archimer.ifremer.fr/doc/00096/20728/

Hailegeorgis, D., Lachkar, Z., Rieper, C., and Gruber, N. (2021). A Lagrangian study of the contribution of the Canary coastal upwelling to the open North Atlantic nitrogen budget. In Ocean Sciences Meeting. AGU. https://doi.org/10.5194/bg-18-303-2021

Hall DK, Riggs GA (2007) Accuracy assessment of the MODIS snow-cover products. Hydrol Process, 21: 1534– 1547. https://10.1002/hyp.6715.

Halpern D. (2002). Offshore Ekman Transport and Ekman Pumping Off Peru During the 1997–1998 EL Niño. Geophys. Res. Lett. 29 (5), 19–11. doi: 10.1029/2001GL014097

Hazeleger W, Severijns C, Semmler T, et al (2010) EC-Earth: A Seamless Earth-System Prediction Approach in Action. Bull Am Meteorol Soc 91:1357–1364. https://doi.org/10.1175/2010BAMS2877.1

Hersbach, H., Bell, B., Berrisford, P., Hirahara, S., Horanyi, A., Munoz-Sabater, J., Nicolas, J., Peubey, C., Radu, R., Schepers, D., Simmons, A., Soci, C., Abdalla, S., Abellan, X., Balsamo, G., Bechtold, P., Biavati, G., Bidlot, J., Bonavita, M., . . . Thepaut, J. N. (2020). The ERA5 global reanalysis. Quarterly Journal of the Royal Meteorological Society, 146(730), 1999-2049. https://doi.org/10.1002/qj.3803

Hibler, W. D. (1979), A dynamic thermodynamic sea ice model, J. Phys. Oceanogr., 9, 815–846. https://doi.org/10.1175/1520-0485(1979)009<0815:ADTSIM>2.0.CO;2

Ikazaki K. (2015) Desertification and a new countermeasure in the Sahel, West Africa. Soil Sci. Plant Nutr. 61, 372–383. doi:10.1080/00380768.2015.1025350

Izquierdo A, Mikolajewicz U (2019) The role of tides in the spreading of Mediterranean Outflow waters along the southwestern Iberian margin. Ocean Model 133:27-43. https://10.1016/j.ocemod.2018.08.003, 2019

Jacob D (2001) A note to the simulation of the annual and interannual variability of the water budget over the Baltic Sea drainage basin. Meteorol Atmos Phys 77(1-4):61-73. https://10.1007/s007030170017

Jacox,M.G., and Edwards,C.A. (2011). Effects of stratification and shelf slope on nutrient supply in coastal upwelling regions. J.Geophys.Res. 116,C03019.doi:10.1029/2010jc006547

Jacox,M.G., Bograd,S.J. Hazen,E.L.,and Fiechter,J. (2015). Sensitivity of the California Current nutrient supply to wind,heat,and remote ocean forcing. Geophys.Res. Lett. 42, 5950 – 5957. doi:10.1002/2015gl065147

Jacox MG, Edwards CA, Hazen EL, Bograd SJ (2018) Coastal upwelling revisited: Ekman, Bakun, and improved upwelling indices for the U.S. West Coast. J Geophys Res. https://doi.org/10.1029/2018JC014187

Jing Z, Wang S, Wu L, Wang H, Zhou S, Sun B, Chen Z, Ma X, Gan B, Yang H, (2023) Geostrophic flows control future changes of oceanic eastern boundary upwelling. Nat. Clim. Chang. 13, 148–154. https://doi.org/10.1038/s41558-022-01588-y

Jones RG, Noguer M, Hassell DC, Hudson D, Wilson SS, Jenkins GJ, Mitchell JFB (2004) Generating high resolution climate change change scenarios using PRECIS. Met Office Hadley Centre, Exeter, UK.

Jones CD, Hughes JK, Bellouin N, Hardiman SC, Jones GS, Knight J, Liddicoat S, O'Connor FM, Andres RJ, Bell C, Boo K-O, Bozzo A, Butchart N, Cadule P, Corbin KD, Doutriaux-Boucher M, Friedlingstein P, Gornall J, Gray L, Halloran PR, Hurtt G, Ingram WJ, Lamarque J-F, Law RM, Meinshausen M, Osprey S, Palin EJ, Parsons Chini L, Raddatz T, Sanderson MG, Sellar AA, Schurer A, Valdes P, Wood N, Woodward S, Yoshioka M, Zerroukat M (2011) The HadGEM2-ES implementation of CMIP5 centennial simulations. Geosci Model Dev 4:543–570. https://doi.org/10.5194/gmd-4-543-2011

Jungclaus JH, Fischer N, Haak H, Lohmann K, Marotzke J, Matei D, Mikolajewicz U, Notz D von Storch JS (2013) Characteristics of the ocean simulations in MPIOM, the ocean component of the MPI-Earth system model. J Adv Model Earth Sy 5:422– 446. https://10.1002/jame.20023

Kämpf J, Chapman P (2016) The canary/Iberia current upwelling system. In Upwelling Systems of the World 203-250. https://10.1007/978-3-319-42524-5_6

Laprise, R. (2008). Regional climate modelling.Journal of Computational Physics,227(7):3641–3666.

Levang, S.J. & Schmitt, R. W. (2020). What Causes the AMOC to Weaken in CMIP5?, Journal of Climate, 33 (4), 1535-1545. https://doi.org/10.1175/JCLI-D-19-0547.1

Levitus S, Boyer TP, Conkright ME, O'Brien T, Antonov J, Stephens C, Stathoplos L, Johnson D, Gelfeld, R (1998) World Ocean Database 1998, vol.1, Introduction, NOAA Atlas NESDIS 18, Ocean Clim. Lab., Natl. Oceanogr. Data Cent., U.S. Gov. Print. Off., Washington, D.C.

Levitus, S., Antonov, J.I., Boyer, T.P., Stephens, C., (2000) Warming of the world ocean. Science 287, 2225–2229. https://doi.org/10.1126/science.287.5461.2225.

Levitus, S., Antonov, J., Boyer, T.P., (2005) Warming of the world ocean, 1955–2003. Geophys. Res. Lett. 32 (2).

Li H, Kanamitsu M, Hong SY (2012) California reanalysis downscaling at 10 km using an ocean-atmosphere coupled regional model system. J Geophys Res 117:D12118. https://doi.org/10.1029/2011JD017372

Lovecchio E, Gruber N, Münnich M, Lachkar Z (2017) On the long-range offshore transport of organic carbon from the Canary Upwelling System to the open North Atlantic. Biogeosciences 14 (13), 3337–3369. https://doi.org/10.3929/ethz-b-000190480.

Lovecchio E, Gruber N, Münnich M (2018) Mesoscale contribution to the long-range offshore transport of organic carbon from the Canary Upwelling System to the open North Atlantic.Biogeosciences 15:5061–5091. https://doi.org/10.5194/bg-15-5061-2018

Macias, D., Landry, M.R., Gershunov, A., Miller, A.J. and Franks, P.J.S. (2012). Climatic control of upwelling variability along the western North American coast. PLo SONE 7:e30436.doi:10.1371/journal.pone.0030436

Maier-Reimer E, Kriest I, Segschneider J, Wetzel P (2005) The HAMburg Ocean Carbon Cycle Model HAMOCC5.1 Technical Description Release 1.1, Ber. Erdsystemforschung, 14, http://hdl.handle.net/11858/00-001M-0000-0011-FF5C-D

Marsland SJ, Haak H, Jungclaus JH, Latif M, Roeske F (2003) The Max-Planck- Institute global ocean/sea icemodel with orthogonal curvilinear coordinates. Ocean Model 5(2):91–127. https://doi.org/10.1016/S1463-5003(02)00015-X

Mason E, Colas F, Molemaker J, Shchepetkin AF, Troupin C, McWilliams JC, Sangrà P (2011) Seasonal variability of the Canary current: a numerical study. J Geophys Res Oceans 116(6):1–20. https://doi.org/10.1029/2010JC006665

Marotzke, J., Müller, W. A., Vamborg, F. S., Becker, P., Cubasch, U., Feldmann, H., et al. (2016). MiKlip: A national research project on decadal climate prediction. Bulletin of

the American Meteorological Society, 97(12), 2379–2394. https://doi.org/10.1175/BAMS-D-15-00184.1

Menge, B.A., Menge, D.N.L., (2013). Dynamics of coastal meta-ecosystems: the intermittent upwelling hypothesis and a test in rocky intertidal regions. Ecol. Monogr. 83, 283–310. https://doi.org/10.1890/12-1706.1

Menna M, Faye S, Poulain PM, Centurioni L, Lazar A, Gaye A, Sow B, Dagorne D (2016) Upwelling features off the coast of north-western Africa in 2009–2013. Bollettino Di Geofisica Teorica Ed Applicata, 57:71–86. https://doi.org/10.4430/bgta0164

Merchant CJ, Embury O, Bulgin CE, Block T, Corlett G, Fiedler E, Good SA, Mittaz J, Rayner N, Berry D, Eastwood S (2019) Satellite-based time-series of sea-surface temperature since 1981 for climate applications. Nat Sci Data 6:223. http://doi.org/10.1038/s41597-019-0236-x

Mikolajewicz U, Sein DV, Jacob D, Königk T, Podzun R, Semmler T (2005) Simulating Arctic sea ice variability with a coupled regional atmosphere-ocean-sea ice model. Meteorol Zeitschrift 14(6):793–800. http://hdl.handle.net/11858/00-001M-0000-0011-FF70-E

Miranda, P.M.A., Alves, J.M.R., Serra, N., (2013) Climate change and upwelling: response of Iberian upwelling to atmospheric forcing in a regional climate scenario. Clim. Dyn. 40 (11-12), 2813–2824. https://doi.org/10.1007/s00382-012-1442-9

Mittelstaedt, E., (1991) The ocean boundary along the northwest African coast: circulation and oceanographic properties at the sea surface. Progress in Oceanography 26 (4), 307–355. https://doi.org/10.1016/0079-6611(91)90011-A

Narayan, N., Paul, A., Mulitza, S., & Schulz, M. (2010). Trends in coastal upwelling intensity during the late 20th century. Ocean Science, 6(3), 815-823. doi:10.5194/os-6-815-2010

Ning H, Li-Juan L, Bin W (2014) The role of the aerosol indirect effect in the northern Indian Ocean warming simulated by CMIP5 models. Atmos. Oceanic Sci Lett 7:411–416. https://doi.org/10.1080/16742834.2014.11447199

Nykjær, L., Van Camp, L., (1994) Seasonal and interannual variability of coastal upwelling along northwest Africa and Portugal from 1981 to 1991. Journal of Geophysical Research: Oceans 99 (C7), 14197–14207. https://doi.org/10.1029/94JC00814

Oerder, V., Colas, F., Echevin, V., Codron, F., Tam, J., Belmadani, A., (2015) Peru-Chile upwelling dynamics under climate change. J. Geophys. Res. Oceans 120, 1152–1172. https://doi.org/10.1002/2014JC010299.

Oyarzún D, Brierley CM (2018) The future of coastal upwelling in the Humboldt current from model projections. Clim Dyn 52:599–615. https://doi.org/10.1007/s00382-018-4158-7

Pardo PC, Padín XA, Gilcoto M, Farina-Busto L, Pérez FF (2011) Evolution of upwelling systems coupled to the long-term variability in sea surface temperature and Ekman transport. Clim Res 48(2–3):231–46. https://doi.org/10.3354/cr00989

Parras-Berrocal I, Vázquez R, Cabos W, Sein D, Mañanes R, Perez-Sanz J, Izquierdo A (2020) The climate change signal in the Mediterranean Sea in a regionally coupled ocean-atmosphere model. Ocean Sci 16:743–765. https://doi.org/10.5194/os-16-743-2020

Pauly D, Christensen V (1995) Primary production required to sustain global fisheries. Nature 374:255–257. https://doi.org/10.1038/374255a0

Pelegrí JL, Aristegui J, Cana L, González-Dávila M, Hernández-Guerra A, Hernández-León S, Marrero-Díaz A, Montero MF, Sangrá P, Santana-Casiano M (2005) Coupling between the open ocean and the coastal upwelling region off northwest Africa: water recirculation and offshore pumping of organic matter. Journal of Marine Systems 54:3–37. https://doi.org/10.1016/j.jmarsys.2004.07.003

Pelegri, JL, Marrero-Diaz A, Ratsimandresy AW (2006) Nutrient irrigation of the North Atlantic. Progress in Oceanography 70:366–406. https://doi.org/10.1016/j.pocean.2006.03.018

Pelegrí JL, Benazzouz A (2015) Coastal upwelling off North-West Africa. In: Valdés, L.1 and Déniz-González, I.(eds). Oceanographic and biological features in the Canary Current Large Marine Ecosystem. IOC-UNESCO, Paris. IOC Technical Series, No. 115: 383. http://hdl.handle.net/1834/9135

Pickett, M. H., Paduan, J. D. (2003). Ekman transport and pumping in the California Current based on the U.S. Navy's high-resolution atmospheric model (COAMPS). Journal of Geophysical Research, 108(C10), 3327. https://doi.org/10.1029/2003JC001902

Pires, A.C., Nolasco, R., Rocha, A., Ramos, C., Dubert, J., (2015) Climate change in the Iberian Upwelling System: a numerical study using GCM downscaling. Clim. Dyn. 47 (1), 451–464. https://doi.org/10.1007/s00382-015-2848-y

Rechid, D., and D. Jacob (2006), Influence of monthly varying vegetation on the simulated climate in Europe, Meteorol. Z., 15, 99–116. 10.1127/0941-2948/2006/0091

Relvas P, Luis J, Santos AMP (2009) Importance of the mesoscale in the decadal changes observed in the northern Canary upwelling system. Geophys. Res. Lett. 36. https://doi.org/10.1029/2009GL040504

Renault L, Deutsch C, McWilliams JC, Frenzel H, Liang JH, Colas F (2016) Partial decoupling of primary productivity from upwelling in the California current system. Nat Geosci 9(7):505–508. https://doi.org/10.1038/ngeo2722

Renault, L., Hall, A., McWilliams, J. C. (2016). Orographic shaping of US West Coast wind profiles during the upwelling season. Climate Dynamics, 46(1–2), 273–289. https://doi.org/10.1007/s00382-015-2583-4

Reynolds RW, Smith TM, Liu C, Chelton DB, Casey KS, Schlax MG (2007) Daily High-Resolution-Blended Analyses for sea surface temperature. J Climate 20(22):5473-5496. https://doi.org/10.1175/2007JCLI1824.1

Rockel B, Will A, Hense A (2008) The regional climate model COSMO-CLM (CCLM). Meteorol Z 17(4):347–348. https://doi.org/10.1127/0941-2948/2008/0309

Roxy M, Ritika K, Terray P, Murtugudde R, Ashok K, Goswami BN (2015) Drying of Indian subcontinent by rapid Indian Ocean warming and a weakening land-sea thermal gradient. Nat Commun 6:7423. https://doi.org/10.1038/ncomms8423

Rummukainen, M.(2010). State-of-the-art with regional climate models. Wiley Inter-disciplinary Reviews: Climate Change, 1(1):82–96. https://doi.org/10.1002/wcc.8

Rykaczewski, R. R., Checkley, D. M. (2008). Influence of ocean winds on the pelagic ecosystem in upwelling regions. Proceedings of the National Academy of Sciences, 105(6), 1965–1970. https://doi.org/10.1073/pnas.0711777105

Rykaczewski RR, Dunne JP, Sydeman WJ, Garcia-Reyes M, Black BA, Bograd SJ (2015) Poleward displacement of coastal upwelling-favorable winds in the ocean's eastern boundary currents through the 21st century. Geophys Res Lett 42:6424–6431. https://doi.org/10.1002/2015GL064694

Samuelsson P, Gollvik S, Jansson C, Kupiainen M, Kourzeneva E, van de Berg WJ (2015) The surface processes of the Rossby Centre regional atmospheric climate model (RCA4). SMHI Rep 157, 58.

Sangrá P (2015) Canary Islands eddies and coastal upwelling filaments off North-west Africa. In: Oceanographic and biological features in the Canary Current Large Marine Ecosystem.Valdés, L. and Déniz-González, I. (eds). IOC-UNESCO, Paris. IOC Technical Series, No. 115, pp. 105-114. http://hdl.handle.net/1834/9181.

Sangrá P, Troupin C, Barreiro-González B, Desmond Barton E, Orbi A, Arístegui J (2015) The Cape Ghir filament system in August 2009 (NW Africa). J Geophys Res Oceans 120: 4516–4533, https://doi.org/10.1002/2014JC010514.

Santana-Falcón Y, Benavides M, Sangrà P, Mason E, Barton ED, Orbi A, Arístegui J (2016) Coastal–offshore exchange of organic matter across the Cape Ghir filament (NW Africa) during moderate upwelling. J. Mar. Syst. 154, 233–242. https://doi.org/ 10.1016/j.jmarsys.2015.10.008.

Santana-Falcón Y, Mason E, Arístegui J (2020) Offshore transport of organic carbon by upwelling filaments in the Canary Current System. Prog Oceanogr 184(April):102322. https://doi.org/10.1016/j.pocean.2020.102322

Santos, F., DeCastro, M., Gómez-Gesteira, M., & Álvarez, I. (2012). Differences in coastal and oceanic SST warming rates along the Canary upwelling ecosystem from 1982 to 2010. Continental Shelf Research, 47, 1-6. http://dx.doi.org/10.1016/j.csr.2012.07.023

Sein DV, Mikolajewicz U, Gröger M, Fast I, Cabos W, Pinto JG, Hagemann S, Semmler T, Izquierdo A Jacob D (2015) Regionally coupled atmosphere-ocean-sea ice-marine biogeochemistry model ROM: 1. Description and validation. J Adv Model Earth Sy 7:268–304. https://doi.org/10.1002/2014MS000357

Sein DV, Koldunov NV, Danilov S, Wang Q, Sidorenko D, Fast I, Rackow, T, Cabos W, Jung T (2017) Ocean modeling on a mesh with resolution following the local rossby radius. J of Adv in Model E Sys 9:2601–2614. https://doi.org/10.1002/2017MS001099

Sein DV, Gröger M, Cabos W, Alvarez-Garcia FJ, Hagemann S, Pinto JG, Izquierdo I, de la vara A, Koldunov NV, Dvornikov AY, Limareva N, Aleekseva E, Martinez-Lopez B, Jacob D (2020) Regionally coupled atmosphere - ocean - marine biogeochemistry model ROM: 2. Studying the climate change signal in the North Atlantic and Europe. Journal of Advances in Modeling Earth Systems. 0–3 p. https://onlinelibrary.wiley.com/doi/abs/10.1029/2019MS001646

Sherman, K., Hempel, G. (2008). The UNEP Large Marine Ecosystem Report: A perspective on changing conditions in LMEs of the world's Regional Seas. http://hdl.handle.net/20.500.11822/2186

Soares PMM, Lima DCA, Semedo A, Cardoso RM, Cabos W, Sein DV (2019) Assessing the climate change impact on the North African offshore surface wind and coastal low-level jet using coupled and uncoupled regional climate simulations. Clim Dyn 1-22. https://doi.org/10.1007/s00382-018-4565-9

Soares PM, Lima DC, Semedo A, Cabos Narvaez WD, Sein D (2019) Climate change impact on the Northwestern African offshore wind energy resources , Environmental Research Letters . https://doi: 10.1088/1748-9326/ab5731

Sousa MC, de Castro M, Álvarez I, Gomez-Gesteira M, Dias JM (2017a) Why coastal upwelling is expected to increase along the Western Iberian Peninsula over the next century? Sci Total Environ 592:243–251. https://doi.org/10.1016/j.scitotenv.2017.03.046

Sousa MC, Alvarez I, deCastro M, Gomez-Gesteira M, Dias JM (2017b) Seasonality of coastal upwelling trends under future warming scenarios along the southern limit of the Canary upwelling system. Prog Oceanogr153:16–23. https://doi.org/doi:10.1016/j. pocean.2017.04.002

Sousa, M.C., Ribeiro, A., Des, M., Gomez-Gesteira, M., deCastro, M., Dias, J.M., (2020) NW Iberian Peninsula coastal upwelling future weakening: competition between wind

intensification and surface heating. Sci. Total Environ. 703, 134808. https://doi.org/10.1016/j.scitotenv.2019.134808

Stramma, L., (1984). Geostrophic transport in the warm water sphere of the eastern subtropical North Atlantic. J. Mar. Res. 42 (3), 537–558. https://doi.org/10.1357/002224084788506022.

Stevens, B., and S.Bony (2013), Water in the atmosphere, Phys. Today, 66(6), 29– 34. https://doi.org/10.1063/PT.3.2009

Stommel, H. M., (1958) The Gulf Stream: A Physical and Dynamical Description, 202 pp., Univ. Calif. Press, Berkeley, Calif.

Sydeman WJ, Garcia-Reyes M, Schoeman DS, Rykaczewski RR, Thompson SA, Black BA, Bograd SJ (2014) Climate change and wind intensification in coastal upwelling ecosystems. Science 345:77–80. https://doi.org/10.1126/science.1251635

Sylla A, Mignot J, Capet X, Gaye AT (2019) Weakening of the Senegalo–Mauritanian upwelling system under climate change. Clim Dyn 53(7–8):4447–73. https://doi.org/10.1007/s00382-019-04797-y

Takhsha M, Nikiéma O, Lucas-Picher P, Laprise R, Hernández-Díaz L, Winger K (2017) Dynamical downscaling with the fifth-generation Canadian regional climate model (CRCM5) over the CORDEX Arctic domain: Effect of large-scale spectral nudging and of empirical correction of sea-surface temperature. Clim Dyn. 126. https://doi.org/10.1007/s00382-017-3912-6

Taylor, K. E., R. J. Stouffer, and G. A. Meehl (2012), An overview of CMIP5 and the experiment design, Bull. Am. Meteorol. Soc., 93, 485–498.

Troupin C, Mason E, Beckers JM, Sangrà P (2012) Generation of the Cape Ghir upwelling filament: A numerical study. Ocean Model. 2012;41:1–15. https://doi.org/10.1016/j.ocemod.2011.09.001

Valcke S (2013) The OASIS3 coupler: a European climate modelling community software. Geosci Model Dev 6:373- 388. https://doi.org/10.5194/gmd-6-373-2013

van Meijgaard E, van Ulft LH, van den Berg WJ, Bosveld FC, van den Hurk BJJM, Lenderink G, Siebesma AP (2008) The KNMI regional atmospheric climate model RACMO version 2.1. KNMI Tech. Rep. TR-302, 43.

Van Camp, L., Nykjaer, L., Mittelstaedt, E., Schlittenhardt, P., (1991). Upwelling and boundary circulation off Northwest Africa as depicted by infrared and visible satellite observations. Progress in Oceanography 26 (4), 357–402. https://doi.org/10.1016/0079-6611(91)90012-B

Varela R, Alvarez I, Santos F, deCastro M, Gomez-Gesteira M (2015) Has upwelling strengthened along worldwide coasts over 1982–2010? Sci Rep 5. https://doi.org/10.1038/srep10016

Varela, R., Rodríguez-Díaz, L., de Castro, M., & Gómez-Gesteira, M. (2022). Influence of Canary upwelling system on coastal SST warming along the 21st century using CMIP6 GCMs. Global and Planetary Change, 208, 103692. https://doi.org/10.1016/j.gloplacha.2021.103692

Vázquez, R., Parras-Berrocal, I., Cabos, W., Sein, D. V., Mañanes, R., Perez, J. I., and Izquierdo, A (2019): Climate Evaluation of a High Resolution Regional Model over the Canary Current Upwelling System, in: Lecture Notes in Computer Science, 240–252, Springer International Publishing, https://doi.org/10.1007/978-3-030-22747-0_19

Vázquez, R., Parras-Berrocal, I., Cabos, W., Sein, DV., Mañanes, R. and Izquierdo, A. (2022) Assessment of the Canary current upwelling system in a regionally coupled climate model. Clim Dyn 58, 69–85. https://doi.org/10.1007/s00382-021-05890-x

Voldoire A, Sanchez-Gomez E, Salas y Mélia D, Decharme B, Cassou C, Sénési S, Valcke S, Beau I, Alias A, Chevallier M, Déqué M, Deshayes J, Douville H, Fernandez E, Madec G, Maisonnave E, Moine M-P, Planton S, Saint-Martin D, Szopa S, Tyteca S, Alkama R, Belamari S, Braun A, Coquart L, Chauvin F (2013) The CNRM-CM5.1 global climate model: description and basic evaluation. Clim Dyn 40:2091-2121. https://doi.org/10.1007/s00382-011-1259-y

Wang DW, Gouhier TC, Menge BA, Ganguly AR (2015) Intensification and spatial homogenization of coastal upwelling under climate change. Nature 518. https://doi.org/10.1038/nature14235

Wang, J., Guan, Y., Wu, L., Guan, X., Cai, W., Huang, J., Dong, W., and Zhang, B. (2021): Changing Lengths of the Four Seasons by Global Warming, Geophys. Res. Lett., 48, https://doi.org/10.1029/2020GL091753.

Wang, Q., J. A. Kalogiros, S. R. Ramp, J. D. Paduan, G. Buzorius, and H. Jonsson, (2011): Wind Stress Curl and Coastal Upwelling in the Area of Monterey Bay Observed during AOSN-II. J. Phys. Oceanogr., 41, 857–877, https://doi.org/10.1175/2010JPO4305.1.

Wang, Y., Castelao, R.M., Yuan, Y., (2015) Seasonal variability of alongshore winds and sea surface temperature fronts in Eastern Boundary Current Systems. J. Geophys. Res. Oceans 120 (3), 2385–2400. https://doi.org/10.1002/2014JC010379

Ward ND, Megonigal JP, Bond-Lamberty B, Bailey VL, Butman D, Canuel EA, Diefenderfer H, Ganju NK, Goñi MA, Graham EB, Hopkinson CS, Khangaonkar T, Langley JA, McDowell NG, Myers-Pigg AN, Neumann RB, Osburn CL, Price RM, Rowlnad J, Sengupta A, Simard M, Thornton PE, Tzortziou M, Vargas R, Weisenhorn PB, Hopkinson CS (2020) Representing the function and sensitivity of coastal interfaces in Earth system models. Nat Commun 11, 2458. https://doi.org/10.1038/s41467-020-16236-2

Wooster WS, Bakun A, McLain D (1976) The seasonal upwelling cycle along the eastern boundary of the North Atlantic. J. Mar. Res. 34(2), 131–141.

Xie, S. P., Deser, C., Vecchi, G. A., Collins, M., Delworth, T. L., Hall, A., et al. (2015). Towards predictive understanding of regional climate change. Nature Climate Change, 5(10), 921–930. https://doi.org/10.1038/nclimate2689

Xiu P, Chai F, Curchitser E, Castruccio F (2018) Future changes in coastal upwelling ecosystems with global warming: The case of the California Current System. Sci Rep 8, 2866. https://doi.org/10.1038/s41598-018-21247-7

Zhou, L. M. (2016). Desert Amplification in a Warming Climate. Scientific Reports, 6. https://doi.org/ARTN3106510.1038/srep31065

Annex

Summary of Scientific activities

Publications in international journals

Parras-Berrocal, I. M., **Vázquez, R.,** Cabos, W., Sein, D. V., Álvarez, O., Bruno, M., and Izquierdo, A. (2023) Dense water formation in the Eastern Mediterranean under global warming scenario, EGUsphere [preprint], https://doi.org/10.5194/egusphere-2023-159

Parras-Berrocal, I. M., **Vázquez, R**., Cabos, W., Sein, D. V., Álvarez, O., Bruno, M., and Izquierdo, A. (2022) Surface and Intermediate Water Changes Triggering the Future Collapse of Deep Water Formation in the North Western Mediterranean, Geophys. Res. Lett., 49, e2021GL095404, https://doi.org/10.1029/2021GL095404.

Vázquez, R., Parras-Berrocal, I., Cabos, W., Sein, DV., Mañanes, R. and Izquierdo, A. (2022) Assessment of the Canary current upwelling system in a regionally coupled climate model. Clim Dyn 58, 69–85. https://doi.org/10.1007/s00382-021-05890-x

Parras-Berrocal I., **Vázquez R**., Cabos W., Sein D., Mañanes R., Perez-Sanz J., and Izquierdo A. (2020) The climate change signal in the Mediterranean Sea in a regionally coupled ocean-atmosphere model, Ocean Sci. 16:743–765. DOI : https://doi.org/10.5194/os-2019-42.

Vázquez R., Parras-Berrocal I.M., Cabos W., Sein D.V., Mañanes R., Perez J.I., Izquierdo A. (2019) Climate Evaluation of a High-Resolution Regional Model over the Canary Current Upwelling System. In: Rodrigues J. et al. (eds) Computational Science – ICCS 2019. ICCS 2019. Lecture Notes in Computer Science, vol 11539. Springer, Cham. DOI: https://doi.org/10.1007/978-3-030-22747-0_19

Publications in Preparation

Vázquez R., Parras-Berrocal I.M., Shunya K., Cabos W., Sein D.V., Izquierdo A. (2023) Seasonality of coastal upwelling trends in the Mauritania-Senegalese region under climate change scenarios. **Submitted to Science of the Total Environment.**

Vázquez R., Parras-Berrocal I.M., Cabos W., Sein D.V., Mañanes R., Bolado-Penagos M., Izquierdo A. (2023) Climate change in the Canary current upwelling system: The role of ocean stratification and wind. **In Preparation.**

Koseki S, **Vázquez R,** Cabos W, Gutiérrez-Escribano C, Sein DV (2023) Dakar Niño variability under global warming investigated by a high-resolution regional coupled model. **In Preparation.**

Cabos W, de la Vara A, **Vázquez R**, Koseki S, Sein DV (2023) Impact of model's resolution on the climate change signal in the South Eastern Tropical Atlantic. **In Preparation**

International conferences

Koseki, S., **Vázquez, R.,** Cabos, W., Guitérrez, C., and Sein, D. (2023) Dakar Niño variability under global warming investigated by a high-resolution regional coupled model, EGU General Assembly 2023, Vienna, Austria, 24–28 Apr 2023, EGU23-8344, https://doi.org/10.5194/egusphere-egu23-8344. (*Poster*)

Parras Berrocal, I. M., **Vázquez, R.,** Cabos, W., Sein, D. V., Álvarez, O., Bruno, M., and Izquierdo, A. (2023) Dense water formation in the Eastern Mediterranean under global warming scenario, EGU General Assembly 2023, Vienna, Austria, 24–28 Apr 2023, EGU23-13187, https://doi.org/10.5194/egusphere-egu23-13187. (*Oral presentation)*

Vázquez R., Parras-Berrocal I.M., Shunya K., Cabos W., Sein D.V., Izquierdo A. (2023) Seasonality of coastal upwelling trends in the Mauritania-Senegalese region under climate change scenarios. CLIVAR: Towards an integrated view of climate, Madrid, Spain (*Poster*)

Vázquez R., Parras-Berrocal I.M., Cabos W., Sein D.V., Mañanes R., Bolado-Penagos M., Izquierdo A. (2022) Climate change in the Canary current upwelling system: The role of ocean stratification and wind. XII Internacional de la Asociación Española de Climatología (AEC), Santiago de Compostela, Spain, (*Poster*)

Koseki, S., **Vázquez, R.,** Cabos, W., Guitérrez, C., and Sein, D. (2023) Dakar Niño variability under global warming investigated by a high-resolution regional coupled model. CLIVAR: Towards an integrated view of climate, Madrid, Spain (*Poster*)

Vázquez R., Parras-Berrocal I.M., Cabos W., Sein D.V., Mañanes R., Bolado-Penagos M., Izquierdo A. (2022) Climate change in the Canary current upwelling system: The role of ocean stratification and wind. VII Expanding Ocean frontiers, Las Palmas de Gran Canaria, Spain, (*Poster*)

Parras-Berrocal, I. M., **Vázquez, R.,** Cabos, W., Sein, D. V., Álvarez, O., Bruno, M., and Izquierdo, A. (2023) Dense water formation in the Eastern Mediterranean under global warming scenario. VII Expanding Ocean Frontiers, Las Palmas de Gran Canaria, Spain, (*Poster*)

Vázquez R., Parras-Berrocal I.M., Cabos W., Sein D.V., Mañanes R., Bolado-Penagos M., Izquierdo A (2021) The climate change effects in the Canary Current Upwelling Systems. Wind and Ocean stratification, complementary or competitives?. III Jis del Mar, Motril, Spain (*Oral presentation*).

Parras-Berrocal, I. M., **Vázquez, R.,** Cabos, W., Sein, D. V., Álvarez, O., Bruno, M., and Izquierdo, A. (2021) Will deep water formation collapse in the Northwestern Mediterranean sea at the end of 21st century?. III Jis del Mar, Motril, Spain, (*Oral presentation*)

Sirviente, S. Bolado-Penagos, M., **Vázquez, R.**, Parras-Berrocal, I., Jiménez-Rincón, J., Caballero, A., Izquierdo, A. (2021) Rio San Pedro Coastal Environmental Observation Platform (POCARISA). 2nd Ocean Observers Workshop, Plouzané, France. (*Oral presentation*)

Pérez Cayeiro, M.L., Arcila Garrido, M., Chica-Ruíz, J.A., Buonocure, C**., Vázquez, R**., Gómiz Pascual, J.J., Ramírez Guerrero, G. (2020) Evaluación de servicios ecosistémicos culaturales: Caso de estudio de la cuenca del río Barbate. XI Congreso Ibérico de Gestión y Planificación del Agua, Zaragoza, Spain (*Oral presentation*)

Parras-Berrocal, I. M., **Vázquez, R.,** Cabos, W., Sein, D. V., Álvarez, O., Bruno, M., and Izquierdo, A. (2020) Will deep water formation collapse in the Northwestern Mediterranean sea at the end of 21st century?. VI Expanding Ocean Frontiers, Barcelona, Spain, (*Oral presentation*)

Vázquez R., Parras-Berrocal I.M., Cabos W., Sein D.V., Mañanes R., Perez J.I., Izquierdo A (2019) Climate Evaluation of a High-Resolution Regional Model over the Canary Current Upwelling System. International Conference on Computational Science, Faro, Portugal (*oral presentation*)

Internship abroad

The author did a national research internship within the Research Group "Climate Physics Group" at the University of Alcala (Alcala de Henares, Spain) from 18th to 23rd April 2021 under the supervision of Dr. William David Cabos Narváez.

The author did an international research internship in the Alfred Wegener Institute for Polar and Marine research (AWI) at the Climate Dynamics section from 1st February to 30th April 2022, under the supervision of Prof. Dr. Sergey Danilov on the topic "Climate change in the Canary Current Upwelling System (CCUS) from the AWI climate models".

Scientific courses and complementary skills

2023. 1st Breezes Workshop (BREW), including the (oral) presentation of the following work: Tendency of the Azores' high-pressure and Iberian Peninsula thermal low and their influence on breezes in the Gulf of Cádiz. University of Cádiz (5 hours)

2022. Participation in European Researchers' Night. University of Cádiz (8hours)

2022. Coastal Risk Evaluation and Ecosystem Services, organized by the University of Ferrara (3 hours)

2021. Seminar "Climate and Oceanography" organized by the Oceanography Physics Group of the University of Cádiz (5 hours)

2021. Participation in "Ocean Hackathon" as mentor of data. Zona Franca de Cádiz (15 hours)

2021. Seminar in "Future Bootcamp". SEA-EU alliance activity. University of Malta (10 hours).

2021. Participation in European Researchers' Night. University of Cádiz (14 hours)

2021. Use of Google drive and collaborative work. Google drive forms. University of Cádiz (25 hours)

2020. English B.2.2 Certificated Course. Modern Language Centre (CSLM). University of Cádiz (25 hours)

2020. Online workshop in "Operational Oceanography". University of Algarve (7.5 hours)

2020. Search, management and communication of scientific information. University of Cádiz Doctorate School (EDUCA). (35 hours).

2020. Participation in "Ocean Hackathon" as mentor of data. Zona Franca de Cádiz (15 hours)

2019. Oceanography and Programming oriented to objects with Python. University of Cádiz Doctorate School (EDUCA). (20 hours).

2019. Development of a water resource management platform during low water periods in the SUDOE region (Interreg SUDOE). University of Cádiz (75 hours)

2019. Learninng "WordPress". University of Cádiz (25 hours)

Project collaboration

SIHROCO (**2023**). Study of the Impact of climate change on Hybrid marine Renewable energy projects using high resOlution simulations with a regional COupled model (SIHROCO). (I+D+I PID2021-128656OB-I00; 161.753,00 €). Leader researcher Dr. William David Cabos Narváez. Financed by the Spaninsh Ministry of Science and Innovation (2022-2025).

WINDABL (**2023**). How are the surface thermally driven WINDs influenced by the vertical and horizontal structure of the Atmospheric Boundary Layer?. (PR2022-055; 10000€). Leader researcher Dr. Carlos Román Cascón. Financed by the University of Cádiz (2023).

POCARISA (**2021**). Proyecto de Observatorio Costero Ambiental del Río San Pedro (POCARISA). Educational innovation Project (1486 €). Leader researcher Dr. Alfredo Izquierdo González. Financed by the University of Cádiz

El aprendizaje del Cambio Climático en la Universidad. Desde el tratamiento de las concepciones alternativas al juego como herramienta didáctica (**2021**). Educational innovation Project (1500 €). Leader researcher Dr. Marina Bolado Penagos. Financed by the University of Cádiz

Observatorio Ambiental Parque Natural Bahía de Cádiz (**2021**). Educational innovation Project (1800 €). Leader researcher Dr. Javier Benavente. Financed by the University of Cádiz.

Teaching experience

Teaching collaboration in Marine Sciences Degree. **2020/2021**. Subject Physics Oceanography, Fluid mechanics and Geophysics and Tectonics, Applied Physics Department, University of Cádiz (37 hours).

Teaching collaboration in Environmental Sciences Degree. **2020/2021**. Subject Environmental pollution assessment and Climate change, Applied Physics Department, University of Cádiz (23 hours).

Teaching collaboration in Marine Sciences Degree. **2021/2022**. Subject Physics Oceanography and Fluid mechanics, Applied Physics Department, University of Cádiz (45 hours).

Teaching collaboration in Environmental Sciences Degree. **2021/2022**. Subject Environmental pollution assessment, Applied Physics Department, University of Cádiz (15 hours).

Teaching collaboration in Marine Sciences Degree. **2022/2023**. Subject Physics Oceanography and Fluid mechanics, Applied Physics Department, University of Cádiz (8 hours).

Teaching collaboration in Environmental Sciences Degree. **2022/2023**. Subject Environmental pollution assessment, Applied Physics Department, University of Cádiz (15 hours).